SVSF ESTIMATION FOR TARGET TRACKING WITH MEASUREMENT ORIGIN UNCERTAINTY

SVSF (SMOOTH VARIABLE STRUCTURE FILTER) ESTIMATION FOR TARGET TRACKING WITH MEASUREMENT ORIGIN UNCERTAINTY

BY

MINA ATTARI, M.Sc., B.Sc.

A Thesis Submitted to the School of Graduate Studies in Partial Fulfilment of the Requirements for the Degree of Doctor of Philosophy

McMaster University

DOCTOR OF PHILOSOPHY (2016), McMaster University, Hamilton, Ontario (Mechanical Engineering)

TITLE:	SVSF Estimation for Target Tracking with Measurement Origin Uncertainty
AUTHOR:	Mina Attari
	B.Sc. (Tabriz University)
SUPERVISOR:	Dr. Saeid Habibi
NUMBER OF PAGES:	xvii, 207

Abstract

The main idea of this thesis is to formulate the smooth variable structure filter (SVSF) for target tracking applications in the presence of measurement origin uncertainty. Tracking, by definition is the recursive estimation of the states of an unknown target from indirect, inaccurate and uncertain measurements. The measurement origin uncertainty introduces the data association problem to the tracking system.

The SVSF estimation strategy was first presented in 2007. This filter is based on sliding mode concepts formulated in a predictor-corrector form. Essentially, the SVSF uses an existence subspace and smoothing boundary layer to bind the estimated state trajectory to within a subspace around the true trajectory. The SVSF is demonstrated to be robust to modeling uncertainties and provide extra measures of performance such as magnitude of the chattering signal. Therefore, with respect to specific nature of car tracking problems that involves modeling uncertainty, it was hypothesized that a robust estimation strategy such as the SVSF, would improve the performance of the tracking system and give more robust tracking results. Also, having the extra information provided by the SVSF strategy, i.e. the chattering magnitude signal, would lead to algorithms that could better account for measurement origin uncertainty in the context of the data association process. Further to these hypotheses, this research has focused on investigating the performance of the SVSF in the target tracking problems, advancing the development of the SVSF, and employing its characteristics to deal with data association problems.

The performance of the SVSF, in its current form, can be improved when there is fewer measurements than states by using its error covariance in target tracking.

As the first contribution in this research, the SVSF is formulated in the context of target tracking in clutter and combined with data association algorithms, resulting in the SVSF-based probabilistic data association (PDA) and joint probabilistic data association (JPDA) for non-maneuvering and maneuvering targets. The results are promising in the tracking scenarios with modeling uncertainties. Therefore, the thesis is then expanded by generalizing the covariance of the SVSF for the cases where the number of measurements is less than the number of states. The generalized covariance formulation is then used to derive a generalized variable boundary layer (GVBL) SVSF. This new derivation gives an estimation method that is optimal in the MMSE sense and in the meantime preserves the robustness of the SVSF. The proposed algorithm improves the performance measures and makes a more reliable tracking algorithm.

This thesis explores the hypothesis that multiple target tracking performance can be substantially improved by including chattering information from SVSF-based filtering in the data association method. A Bayesian framework is used to formulate a new set of augmented association probabilities which include the chattering information. The simulation and experimental results demonstrate that the proposed augmented probabilistic data association improves the performance of the tracking system including maneuvering cars, in particular for highly cluttered environments.

The derived methods are applied on simulations and also on real data from an experimental setup. This thesis is made up of a compilation of papers that include three conference papers and three journal papers.

Acknowledgment

Foremost, I express my deep appreciation to my supervisor, Dr. Saeid Habibi, for his support, generosity, and guidance through my PhD. This journey was an impossible one without his mentorship, wisdom, and thoughtful insight. Furthermore, I would like to convey my gratitude to Dr. Andrew Gadsden who helped me overcome the initial challenges and dive into the research, and Mr. Cam Fisher for his continuous support and technical insight. I would also like to thank my supervisory committee Dr. Ali Emadi, Dr. Stephen Veldhuis, and Dr. Thia Kirubarajan for their helpfulness and support.

I also would like to express my gratitude to my friends and colleagues in McMaster University who helped me go through my PhD study and finalize it. I am especially indebted to Dr. Bahram Marami for his support and friendship.

I am also deeply grateful to my beloved parents, Ayoub and Manizheh, wonderful parents-in-law, Alireza and Fatemeh, and siblings, Peyman and Nasrin for their encouragement and support throughout my life. I owe any achievement I ever had to my parents, and warmth of my heart to my sister.

Finally, I thank Atta, my soulmate and my inspiration. Nothing was possible without his unconditional love, support and motivation.

Contents

List of Figures

List of Tables

Declaration of Academic Achievement

This research presents analytical and computational work carried out solely by Mina Attari, herein referred to as “the author”, with advice and guidance provided by the academic supervisor Dr. Saied Habibi. Information that is presented from outside sources which has been used towards analysis or discussion, has been cited when appropriate, all other materials are the sole work of the author.

Chapter 1

General Introduction

Multiple target tracking (MTT) is an ever-increasing field of research with a wide range of application areas. The initial dawn of the research field was mainly driven by military applications, including state estimation of aircrafts using on-ground radar systems. Since its inception, the application field for MTT has greatly expanded to include biological systems, environmental studies, finance, air traffic surveillance and automotive safety systems. The MTT system is based on estimation theory which involves a recursive extraction and estimate of unknown variables from measurements over time. In general, the unknown variable could be the temperature of the room, the movement of a blood cell, or the stock value in a financial market. In the setting of the MTT systems, the variables of interest are commonly the position, velocity and possibly the acceleration of the objects or targets, often referred to as *states*.

The target states evolve in time and to make a prediction of their future value, a model known as a *process model* or *motion model* is used. Typically, a process noise needs to be added to the motion model to reflect modeling errors. Given the knowledge of the current state, in the next step state is predicted using the motion model. The predicted value along with the additional information is used to update the state. Typically, the source of the additional information is measurements from sensors, such as radar, camera, LiDAR, etc. The sensory data in turn relate to the states through a model called the *measurement model*.

To account for the measurement errors and potential sensor imprecisions, a realistic measurement model includes a measurement noise term.

Apart from the process and measurement uncertainties, often in MTT systems the measurement origin uncertainty must also be resolved. The measurement origin uncertainty is translated into data association uncertainty and occurs when the origin of the measurements from the remote sensing device are not certain, i.e. not necessarily from the target of interest. This uncertainty occurs when the target is not detectable, the targets are interfering, or some measurements are received from clutter as false alarms. Another issue to address in a generic MTT system is the track management which is caused by targets entering and exiting the sensor's field of view. These require algorithms to manage the initiation, confirmation and possibly deletion of tracks.

The title of this thesis is "SVSF estimation for target tracking with measurement origin uncertainty". Several aspects of the SVSF is modified in this context and the potential of the SVSF to improve the MTT system is exploited. Section 1.1 provides the theme and objectives of this dissertation. In section 1.2 the outline and the overview of the thesis chapters are presented. Section 1.3 reviews the background and literature on several topics including multiple target tracking, estimation, gating and data association, and track management. Finally, section 1.4 is devoted to overall proposed car tracking system including the experimental setup, different simulation models and scenarios, and the potential application areas.

1.1 Theme and Objective of Dissertation

In compliance with the regulations of McMaster University, this dissertation is assembled as a sandwich thesis format composed of three conference and three journal articles. These articles represent the independent work of the author of this dissertation.

The articles in the dissertation follow a cohesive flow aimed at defining and investigating the Smooth Variable Structure Filter (SVSF) in the context of tracking in the presence of measurement origin uncertainty. The general theme is based on the following:

i. To examine the performance of the combination of probabilistic data association methods and SVSF (Conference papers *a*, *b* and *c*)
   a. To formulate and simulate the SVSF-based single target tracking in clutter (Conference paper *a*).
   b. To investigate the SVSF-based multiple target tracking in clutter (Conference paper *b*).
   c. To examine the SVSF-based maneuvering target tracking in clutter (Conference paper *c*).

ii. To generalize the covariance derivation of the SVSF and examine the performance of the covariance modified SVSF for tracking in the presence of clutter (Journal paper I).

iii. To generalize the optimal formulation of the SVSF, namely the variable boundary layer SVSF, and examine its improvements in dealing with target tracking with measurement origin uncertainty (Journal paper II).

iv. To formulate an augmented set of association probabilities using the extra information provided by the SVSF and to investigate its performance (Journal paper III).

Explanation of the basic concepts and related literature review are provided throughout the papers. Additionally, section 1.3 is dedicated to provide a cohesive overview of the entire thesis.

1.2 Thesis Outline

The thesis contains six chapters. The chapters and the associated papers as listed in Section 1.1 are briefly described and listed as follows.

1.2.1 Chapter II: SVSF-Based Target Tracking - Papers a, b, and c

The following papers are contained in this chapter:

a. M. Attari, S. A. Gadsden, S. Habibi, "Target Tracking Formulation of the SVSF as a Probabilistic Data Association Algorithm", American Control Conference (ACC), Washington D.C., June 17-19, 2013

b. M. Attari, S. A. Gadsden, S. Habibi, "A Multi-Target Tracking Formulation of the SVSF with the Joint Probabilistic Data Association Technique", ASME 2014 Dynamic Systems and Control Conference (DSCC), San Antonio, TX, October 22-24, 2014

c. M. Attari, and S. Habibi, "Automotive Tracking Techniques Using a New IMM based PDA-SVSF", International Mechanical Engineering Congress and Exposition (IMECE), Montreal, QC, November 14-20, 2014

Preface: Prior research demonstrate some promising characteristic of the SVSF, particularly its robustness to modeling uncertainties and also extra sources of information

it provides. These properties motivated the first steps to explore the SVSF in the context of target tracking in the presence of measurement origin uncertainty. The well-studied probabilistic data association (PDA), joint probabilistic data association (JPDA) and interacting multiple model (IMM) are combined with SVSF and compared to their Kalman filter (KF) based counterparts. The performance measure is the root-mean-squared-error (RMSE) of the estimation that is averaged over a number of Monte Carlo runs. The comparison results confirm a performance improvement of the SVSF-based algorithms over the KF-based methods for the cases involving modeling uncertainties. These promising results encouraged further research on advancing the development of the SVSF and employing its characteristics to deal with data association problem.

1.2.2 Chapter III: Generalized Covariance SVSF, Journal Paper I

This Chapter consists of a paper that is currently under review (submitted on December 2014):

M. Attari, S. A. Gadsden, and S. Habibi, "Target Tracking Formulation of the SVSF with Data Association Techniques", IEEE Trans. on Aerospace & Electronic Systems.

Preface: After a preliminary demonstrative investigation of the SVSF, this paper elaborates on the generalization of the covariance formulation of the SVSF. This generalization considers the cases where the number of measurements is less than the number of states. This was an essential step to employing the SVSF in target tracking algorithms. The reason is that in a generic tracking scenario, the estimation of position, velocity and possibly acceleration is required. However the direct measurements of these variables are not always available. In this paper, the generalized covariance formulation of the SVSF (covariance-

modified SVSF, CM-SVSF) is used with probabilistic data association methods and explored and compared with KF-based methods for different tracking scenarios.

1.2.3 Chapter IV: Generalized Variable Boundary Layer SVSF, Journal Paper II

This Chapter consists of a paper that is accepted and available online:

M. Attari, Z. Lou, and S. Habibi, "An SVSF-Based Generalized Robust Strategy for Target Tracking in Clutter", IEEE Trans. on Intelligent Transportation Systems, DOI: 10.1109/TITS.2015.2504331, 23 Dec. 2015

Preface: This paper expands on the results of the above mentioned papers and provides a generalized variable boundary layer SVSF (GVBL-SVSF). This new derivation gives an estimation method that is optimal in the MMSE sense and in the meantime preserves the robustness of the SVSF to modeling uncertainties. The GVBL-SVSF is combined with probabilistic data association methods and tested under simulation scenarios as well as in an experimental set up. The experimental setup used for data acquisition includes a Ford escape car equipped with a Velodyne HDL32 LiDAR (Light Detection and Ranging) sensor. The LiDAR provides a 3D point cloud in each frame with a frame rate of 0.1 second. The point cloud data is processed and the vehicle-like objects are detected. The centre-points of these objects are in turn fed into the tracking algorithm. The performance of the GVBL-SVSF is then compared with the KF-based methods.

1.2.4 Chapter V: SVSF-Based Augmented Probabilistic Data Association, Journal Paper III

This Chapter consists of a paper that is currently under review (submitted on December 2015):

M. Attari, and S. Habibi, Augmented Probabilistic Data Association based on SVSF Estimation, IEEE Trans. on Aerospace and Electronic Systems

Preface: This paper completes the formulation of the SVSF estimation strategy in the context of target tracking in clutter. The probabilistic data association method is augmented to include the chattering information provided by SVSF-based filtering. The chattering magnitude signal is probabilistically analyzed and its probability distribution function is derived. Then, a Bayesian inference is used to formulate a new set of association probabilities which included the chattering information. This augmented probabilistic data association (APDA) method in conjunction with GVBL-SVSF is simulated and tested. The results are compared with the KF-based probabilistic data association.

1.2.5 Chapter VI: General Conclusion

This chapter provides the general concluding remarks of the thesis. The objective and main focus of the thesis is discussed. Supporting arguments and confirmation of the research hypotheses for each chapter are highlighted and a general overview of the results are presented.

1.3 Background and Literature Review

In this section, a brief introductory review is provided on multiple target tracking (MTT) system and its constituent blocks. A literature review of related work is presented in an attempt to provide a cohesive context to the published papers and the remaining chapters of this thesis. A review on estimation strategies with an emphasis on the smooth variable structure filter is provided. Also, the concept of data association to deal with measurement

origin uncertainty is briefly discussed. The track management, as a constituent block in every generic MTT system is also reviewed. The overall proposed car tracking system is then discussed and the car motion models, simulation scenarios, experimental set-up and the application areas are discussed to provide a cohesive picture of the research which is later presented in more details in the remaining chapters.

1.3.1 Multiple Target Tracking System

Target tracking algorithms have been used in a wide-variety of applications; ranging from air traffic control and monitoring, to data processing of medical images [1]. Most recently, target tracking systems are being applied to the area of autonomous vehicle research. For example, intelligent and cognitive vehicles make use of target tracking algorithms for active safety and advanced driver assistance systems (ADAS) [2, 3]. In surveillance and monitoring systems, the fundamental role of tracking algorithms is to interpret the surrounding environment using sensory information in an effort to form target tracks and estimates [1, 4]. Recent research on car safety systems shows that major improvements can be achieved if the information of the surrounding environment is added to the information of the internal states of the car in order to assist the driver to take appropriate decisions using tracking algorithms [3, 2].

Tracking is the estimation of the state of a moving object [4]. A vehicle tracking algorithm is used to interpret the environment by analyzing sensor information, which are typically noise-corrupted observations. These are then partitioned into tracks (of vehicles) based on their origin, in an effort to estimate their position, velocity, or other quantities of interest [1]. Figure 1.1 illustrates typical elements in a conventional tracking system.

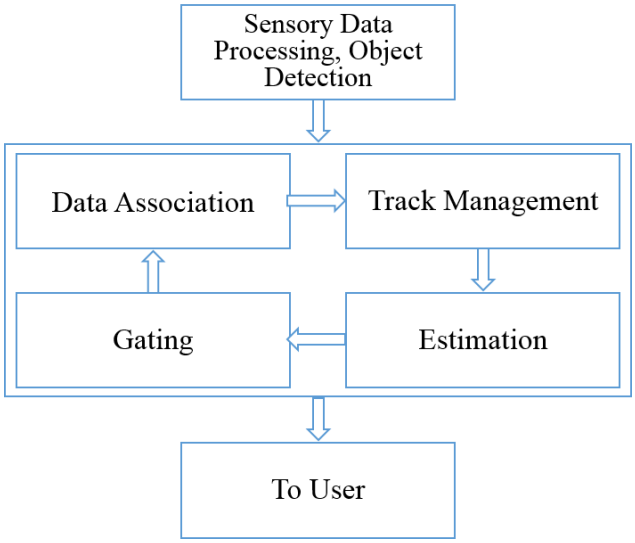

Figure 1.1 Basic elements of a conventional multiple target tracking system

The fundamental blocks of a multiple target tracking (MTT) system are: (i) estimation, (ii) gating and data association, and (iii) track management. An introduction to these typical functions and the manner in which they interrelate is provided as follows. The main distinction between an MTT system and a conventional estimation problem is the measurement origin uncertainty issue in the MTT system. A track is a state trajectory estimated from a set of received measurements that are associated with the same target in time. The source of the measurements might be uncertain because of the random false alarms, clutter, or interfering targets. The gating and data association blocks of an MTT system are responsible for this measurement to track association issues. Once the measurement association is resolved, the estimation block functions to update the tracks and provide the proper output for the user. The track management block is responsible for initializing the new tracks and properly validating them. It also ensures that tracks that are no longer detected or are unlikely to exist, get deleted. The fundamental blocks and their functions are further discussed in the following sections.

1.3.2 Estimation

A general recursive estimation problem aims at recursively calculating the posterior probability density function of the state of the system, given all the previous measurements. In a general Bayesian framework, this problem translates into the calculation of an integral [5], which is seldom analytically solvable, and requires to keep track of an infinite many moments of prior information. However, if both the system and measurement models are linear with additive Gaussian noise, the optimal solution in the minimum mean square error (MMSE) sense is analytically derivable and tractable. This assumption is named linear-Gaussian (LG) assumption and results in the well-studied Kalman filter [6].

1.3.2.1 Kalman Filter

The Kalman filter was first presented in 1960s [7] and quickly became one of the most commonly used estimation methods [6, 8]. Using the LG assumption, the system and measurement models are expressed by a linear set of equations as follows:

$$x(k+1) = Ax(k) + Bu(k) + v(k) \tag{1.1}$$

$$z(k) = Cx(k) + w(k) \tag{1.2}$$

where $v(k)$ and $w(k)$ are zero mean white Gaussian process noise and measurement noise, with covariance matrices $Q(k)$ and $R(k)$, respectively. The KF algorithm is based on two main steps. The first step is referred to as the prediction step, and consists of the following equations:

$$\hat{x}(k+1|k) = A\hat{x}(k|k) + Bu(k) \tag{1.3}$$

$$\hat{z}(k+1|k) = C\hat{x}(k+1|k) \tag{1.4}$$

$$P(k+1|k) = AP(k|k)A^T + Q(k) \tag{1.5}$$

The state estimates are first predicted in (1.3), and the corresponding state error covariance is calculated as per (1.5). Equation (1.4) gives the predicted measurement. These values are then used in the updated step, which consists of the following equations:

$$K(k+1) = P(k+1|k)C^T[CP(k+1|k)C^T + R(k+1)]^{-1} \tag{1.6}$$

$$\hat{x}(k+1|k+1) = \hat{x}(k+1|k) + K(k+1)[z(k+1) - \hat{z}(k+1|k)] \tag{1.7}$$

$$P(k+1|k+1) = [I - K(k+1)C]P(k+1|k) \tag{1.8}$$

Equations (1.3)-(1.8) summarize the KF solution for linear estimation problems. The process is repeated iteratively.

For many practical applications the LG assumption is too restrictive. If the LG assumption is violated, the KF results in a suboptimal solution and can become unstable [9]. Nonlinear estimation problems deal with the following format of the system and measurement models:

$$x(k+1) = f\big(x(k), u(k)\big) + v(k) \tag{1.9}$$

$$z(k+1) = h\big(x(k+1)\big) + w(k) \tag{1.10}$$

Many variations of the KF have been presented in literature [6, 10] to deal with the system of (1.9) and (1.10). The most popular and simplest strategy is the Extended KF (EKF), which uses a first order linearization of the nonlinearities [11, 10] to analytically propagate the random Gaussian variables. The partial derivatives yield the linearized system and measurement matrices as follows [6]:

$$A(k) = \left.\frac{\partial f(x(k))}{\partial x}\right|_{x=\hat{x}(k|k)} \tag{1.11}$$

$$C(k+1) = \left.\frac{\partial h(x(k+1))}{\partial x}\right|_{x=\hat{x}(k+1|k)} \tag{1.12}$$

Equations (1.11) and (1.12) are used in the same framework of KF filtering to formulate the EKF.

An alternative to EKF is Unscented Kalman filter (UKF) that uses a deterministic sampling approach to approximate the mean and covariance and captures the nonlinearities to the second order of Taylor series expansion [9]. The KF, EKF and UKF use mean and covariance to describe the posterior probability distribution function, either exactly or by some sort of approximation, which implicitly assume that the Gaussian distribution is an adequately valid approximation. For the case when the Gaussian assumption is breached, one solution is to approximate the non-Gaussian distribution with a Gaussian mixture for the cost of increasing computational complexity [11]. The PF or sequential Monte Carlo method is proposed for nonlinear non-Gaussian systems [12]. The state probability distribution is approximated by a large number of Monte Carlo independent identical distribution samples, namely particles [12]. The PF is expensive in implementation, yet powerful in handling difficult problems [12].

The KF yields suboptimal results and is prone to instability if the LG assumption does not hold [11]. In an effort to reduce the effects of modeling uncertainties, robust Kalman filtering has been suggested [13, 14, 11]. These techniques try to deal with uncertainties in the system and measurement matrices, or noise covariance matrices. When dealing with uncertainties in the system and measurement matrices, the robust estimator is designed such that it gives an upper bound on the error variance for any allowed modeling uncertainty

[13, 14]. When the uncertainties in noise covariance matrices are dealt with, the KF gain is derived to minimize the estimation error covariance as well as its variation due to changes in process and measurement noise covariance matrices. In this way the sensitivity of the estimation error covariance to changes in the process and measurement noise covariances is reduced [11].

1.3.2.2 Smooth Variable Structure Filter

The smooth variable structure filter (SVSF) is the core concept behind the research presented in this thesis. In this section a brief review of the method is provided.

The smooth variable structure filter (SVSF) is a revised form of the variable structure filter (VSF), and was first presented in 2007 [15]. The VSF-based methods is a group of robust estimation techniques [16], where similar to sliding mode concept, the stability of the filter is guaranteed given bounded parametric uncertainties [16]. Similar to the KF strategy, the SVSF consists of two main steps: prediction and update. However, the main difference lies in how the SVSF gain is formulated. Conceptually, by use of the SVSF corrective gain, the SVSF converges the estimated state trajectory to within an existence subspace around the true trajectory. The width of the existence subspace is a function of uncertain dynamics due to uncertainties. Once the estimated states are in that subspace, they switch back and forth across the true trajectory and will remaining within this subspace [15]. This switching effect is referred to as chattering and for a normal operating condition is filtered out by using a smoothing function [15]. However, the magnitude of the chattering signal, if it exists, is an indicator of modeling uncertainty [15]. Therefore, in addition to conventional filter performance measures, the SVSF provides a unique set of performance indicators, which quantifies the degree of uncertainty [15].

The SVSF, in its original form [15], did not have a covariance formulation. In [17], an iterative strategy for generating an error covariance matrix was proposed. The error covariance was then used for obtaining a variable and optimal smoothing boundary layer in [17]. To deal with the cases when there are fewer measurements than states, a Luenberger observer based approach was originally adopted in [15]. In later modifications of the SVSF, as in [17], however, this approach was not used. In Chapter III of this thesis, the SVSF covariance formulation is modified to a general form to include the case when there are fewer number of measurements than states. In Chapter IV, based on the generalized covariance derivation of Chapter III, a generalized variable boundary layer form of [17] is presented.

1.3.2.3 Interacting Multiple Model

A real-world system may behave according to a number of different operating regimes. For example a moving car may travel straight with a constant speed, or may have a coordinated turn [6]. The operating modes may differ in noise level or their structure. Such systems are called hybrid systems [6]. Hybrid systems are characterized by their state that evolves according to a stochastic difference (or differential) equation model, and their mode that is governed by a discrete stochastic process [18]. In these systems, the implementation of adaptive estimation, which adapts to different operating modes in an effort to minimize the estimation error, is more desirable [6]. The so-called multiple model (MM) algorithms assume that the behaviour of the system can be modeled with a finite number of models [6]. In the static MM algorithm the system evolves on a fixed model and no switching happens among models during the estimation process evolution [19]. In contrast, in the dynamic MM estimator, the mode the system is in can undergo switching in time based on a homogeneous Markov chain with known transition probabilities [20, 21]. Compared with the static MM approach, the main advantage of dynamic MM algorithms is that the a priori

switching probabilities make these algorithms alert to regime changes while the static MM approach goes toward the single-mode hypothesis [18]. The dynamic MM algorithms include generalized Pseudo-Bayesian (GPB) [6, 22], and interacting multiple model (IMM) [6, 23, 24].

The GPB methods combine histories of models that differ in older models [6]. In first-order GPB (GPB1), only the possible models in the last sampling step are considered. In second-order GPB (GPB2) the possible models in the last two sampling steps are considered [6]. The IMM estimator is a suboptimal dynamic MM filter that has been demonstrated to be one of the most computationally effective hybrid state estimation schemes [21]. The main feature of this algorithm is that it is the best compromise available between computational complexity and performance [6, 25]; its computational requirements are almost linear in the number of models (as for GPB1), whereas its performance is almost the same as that of an algorithm with quadratic computational complexity (as for GBP2) [6, 20]. The IMM uses several filters in parallel for a finite number of target maneuvers. Its algorithm is composed of four main steps [6]: *interaction* or mixing the individual filter estimates with respect to the predicted model probabilities; *model-matched filtering* or state prediction and update of each filter using its own dynamic model assumptions; *model probability update* or updating the model probability of each model with respect to the innovation error; and *estimate combination* or combination of state estimate as a weighted sum of model-matched estimates, for output purposes. Figure 1.2 illustrates one cycle of the IMM estimator.

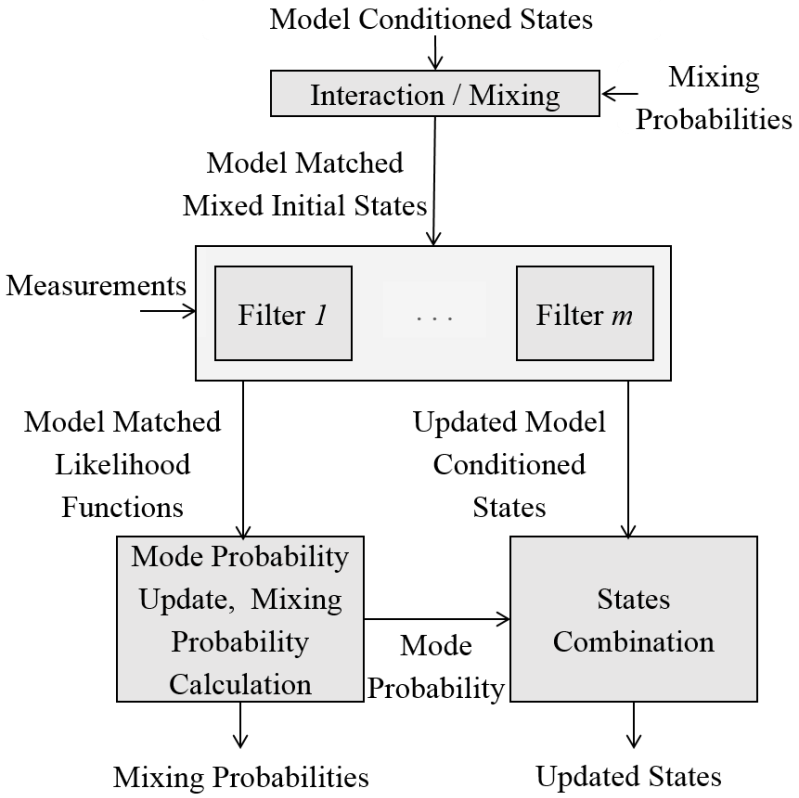

Figure 1.2 One cycle of the IMM estimator

In IMM method the state at time k is estimated under each possible current model using m filters, where each filter uses a different combination of previous model-conditioned estimates [6, 20]. One cycle of the IMM estimation consists of the following [6, 20]:

1. Computation of the mixed initial conditions for the model matched filter i is performed:

$$\hat{x}^{0i}_{k-1|k-1} = \sum_{j=1}^{m} \hat{x}^{j}_{k-1|k-1} \mu^{j|i}_{k-1|k-1} \quad i = 1, \dots, m \tag{1.13}$$

where $\mu_{k-1|k-1}^{j|i} = \frac{p_{ji}\mu_{k-1}^{j}}{\sum_{j=1}^{m} p_{ji}\mu_{k-1}^{j}}$ and, p_{ji} is the model switching probability and μ_{k-1}^{j} is the model probability at the time $k-1$. The covariance corresponding to above state estimation is as follows:

$$P_{k-1|k-1}^{0i} = \sum_{j=1}^{m} \mu_{k-1|k-1}^{j|i}\{P_{k-1|k-1}^{j} + (\hat{x}_{k-1|k-1}^{j} - \hat{x}_{k-1|k-1}^{0i})(\hat{x}_{k-1|k-1}^{j} - \hat{x}_{k-1|k-1}^{0i})'\} \qquad i = 1, \dots, m \tag{1.14}$$

2. Likelihood function for each of model-matched filters is calculated. The estimate (1.13) and the associated covariance (1.14) are used as inputs to each model-matched filter to calculate the likelihood function corresponding to m filters, as follows:

$$\Lambda_k^i = \mathcal{N}\left[z_k; \hat{z}^i{}_{k|k-1}(\hat{x}_{k-1|k-1}^{0i}), S_k^i(P_{k-1|k-1}^{0i})\right] \qquad i = 1, \dots, m \tag{1.15}$$

3. The model probabilities are updated:

$$\mu_k^i = \frac{\Lambda_k^i \sum_{j=1}^{m} p_{ji}\mu_{k-1}^{j}}{\sum_{i=1}^{m} \Lambda_k^i \sum_{j=1}^{m} p_{ji}\mu_{k-1}^{j}} \tag{1.16}$$

4. Combined model-conditioned state estimate and covariance matrix are calculated. Combination of the model-conditioned estimates and their corresponding covariances is done according to the following mixture equations:

$$\hat{x}_{k|k} = \sum_{i=1}^{m} \hat{x}_{k|k}^{i}\,\mu_k^i \tag{1.17}$$

$$P_{k|k} = \sum_{i=1}^{m} \mu_k^i\{P_{k|k}^{i} + (\hat{x}_{k|k}^{i} - \hat{x}_{k|k})(\hat{x}_{k|k}^{i} - \hat{x}_{k|k})'\} \tag{1.18}$$

This combination is only for output purposes and is not part of the recursion of the algorithm [6].

1.3.3 Gating and Data Association

In a conventional estimation algorithm, any uncertainty in measurement-to-track association is disregarded. In a practical MTT system, however, it is seldom known that which measurements is originated from which target. This uncertainty is known as data association problem. Algorithms are required to be in place to find the likely measurement-to-track associations. To illustrate the problem, suppose a sensor is mounted on a vehicle observing the traffic as in Figure 1.3. At time k, there are 2 targets in the traffic, but 5 measurements are received. The data association algorithm is responsible to find out which of the received measurements (if any) are likely to belong to the targets of interest.

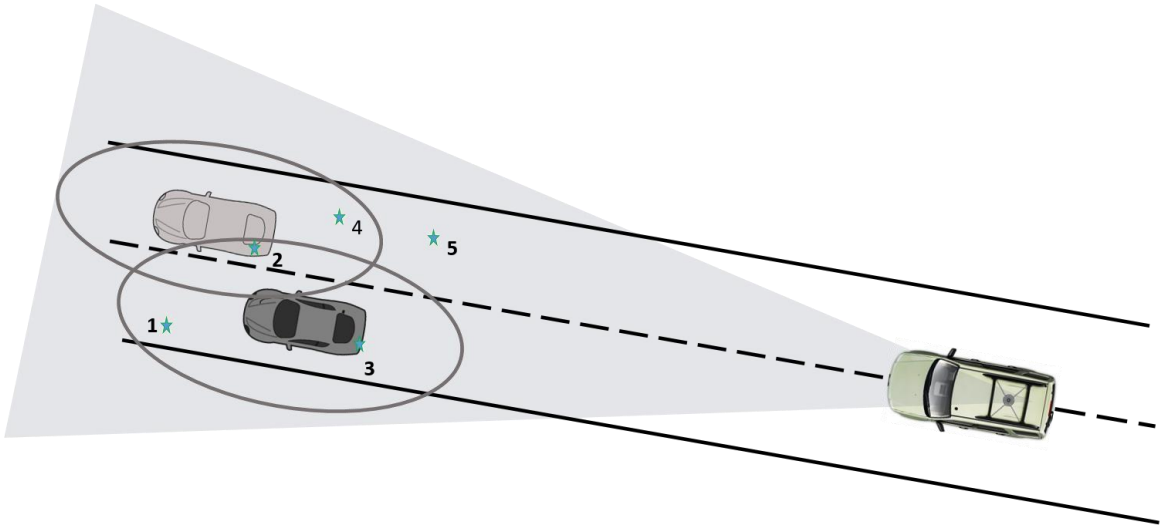

Figure 1.3 Illustration of the data association problem

A convenient approach to reduce the computational load of the data association algorithm is to remove unlikely measurement-to-track associations. This method is called gating. Therefore, to avoid searching the entire measurement set for the measurements originated from a specific target, an ellipsoidal gate is set up for each track, or rather around the predicted measurement of each track, $\hat{z}^i(k+1|k)$, and such a gate is called a validation region [5]. In this way, the number of possible measurement-to-track assignments is limited. The validation region is defined as a stochastic distance to the predicted measurements, as follows [5]:

$$d_{i,j}^2 = \left[z_{k+1}^i - \hat{z}^j(k+1|k)\right]^T S_{k+1}^T \left[z_{k+1}^i - \hat{z}^j(k+1|k)\right] \tag{1.19}$$

$$\mathcal{V}^j(k+1,\gamma) = \left\{z : d_{i,j}^2 \leq \gamma\right\} \tag{1.20}$$

where γ is the gate threshold, and $z_{k+1} - \hat{z}^j(k+1|k)$ is the residual between a received measurement and the predicted measurement of the track, that is assumed to be Gaussian distributed. Therefore, $d_{i,j}^2$ is Chi-squared distributed. This assumption is used to determine the gate threshold [4]. All the measurements that satisfy the gate criterion, are later considered in the data association algorithm. Figure 1.4 shows the validation gates and received measurements for two hypothetical targets.

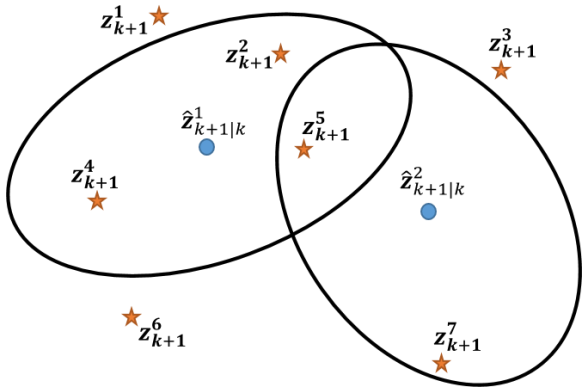

Figure 1.4 Validation region,

several measurements z^i_{k+1} in the ellipsoidal validation region of two targets centered at their predicted measurements $\hat{z}^j_{k+1|k}$ ($i = 1,..,7$ and $j = 1,2$)

If more than one measurement falls within the gate, then an association uncertainty arises. It is required to decide which measurement is originated form the target and therefore should be used to update the track [4]. There are a number of different data association algorithms proposed in the literature [4, 1]. A good review is given in [4, 1]. One of the simplest algorithms is the standard nearest neighbor filter (SNNF). In this method, the single most likely measurement to target association hypothesis is chosen in each time step. The SNNF associates the nearest measurement, in the sense of the statistical distance, target by target and in this manner is similar to a local optimization. This might lead to association of one measurement to several targets, which in turn lead to poor tracking performance and track losses [4]. The global nearest neighbour filter (GNNF) is an extension of SNNF that looks for one single best global association hypothesis, considering all targets and measurements simultaneously [1]. The GNNF is formulized in the form of a convex optimization problem and therefore can be solved by an optimization algorithm such as Auction algorithm [26]. Both SNNF and GNNF make a hard decision on association. This

single assignment made at a certain time might not be the best assignment in retrospect under difficult scenarios with interfering targets and high number of false alarms. This is a drawback of the SNNF and GNNF as a single-hypothesis method.

The probabilistic data association filter (PDA) is one of the most commonly used data association methods [27]. The PDA takes all feasible measurement-to-track association hypotheses into consideration, and calculates the association probability for the track [5]. Hence, it is an all-neighbor data association method. Since the PDA assumes that the track has already been initialized, another algorithm is required to handle the track maintenance. The integrated probabilistic data association (IPDA) is a derivation of the PDA without the aforementioned assumption, that yields the data association probabilities as well as track existence probabilities [28].

The PDA filter is typically formulated for single target tracking in the presence of clutter. Assume that the target track has been initialized. Also, define past information through time $k-1$ about the target trajectory in the form of a normal distribution as follows [5]:

$$p[x_k|Z^{k-1}] = \mathcal{N}[x_k; \hat{x}_{k|k-1}, P_{k|k-1}] \tag{1.21}$$

It is also assumed that if the target is detected, then, there is only one target originated measurement within the validation gate, and the remaining measurements are clutter originated. The number of validated false measurements is Poisson distributed with spatial density λ and their spatial distribution is modeled as independent and identically distributed uniform [5]. The m_k candidate measurements at time k are named as $z^i, i = 1, \dots, m_k$. The set of available measurements at time k are defined as $Z^k = \{z^1, \dots, z^{m_k}\} \cup Z^{k-1}$. For m_k validated measurements in time k, one can describe $m_k + 1$ distinct association hypotheses as [1]:

$$\mathcal{H}_k^i = \{z^i \; is \; target \; originated \;\} \tag{1.22}$$

$$\mathcal{H}_k^0 = \{none \; are \; target \; originated\} \tag{1.23}$$

where $i = 1, \dots, m_k$. Since these hypothesis are mutually exclusive and exhaustive, the use of the total probability theorem is allowed [5, 6]. The minimum variance estimate is written as follows:

$$\hat{x}_{k|k} = \mathbb{E}\{x_k|Z^k\} = \sum_{i=0}^{m_k} \mathbb{E}\{x_k|\mathcal{H}_k^i, Z^k\} P\{\mathcal{H}_k^i|Z^k\} = \sum_{i=0}^{m_k} \hat{x}_{k|k}^i \beta_k^i \tag{1.24}$$

where $\hat{x}_{k|k}^i$ is the updated state given that the ith hypothesis is correct and β_k^i is named association probability which is the conditioned probability of the ith hypothesis [29, 1]. These association probabilities are computed as follows [5, 4] :

$$\beta_k^i = \begin{cases} \dfrac{1 - P_D P_G}{1 - P_D P_G + \sum_{i=1}^{m_k} \mathcal{L}_k^i}, & i = 0 \\ \dfrac{\mathcal{L}_k^i}{1 - P_D P_G + \sum_{i=1}^{m_k} \mathcal{L}_k^i}, & i = 1, \dots, m_k \end{cases} \tag{1.25}$$

where $i = 0$ is association probability of the hypothesis when none of the validated measurements is target originated, P_G is gate probability [4], and P_D is the target detection probability. In addition:

$$\mathcal{L}_k^i = \frac{\mathcal{N}\left[z_k^i; \hat{z}_{k|k-1}, S_k\right] P_D}{\lambda} \tag{1.26}$$

which is the likelihood ratio of the measurement z_k^i, assuming that it is target originated [5]. The combined innovation to be used in the filter update is calculated as a weighted sum of m_k validated measurements, as follows:

$$\tilde{z}_k = \sum_{i=1}^{m_k} \beta_k^i e_{z,k+1|k}^i \tag{1.27}$$

where $e_{z,k+1|k}^i = z_k^i - Cx_{k|k-1}$ [30]. The states are updated with a standard estimation strategy. To update the covariance, the following equation is used:

$$P_{k|k} = \beta_k^0 P_{k|k-1} + [1 - \beta_k^0] P_{k|k}^* + \tilde{P}_k \tag{1.28}$$

where $P_{k|k}^*$ is the covariance matrix and $\tilde{P}_k$ accounts for uncertainty increment due to association uncertainty. It is computed as follows [29]:

$$\tilde{P}_k = K_k \left[\sum_{i=1}^{m_k} \beta_k^i e_{z,k+1|k}^i e_{z,k+1|k}^i{}' - \tilde{z}_k \tilde{z}_k{}' \right] K_k{}' \tag{1.29}$$

The original derivation of the PDA is for single-target tracking in the presence of clutter. For multiple-target tracking, a number of PDA's may be used in parallel [5]. When the target trajectories are interfering, an extension of PDA, named as the joint probabilistic data association (JPDA), is utilized and has improved performance [31]. In JPDA, the association probabilities are calculated in a joint manner across all targets [31]. To calculate the association probabilities, the conditional probabilities of the following joint events are evaluated as follows [5]:

$$\mathcal{H}_k = \bigcap_{i=1}^{m_k} \mathcal{H}_k^{ji} \tag{1.30}$$

where $\mathcal{H}_k^{it_i}$ is the hypothesis that measurement j originated from target t, $0 \leq i \leq m_k$, $0 \leq t \leq T$, k is the time index, t_j is the target that measurement j is associated with, m_k is

the number of measurements, and T is the number of targets [31]. The joint association probabilities are calculated as follows [5]:

$$P\{\mathcal{H}_k|Z^k\} = c\prod_i\left\{\lambda^{-1}\mathcal{L}_k^{t_i}\right\}^{\tau_i}\prod_t(P_D^t)^{\delta_t}(1-P_D^t)^{1-\delta_t} \tag{1.31}$$

where P_D^t is the detection probability of target t; and τ_i and δ_t are the target detection and measurement association indicators, respectively [31]. In addition:

$$\mathcal{L}_k^{t_i} = \mathcal{N}[z_k^i; \hat{z}_{k|k-1}^{t_i}, S_k^{t_i}] \tag{1.32}$$

The state estimation is carried out separately for each target using the marginal association probabilities [5, 31]. These probabilities are obtained from joint probabilities (1.31) by summing the joint hypotheses in which the marginal hypothesis of interest is included, as follows [5]:

$$\beta_k^{it} = P\left\{\mathcal{H}_k^{it}\middle|Z^k\right\} = \sum_{\mathcal{H}:\mathcal{H}^{it}\in\mathcal{H}} P\{\mathcal{H}_k|Z^k\} \tag{1.33}$$

These probabilities are used to create the combined innovation for each target, which is used during the filter update stage.

Further to PDA-based methods, a number of other approaches are suggested to deal with measurement origin uncertainty in the literature. In 1979 the multiple hypothesis tracker (MHT) was presented [32]. In MHT all the measurement-to-track assignments are enumerated; then the infeasible assignments are eliminated using pruning and gating methods, which imposes the risk of the elimination of the correct measurement sequences. Unlike the traditional MHT, the probabilistic multi hypothesis tracking (PMHT) is based

on the calculation of the probability of each measurement belonging to each track by a Bayesian inference [33]. In PMHT, the hard decision of measurement to track is avoided by a joint estimation of the target states and measurement-to-track association probabilities [33]. A literature review of the advances in PMHT is presented in [34]. Another approach to treat multiple targets and observations is a method based on random finite set concept, named as probability hypothesis density (PHD) filter. Some of the approximations to deal with the PHD recursion are suggested, including Sequential Monte Carlo PHD (SMCPHD) filter [35], Cardinalised PHD (CPHD) filter [36] and Gaussian Mixture PHD (GMPHD) filter [37].

1.3.4 Track Management

An essential function in the application of MTT systems is the track management block. This block makes sure that only tracks of sufficient quality continue to carry over frame by frame. The track management can be divided into three main phases [1]:

1. *Track initiation*: a tentative track is initialized for measurements that are not associated with any of the existing and previously identified targets. An initialized track is named as a tentative track.
2. *Track confirmation*: if the subsequent observations indicate that the tentative track truly represents a target; the status of the track is updated from "tentative" to "confirmed". The confirmed track is reported as a real target.
3. *Track deletion*: if the tracking system no longer receives enough information to maintain the validity of a track, the track gets removed and no longer is considered.

The track management can be implemented in several ways [4, 1]. A logic-based track formation procedure follows a logic of m detections out of n frames (m/n) validation rule.

The algorithm states that if a track has been associated to a measurement in m of the last n frames, its status becomes a confirmed track, otherwise it is dropped [4].

An alternative approach of determining the quality and status of a track is based on the concept of track score [1]. A track score is conceptually a hypothesis testing with the following two hypotheses; $\mathcal{H}_0$, the track is originated from clutter, and $\mathcal{H}_1$, the track is originated from real target. The track score is a measure based on a standard detection method as sequential probability ratio test (SPRT) [38], and is calculated using the probability of each hypothesis given the information through time step k , $Z^k = z_k \cup Z^{k-1}$, as follows:

$$s(k) = \frac{P\{\mathcal{H}_1|Z^k\}}{P\{\mathcal{H}_0|Z^k\}} = \frac{p(Z^k|\mathcal{H}_1)P\{\mathcal{H}_1\}}{p(Z^k|\mathcal{H}_0)P\{\mathcal{H}_0\}} \tag{1.34}$$

where $P\{\mathcal{H}_1\}$ and $P\{\mathcal{H}_0\}$ are the prior probability of hypotheses $\mathcal{H}_1$ and $\mathcal{H}_0$, respectively. A recursive form of (1.34), with the assumption of independent measurement noise from frame to frame, is given as follows [1]:

$$s(k) = \frac{p(z_k|\mathcal{H}_1)p(Z^{k-1}|\mathcal{H}_1)P\{\mathcal{H}_1\}}{p(z_k|\mathcal{H}_0)p(Z^{k-1}|\mathcal{H}_0)P\{\mathcal{H}_0\}} = \frac{p(z_k|\mathcal{H}_1)}{p(z_k|\mathcal{H}_0)}s(k-1) \tag{1.35}$$

In application, often the logarithm of the track score, the log likelihood ratio, is used to make the score update a simple summation. As the new set of observations arrive, the track scores get updated. If a track score exceeds confirmation threshold, the corresponding track gets confirmed and is named a confirmed track. On the other hand, if a track score goes below deletion threshold, the corresponding track gets deleted. If a track score is between two thresholds, then the track remains tentative and the decision is postponed until the

arrival of sufficient information. Figure 1.5 shows the flowchart of one cycle of such track management algorithm.

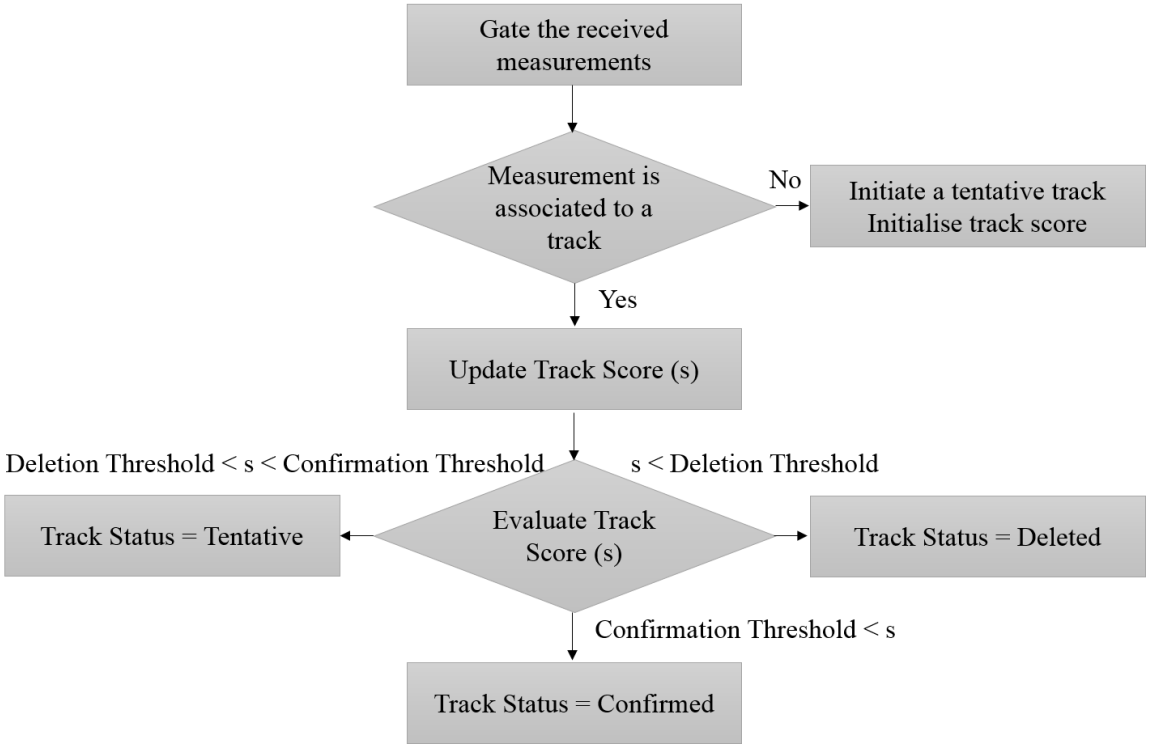

Figure 1.5 Flowchart of one cycle of track management algorithm based on track score

1.4 Overall Proposed Car Tracking System

In this section, the overall proposed car tracking system is discussed. The simulation scenarios and car motion models, experimental set-up and the application areas are included

to provide a cohesive picture of the research which is later discussed in more details in the remaining chapters.

In Figure 1.6 a schematic flowchart of overall proposed car tracking system is presented.

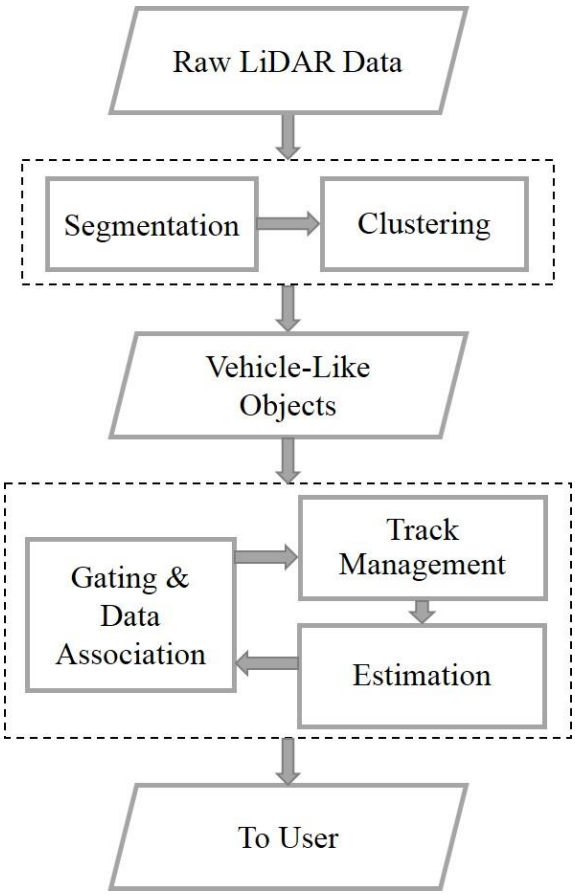

Figure 1.6 Overall proposed car tracking system

The experimental set-up of this project is a LiDAR (light detection and ranging) sensor based perception system. A Ford escape car equipped with a Velodyne HDL-32E LiDAR

sensor is used for data acquisition. The LiDAR sensor and the overall experimental set-up is shown in Figure 1.7.

Figure 1.7 LiDAR sensor and experimental set-up

The principle of operation of the HDL-32E LiDAR is as follows. The sensor creates 360° 3D images by using 32 laser/detector pairs whose housing rapidly spins to scan the surrounding environment. Table 1.1 tabulates the specification of HDL-32E LiDAR sensor [39].

Table 1.1 Velodyne HDL-32E LiDAR specifications

Specification	**Velodyne HDL-32E**
Laser	Class 1- eye safe 903 nm wavelength Time of flight distance measurement Measurement range 70 m (1m to 70m) Max Altitude of Operation 2000m
Sensor	32 laser/detector pairs +10.67 to -30.67 degree field of view (vertical) 360 degree field of view (horizontal) 10 Hz frame rate
Mechanical	Power : 12 V @ 2 Amps Operation voltage : 9-32 VDC Weight: < 2 kg Dimensions: 5.9” height × 3.36” diameter
Output	Approximately 700,000 points/second UDP packets(distance , intensity)

The LiDAR provides a 3D point cloud in each frame with a frame rate of 0.1 second. A point cloud is basically a large collection of points that are placed on a three-dimensional coordinate system with the origin at the sensor. Point cloud data provides a dense representation of the real-world context where one can re-create the referenced objects. The LiDAR 3D point cloud is processed with an algorithm of two steps: segmentation and clustering. The segmentation step tries to find the non-ground points. Once the ground points are removed, in the clustering step, the remaining non-ground points are clustered. The representative points of these vehicle-like objects, in turn, are fed into the MTT system for data association and tracking.

The gating and data association step is a crucial function of the MTT system to disregard the unlikely assignments and to deal with measurement origin uncertainty. As discussed in section 1.3.3, in the first place a validation region is constructed around the predicted

measurement of each track. This validation region is an ellipsoid that discriminates the received measurements based on their statistical distance to the predicted measurement, and in this way eliminates the unlikely measurements from the association process. Then, a measurement to track association algorithm comes to play to resolve the measurement origin uncertainty issue. In the proposed methods of this dissertation, the probabilistic data association (PDA) based methods are used for such task.

In the initial design phases, the SVSF estimation method is generalized and modified. The generalized SVSF is then used as the basis for the further development of the proposed MTT system. The SVSF-based PDA, JPDA and IMM-PDA are used to deal with single, multiple and maneuvering target tracking in clutter, respectively. Also, the chattering information of the SVSF estimation method is employed as an extra source of information to resolve the measurement origin uncertainty in a more efficient manner.

Finally, a track maintenance algorithm is designed to take care of the track initiation and confirmation for new targets entering the field of view of the sensor and track deletion for the existing targets that exit the field of view of the sensor. As discussed in section 1.3.4, the implemented track management system in the proposed car tracking system of this thesis is based on the track score measure.

1.4.1 Simulation Scenarios

Various driving patterns of a vehicle on a road, as depicted in Figure 1.8, include straight line and curve, cut-in-out, U-turn and interchange [40].

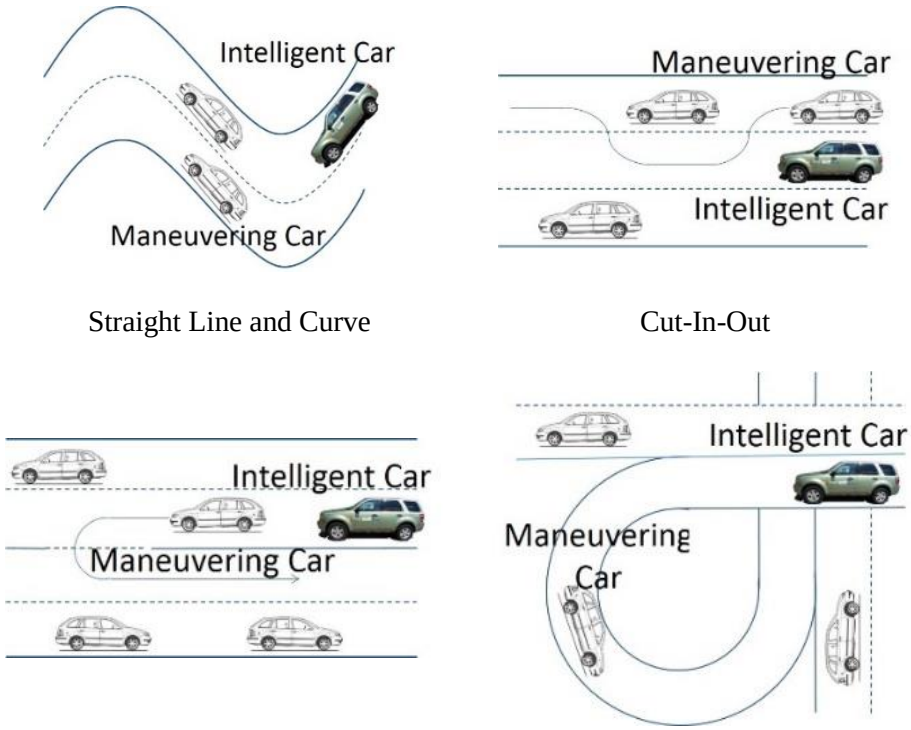

Figure 1.8 Various driving patterns of a vehicle [40]

The driving patterns of Figure 1.8 are simulated using the two models: near constant velocity model and near constant speed turn model as presented below:

The *near constant velocity model* [6, 40] describes the uniform motion and captures constant velocity motions with possible accelerations. There are four states, related to the target position and velocity defined as $x = [\xi\ \eta\ \dot{\xi}\ \dot{\eta}]'$. Note that ξ and η are the position in two Cartesian directions, and $\dot{\xi}$ and $\dot{\eta}$ are the corresponding velocities. This model assumes that the accelerations of the target between two sequential samples are constant and are drawn from a discrete-time zero mean white Gaussian noise. The motion model is defined as follows:

$$x(k+1) = Ax(k) + Bv(k) \tag{1.36}$$

where the system and process noise gain matrices are defined by:

$$A = \begin{bmatrix} 1 & 0 & T_s & 0 \\ 0 & 1 & 0 & T_s \\ 0 & 0 & 1 & 0 \\ 0 & 0 & 0 & 1 \end{bmatrix} \quad , \quad B = \begin{bmatrix} T_s^2/2 & 0 \\ 0 & T_s^2/2 \\ T_s & 0 \\ 0 & T_s \end{bmatrix} \tag{1.37}$$

The white acceleration noise is defined as follows:

$$Q = cov\{v(k)\} = \begin{bmatrix} \sigma_v^2 & 0 \\ 0 & \sigma_v^2 \end{bmatrix} \tag{1.38}$$

The *near constant speed turn model* [6, 40] describes maneuvering car moving at a constant turn rate. The state vector is $x = [\xi\ \eta\ \dot{\xi}\ \dot{\eta}\ \omega]$. Note that ξ and η are the position in two Cartesian directions, and $\dot{\xi}$ and $\dot{\eta}$ are the corresponding velocities and, ω is the angular velocity. The motion model is defined as follows:

$$x(k+1) = Ax(k) + Bv(k) \tag{1.39}$$

where the system and process noise gain matrices are defined by:

$$A = \begin{bmatrix} 1 & 0 & \frac{\sin \omega_k T_s}{\omega_k} & -\frac{1-\cos \omega_k T_s}{\omega_k} & 0 \\ 0 & 1 & \frac{1-\cos \omega_k T_s}{\omega_k} & \frac{\sin \omega_k T_s}{\omega_k} & 0 \\ 0 & 0 & \cos \omega_k T_s & -\sin \omega_k T_s & 0 \\ 0 & 0 & \sin \omega_k T_s & \cos \omega_k T_s & 0 \\ 0 & 0 & 0 & 0 & 1 \end{bmatrix} \quad B = \begin{bmatrix} T_s^2/2 & 0 & 0 \\ 0 & T_s^2/2 & 0 \\ T_s & 0 & 0 \\ 0 & T_s & 0 \\ 0 & 0 & T_s \end{bmatrix} \tag{1.40}$$

The remaining equations are the same as the near constant velocity model.

Different maneuvering and non-maneuvering car simulation scenarios are designed as a combination of different driving patterns.

1.4.2 Application Areas

In the early dawn of multiple target tracking systems, the driving motivation was its military applications, such as estimating the position and velocity of airborne vehicles using ground-based remote sensing. As the scope of research evolved, the developed tools for the original application were applied to several other domains including sonar image processing in unmanned underwater vehicles [41], video image processing [42], medical imaging [43], biomedicine [44], finance [45], automotive safety systems [46, 47], and autonomous or driverless cars [48, 49].

In the automotive sector, car safety systems are divided in two general groups: protective or passive safety systems and preventive or active safety systems. The preventive safety systems are designed to passively protect the car occupants in the case of a crash. These systems are the components of the vehicle such as airbags, seatbelts and the physical structure of the vehicle that are constructed to absorb energy or to hold the driver firmly during the accident.

The preventive safety systems help the driver to avoid an accident by using in-vehicle systems, taking the status of the driver into account. The preventive safety systems, will take the following actions, depending on the significance and timing of the situation:

- inform the driver of the threat as soon as possible;
- warn the driver in the case of no reaction to the information; and
- actively assist or intervene to avoid or mitigate the likely accident.

The preventive safety systems may also assist the driver through the following functions:

- maintain a safe speed keeping a reasonable distance from other vehicles;
- maintain driving within the lanes;
- avoid critical or dangerous overtaking;
- assist the driver to safely pass through intersections; and
- prevent accidents with vulnerable other road users.

In general, preventive safety systems aim to improve the safety of driving by the use of information from the vehicle, surrounding environment, communications and positioning systems. Some of the current preventive safety systems are as follows: forward collision, collision avoidance by breaking, adaptive cruise control, and lane departure warning.

Furthermore, the new generation of automotive safety systems include integrated safety systems that combine the functionalities of passive and active systems. The perceived information from active safety systems is used to improve the protective safety systems. Such improvements may include better positioning of the occupants' seat, pre-tightening of the seat belt, or pre-firing the air bag system.

Several active safety systems use MTT algorithms to assess the situation including the own-vehicle, obstacles, other vehicles on the road, pedestrians, lane markings, curbs, etc. The MTT system is considered to be an efficient solution to provide sufficient awareness of the surrounding environment and desired detection and tracking capabilities. In such intelligent vehicles, the MTT algorithms are designed to resolve the issues related to missing marking line, ambiguity identification, road curvatures and texture changes, variations in lane width, shadows, occluded cars, daylight condition variations and false alarms.

Besides intelligent vehicles equipped with active safety systems, self-deriving or semi-autonomous cars are other application areas that use MTT systems. Statistical data show human error is a major cause in fatal car accidents. A tremendous amount of research has been devoted to make cars safer by using active and passive safety systems. However, the tendency of human beings to make mistakes has been a serious motivation for researchers to try to realize and implement autonomous systems that remove the human element from the car operation. Self-driving cars are being developed by large corporations despite their legal complications. The proposed algorithms will serve the technological evolution taking place towards autonomous vehicles.

Chapter 2

Target Tracking Formulation of the SVSF

2.1 Target Tracking Formulation of the SVSF with PDA (Conference paper *a*)

2.1.1 Abstract

Target tracking algorithms are important for a number of applications, including: physics, air traffic control, ground vehicle monitoring, and processing medical images. The probabilistic data association algorithm, in conjunction with the Kalman filter (KF), is one of the most popular and well-studied strategies. The relatively new smooth variable structure filter (SVSF) offers a robust and stable estimation strategy under the presence of modeling errors, unlike the KF method. The purpose of this paper is to introduce and formulate the SVSF-PDA, which can be used for target tracking. A simple example is used to compare the estimation results of the popular KF-PDA with the new SVSF-PDA.

2.1.2 Introduction

Target tracking algorithms make a fundamental element of surveillance and monitoring systems. These algorithms are used to interpret the environment by analyzing sensor information and partitioning it into tracks based on their origin, in an effort to estimate

quantities of interest [1, 30]. There are numerous applications for target tracking algorithms, including: physics, air traffic control (ATC), ground vehicle monitoring, and data processing for medical images [1]. Recent applications of target tracking algorithms include the automotive industry. These applications include law enforcement systems and vehicle safety systems [3, 2].

The essential issue in multi-target tracking (MTT) systems is dealing with data association uncertainty that occurs when the sensor provides measurements whose origin is uncertain and complex. Data association logics are required to differentiate received sensor data into different categories including targets of interest, background clutter, and false alarms [5]. There are several methods proposed to solve data association problems. A comprehensive survey of the methods is provided in [1] and [30]. In one classification [1], there are two types of data association methods: nearest neighbour association, and all-neighbour's association. The former involves associating the measurement nearest to the predicted measurement of each track. In the latter, one may use all validated measurements for data association.

In the standard nearest neighbour method, the statistical distance is used to predict and associated measurements of each track [4]. However, due to some flaws in this method, the global nearest neighbour method was proposed which takes all of the possible measurement-to-track associations and generates the most probable assignment hypothesis [1]. The probabilistic data association (PDA) method is a type of 'all-neighbour' data association method. It calculates the association probabilities for each probable association hypothesis, and utilizes them to form a combined innovation used for filtering [29]. PDA was originally formulated for single target tracking. An extension of it for multiple targets was named joint probabilistic data association (JPDA), in which the association probabilities are calculated in a combined manner across the targets in a cluster [31].

In the aforementioned methods, the basic filtering algorithm employed is based on the popular Kalman filter (KF). The KF was introduced in the 1960s and remains one of the most popular estimation methods because it yields a statistically optimal solution for linear systems and measurements [7, 8]. A number of extensions were created to formulate the KF for nonlinear systems and to tackle issues with modeling uncertainty and instability [50, 11]. In 2007, the smooth variable structure filter (SVSF) was proposed [15]. It is a recursive predictor-corrector filter based on the sliding mode concept [17]. In the SVSF, a hyper-plane was introduced which is a projection of the true state trajectory, and a corrective gain is applied to force the estimated states to go towards the desired hyper-plane. Once it reaches within a region of the hyper-plane referred to as the existence subspace, the estimated states are forced to remain within this subspace by going back and forth across the hyper-plane or desired state trajectory [15]. Significant features of the SVSF are its robustness, multiple indicators of performance (innovation vector and indicators that quantify the degree of uncertainty and modeling error specific to each state), and the ability to identify the source of uncertainty [15].

This paper introduces the SVSF in a formulation that can be used for target tracking, making use of the probabilistic data association (PDA) technique. The paper is organized as follows. Section 0 provides a brief overview of the KF and SVSF equations. The main PDA algorithm is highlighted in Section 2.1.4. Section 2.1.5 introduces the SVSF-PDA estimation strategy. A simple target tracking example is studied in section 2.1.62.1.7, and the results of the KF-PDA are compared with the SVSF-PDA. The main findings are summarized in the section 2.1.7. Also, the following is a list of the main nomenclature used throughout the paper.

Table 2.1 List of Important Nomenclature and Parameters

Parameter	Definition
$\boldsymbol{x}$	State vector or values
$\boldsymbol{z}$	Measurement (system output) vector or values
$\boldsymbol{w}$	System noise vector
$\boldsymbol{v}$	Measurement noise vector
$\boldsymbol{A}$	Linear system transition matrix
$\boldsymbol{B}$	Linear input gain matrix
$\boldsymbol{C}$	Linear measurement (output) matrix
$\boldsymbol{E}$	SVSF error vector (or matrix)
$\boldsymbol{K}$	Filter gain matrix
$\boldsymbol{P}$	State error covariance matrix
$\boldsymbol{Q}$	System noise covariance matrix
$\boldsymbol{R}$	Measurement noise covariance matrix
$\boldsymbol{S}$	Innovation (measurement error) covariance matrix
$\boldsymbol{e_z}$	Measurement (output) error vector
$\boldsymbol{\gamma}$	SVSF 'memory' or convergence rate
$\boldsymbol{\psi}$	SVSF smoothing boundary layer
$\boldsymbol{diag[a]}$ **or** $\boldsymbol{\bar{a}}$	Diagonal of some vector or matrix a
$\boldsymbol{sat}()$	Saturation function
$\boldsymbol{\lvert a \rvert}$	Absolute value of a
$\boldsymbol{T}$	Transpose of a vector (if superscript) or sample rate
$+$	Pseudoinverse of some non-square matrix
$\circ$	Denotes a Schur product (element-by-element multiplication)
$\sim$	Denotes error or difference
^	Estimated vector or values
$\boldsymbol{k+1\lvert k}$ or $\boldsymbol{k\lvert k-1}$	A priori values
$\boldsymbol{k+1\lvert k+1}$ or $\boldsymbol{k\lvert k}$	A posteriori values

2.1.3 Estimation Strategies

A. Kalman Filter

As described in [17], the success of the KF comes from the optimality of the Kalman gain in minimizing the trace of the a posteriori state error covariance matrix [51, 17]. The following five equations form the core of the KF algorithm, and are used in an iterative fashion. Equations (2.1.1) and (2.1.2) define the a priori state estimate $\hat{x}_{k+1|k}$ based on knowledge of the system A, the previous state estimate $\hat{x}_{k|k}$, the input matrix B, and the input u_k, and the corresponding state error covariance matrix $P_{k+1|k}$, respectively.

$$\hat{x}_{k+1|k} = A\hat{x}_{k|k} + Bu_k \tag{2.1}$$

$$\hat{x}_{k+1|k} = A\hat{x}_{k|k} + Bu_k \tag{2.2}$$

$$P_{k+1|k} = AP_{k|k}A^T + Q_k \tag{2.3}$$

The Kalman gain K_{k+1} is defined by (2.4), and is used to update the state estimate $\hat{x}_{k+1|k+1}$ and the a posteriori state error covariance $P_{k+1|k+1}$.

$$K_{k+1} = P_{k+1|k}C^T\left[CP_{k+1|k}C^T + R_{k+1}\right]^{-1} \tag{2.4}$$

$$\hat{x}_{k+1|k+1} = \hat{x}_{k+1|k} + K_{k+1}\left[z_{k+1} - C\hat{x}_{k+1|k}\right] \tag{2.5}$$

$$P_{k+1|k+1} = [I - K_{k+1}C]P_{k+1|k} \tag{2.6}$$

Note that the KF, in the above form, may be only applied on linear systems and measurements. The most popular and simplest method used to formulate the KF for nonlinear functions is the extended Kalman filter (EKF) [11, 10]. The EKF is conceptually similar to the KF; however, the nonlinear system is linearized according to its Jacobian.

This linearization process introduces uncertainties that can sometimes cause instability [10].

B. Smooth Variable Structure Filter

The smooth variable structure filter (SVSF) is based on the sliding mode concept, formulated in a predictor-corrector fashion. The SVSF estimation strategy is illustrated in Fig. 1. Essentially, a switching gain is utilized which forces the estimates to within a region of the true state trajectory. As previously described, this region is referred to as the existence subspace and is a function of modeling uncertainties and unwanted noise.

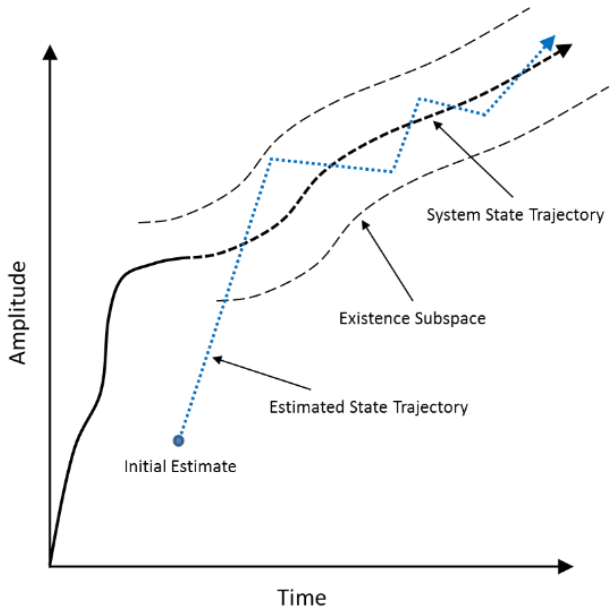

Figure 2.1 SVSF estimation concept [17]

The SVSF estimation method is described by the following series of equations. Note that this formulation includes state error covariance equations as presented in [52], which was

not originally presented in the standard SVSF form [15]. The prediction stage is similar to the KF stage, and is defined by the following equations.

$$\hat{x}_{k+1|k} = A\hat{x}_{k|k} + Bu_k \tag{2.7}$$

$$P_{k+1|k} = AP_{k|k}A^T + Q_k \tag{2.8}$$

$$e_{z,k+1|k} = z_{k+1} - C\hat{x}_{k+1|k} \tag{2.9}$$

The SVSF gain is calculated as follows [17]:

$$K_{k+1} = C^{+} diag\left[\left(\left|e_{z,k+1|k}\right|_{Abs} + \gamma\left|e_{z,k|k}\right|_{Abs}\right) sign\left(\frac{e_{z,k+1|k}}{\psi_i}\right)\right]\left[diag\left(e_{z,k+1|k}\right)\right]^{-1} \tag{2.10}$$

As described in [17], the SVSF gain is a function of: the a priori and a posteriori measurement error vectors $e_{z,k+1|k}$ and $e_{z,k|k}$; the smoothing boundary layer widths ψ_i where i refers to the i^{th} width; the 'SVSF' memory or convergence rate γ with elements $0 < \gamma_{ii} \leq 1$; and the linear measurement matrix C. However, for numerical stability, it is important to ensure that one does not divide by zero in (2.10). This can be accomplished using a simple if statement with a very small threshold (i.e. 1×10^{-12}).

The remaining equations update the SVSF estimate $\hat{x}_{k+1|k+1}$ and the state error covariance matrix $P_{k+1|k+1}$, as well as the a posteriori measurement error $e_{z,k+1|k+1}$ which is used in the next time step.

$$\hat{x}_{k+1|k+1} = \hat{x}_{k+1|k} + K_{k+1}e_{z,k+1|k} \tag{2.11}$$

$$P_{k+1|k+1} = (I - K_{k+1}C)P_{k+1|k}(I - K_{k+1}C)^T + K_{k+1}R_{k+1}K_{k+1}^T \tag{2.12}$$

$$e_{z,k+1|k+1} = z_{k+1} - C\hat{x}_{k+1|k+1} \tag{2.13}$$

Equations (2.7) through (2.13) summarize the SVSF estimation process.

2.1.4 Data Association Principles

PDAF is an algorithm which is basically formulated for tracking single target in clutter. The track is assumed to be initialized and the density of state vector conditioned on the past measurements is approximated by a normal distribution as follows [5]:

$$p[x(k)|Z^{k-1}] = \mathcal{N}[x(k); \hat{x}(k|k-1), P(k|k-1)] \tag{2.14}$$

The algorithm provides some validated measurements around the predicted measurement of the track. The n_m candidate measurements at time k are named as $z^j, j = 1, \dots, n_m$. Thus, the total available validated measurements at time k are $Z^k = \{z^1, \dots, z^{n_m}\} \cup Z^{k-1}$. Also, it is assumed that when the corresponding measurement of the detected target is within the validation gate, then, only one of the validated measurements is originated from the target [5]. The remaining non-target originated measurements are considered as clutter originated or false alarms. The number of such measurements points is assumed to have a Poisson distribution (with spatial density of λ) and the spatial distribution of them is modeled as i.i.d. uniform.

Suppose that there are $n_m(k)$ validated measurements in time step k, then, one can describe $n_m(k) + 1$ distinct events (association hypotheses) as [1]:

$$\mathcal{H}_i(k) = \{z^i \; is \; target \; originated\} \tag{2.15}$$

$$\mathcal{H}_0(k) = \{none \; are \; target \; originated\} \tag{2.16}$$

where $i = 1, \dots, n_m(k)$, then the minimum variance estimate can be written as follows:

$$\begin{aligned} \hat{x}(k|k) = \mathbb{E}\{x(k)|Z^k\} &= \sum_{i=0}^{n_m(k)} \mathbb{E}\{x(k)|\mathcal{H}_i(k), Z^k\} P\{\mathcal{H}_i|Z^k\} \\ &= \sum_{i=0}^{n_m(k)} \hat{x}_i(k|k)\beta_i(k) \end{aligned} \tag{2.17}$$

where $\hat{x}_i(k|k)$ is the updated state given that the ith hypothesis is correct and $\beta_i(k)$ is named association probability which is the conditioned probability of the ith hypothesis. Using the calculations provided in [5] and [4], these association probabilities are computed as follows:

$$\beta_i(\mathrm{k}) = \begin{cases} \dfrac{1 - \mathrm{P_D P_G}}{1 - \mathrm{P_D P_G} + \sum_{\mathrm{i=1}}^{\mathrm{n_m(k)}} \mathcal{L}_\mathrm{i}(\mathrm{k})}, & \mathrm{i} = 0 \\ \dfrac{\mathcal{L}_\mathrm{i}(\mathrm{k})}{1 - \mathrm{P_D P_G} + \sum_{\mathrm{i=1}}^{\mathrm{n_m(k)}} \mathcal{L}_\mathrm{i}(\mathrm{k})}, & \mathrm{i} = 1, \dots, \mathrm{n_m(k)} \end{cases} \tag{2.18}$$

where $i = 0$ is association probability of the hypothesis when none of the validated measurements is originated from the target, P_G is gate probability [4], P_D is the target detection probability and also,

$$\mathcal{L}_i(k) = \frac{\mathcal{N}[z_i(k); \hat{z}(k|k-1), S(k)] P_D}{\lambda} \tag{2.19}$$

which is the likelihood ratio of the measurement $z_i(k)$, if it is originated from the target. After calculation of the association probabilities, the combined innovation to be used in the Kalman filter update is calculated as a weighted sum of $n_m(k)$ validated measurements:

$$\tilde{z}(k) = \sum_{i=1}^{n_m(k)} \beta_i(k)\tilde{z}_i(k) \tag{2.20}$$

where $\tilde{z}_i(k) = z_i(k) - Cx(k|k)$ [30]. Then, the states are estimated as the same procedure in standard Kalman filter. The updated covariance is calculated as follows:

$$P(k|k) = \beta_0(k)P(k|k-1) + [1-\beta_0(k)]P^*(k|k) + \tilde{P}(k) \tag{2.21}$$

Note that $P^*(k|k)$ is the standard KF covariance matrix and $\tilde{P}(k)$ is an increment as an effect of uncertain associations and is computed by [29]:

$$\tilde{P}(k) = K(k)[\sum_{i=1}^{n_m(k)} \beta_i(k)\tilde{z}_i(k)\tilde{z}_i(k)' - \tilde{z}(k)\tilde{z}(k)']K(k) \tag{2.22}$$

2.1.5 Formulation of the SVSF-PDA

In this section, a novel formulation of the SVSF based on the PDA method is introduced, referred to as the SVSF-PDA. Using the notation of previous section and the algorithm provided in [17], the proposed algorithm consists of the following steps.

A. Gating Step

The received measurements are validated based on the assumption made earlier. The validation region is an elliptical region defined for stochastic distance to the predicted measurements as follows [5]:

$$\mathcal{V}(k,\gamma) = \{z: [z-\hat{z}(k|k-1)]'S(k)^{-1}[z-\hat{z}(k|k-1)] \leq \gamma\} \tag{2.23}$$

where γ is the gate threshold corresponding to the gate probability with which the actual measurement lies within the gate (if detected), and $S(k)$ is the covariance of the innovation corresponding to the actual measurement.

B. Prediction Step

In this step, the state estimates and measurements are predicted using motion and measurement models, and then the a priori state error covariance is calculated.

$$\hat{x}(k|k-1) = A(k-1)\hat{x}(k-1|k-1) \tag{2.24}$$

$$P(k|k-1) = A(k-1)P(k-1|k-1)A(k-1)' + Q(k-1) \tag{2.25}$$

$$z(k|k-1) = C(k-1)\hat{x}(k|k-1) \tag{2.26}$$

The association probabilities and the combined innovation are calculated using (2.18) and (2.20), respectively. The a priori measurement error is calculated to be equal to the combined innovation:

$$e_z(k|k-1) = \tilde{z}(k) \tag{2.27}$$

C. State Update Step

For state estimation, the SVSF correction gain is calculated and the states are updated.

$$\hat{x}(k|k-1) = A(k-1)\hat{x}(k-1|k-1) \tag{2.28}$$

$$\hat{x}(k|k) = \hat{x}(k|k-1) + K(k)e_z(k|k-1) \tag{2.29}$$

$$K(k) = C^{+} diag[(|e_z(k|k-1)|_{Abs} + \gamma |e_z(k-1|k-1)|_{Abs}) \circ sat\left(\frac{e_z(k|k-1)}{\psi}\right)][diag(e_z(k|k-1))]^{-1} \quad (2.30)$$

The covariance associated with the updated states is then calculated by (2.21). Note that $P^*(k|k)$ is the SVSF covariance matrix, and is computed by:

$$P^*(k|k) = [I - K(k)C(k)]P(k|k-1)[I - K(k)C(k)]' + K(k)R(k)K'(k) \quad (2.31)$$

Furthermore, $\tilde{P}(k)$ is calculated by (2.22). To obtain the a posteriori measurement error, the actual measurement is required. It is assumed that the combined innovation is the difference between the actual and the predicted measurements:

$$z^a(k) = e_z(k|k-1) + C(k)\hat{x}(k|k-1) \quad (2.32)$$

$$e_z(k|k) = z^a(k) - C(k)\hat{x}(k|k) \quad (2.33)$$

Substitution of (2.32) into (2.33), and using (2.29), yields a posteriori measurement error as:

$$e_z(k|k) = [I - C(k)K(k)]e_z(k|k-1) \quad (2.34)$$

2.1.6 Estimation Problem and Results

A. Problem Setup

In this section, the estimation problem is described. A simple two-dimensional discrete, constant velocity model is implemented [6]. There are four states, related to the target position and velocity (x and y directions), defined as follows: $x = [\xi\ \eta\ \dot{\xi}\ \dot{\eta}]$. Note that ξ and η are the position in two Cartesian directions, and $\dot{\xi}$ and $\dot{\eta}$ are the corresponding

velocities. This model assumes that the accelerations of the target between two sequential samples are constant and are drawn from a discrete-time zero mean white Gaussian noise. The motion model is defined as follows:

$$x(k+1) = Ax(k) + Bv(k) \tag{2.35}$$

where the system and process noise gain matrices are defined by:

$$A = \begin{bmatrix} 1 & 0 & T_s & 0 \\ 0 & 1 & 0 & T_s \\ 0 & 0 & 1 & 0 \\ 0 & 0 & 0 & 1 \end{bmatrix} \tag{2.36}$$

$$B = \begin{bmatrix} T_s^2/2 & 0 \\ 0 & T_s^2/2 \\ T_s & 0 \\ 0 & T_s \end{bmatrix} \tag{2.37}$$

The white acceleration noise is defined as follows:

$$Q = cov\{v(k)\} = \begin{bmatrix} \sigma_v^2 & 0 \\ 0 & \sigma_v^2 \end{bmatrix} \tag{2.38}$$

The measurement function, matrix, and noise covariance are defined respectively as follows:

$$z(k) = Cx(k) + w(k) \tag{2.39}$$

$$C = \begin{bmatrix} 1 & 0 & 0 & 0 \\ 0 & 0 & 1 & 0 \end{bmatrix} \tag{2.40}$$

$$R = cov\{w(k)\} = \begin{bmatrix} \sigma_w^2 & 0 \\ 0 & \sigma_w^2 \end{bmatrix} \tag{2.41}$$

B. Estimation Results

Simulations are run for the KF-PDA and SVSF-PDA algorithms. The parameter values used for the simulations are $T_s = 30\ s$ and $P_D = 0.9$. The clutter is assumed to have a spatial uniform distribution, and the number of cluttered measurements is generated by a Poisson's distribution of $\lambda = 10^{-6}$. The process noise variance is $\sigma_v^2 = 0.01^2$, and the measurement noise variance is $\sigma_w^2 = 7^2$.

The following figure illustrates the simulation results for both the KF-PDA and SVSF-PDA strategies. Both filters are able to successfully track the actual path of the target.

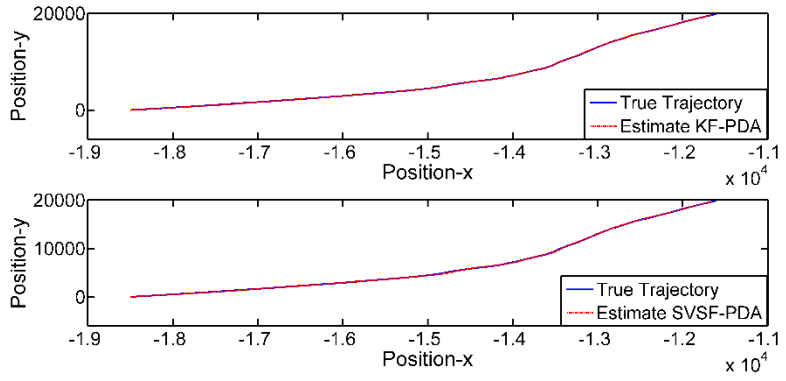

Figure 2.2 PDA-KF and PDA-SVSF estimation results (normal case)

The RMSE errors for the four states of the system are computed and shown in the following table. Note that the SVSF-PDA strategy performed slightly better than the KF-PDA, in terms of RMSE.

Table 2.2 RMSE Estimation Results – Normal Case

Filter	**KF-PDA**	**SVSF-PDA**
ξ	92.4	64.5
$\dot{\xi}$	0.81	0.48
η	210.8	198.5
$\dot{\eta}$	0.83	0.57

To further investigate the robustness of the proposed SVSF-PDA strategy, modeling uncertainty is injected roughly 25% of the way into the simulation in the form of 2% change in the system matrix for 5 iterations. The results are shown in the following figure.

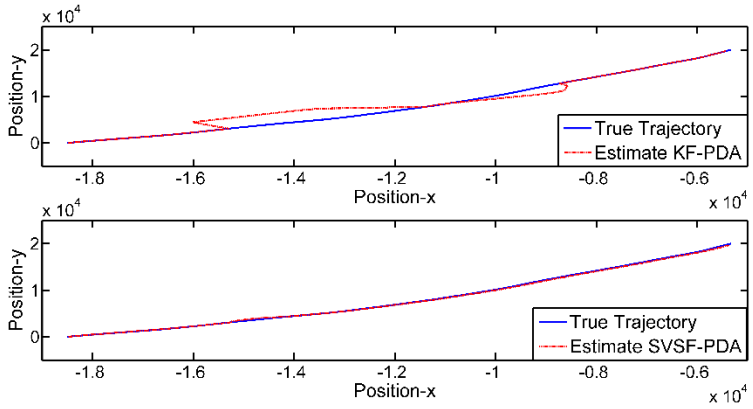

Figure 2.3 KF-PDA and SVSF-PDA estimation results (uncertainty)

The RMSE under this scenario was recalculated, and is shown in the following table.

Table 2.3 RMSE Estimation Results – Uncertainty Case

Filter	KF-PDA	SVSF-PDA
ξ	721.7	125.1
η	284.3	207.3

Note that the SVSF-PDA provided a more stable estimate, as the results did not diverge from the true state trajectory. Furthermore, the x-position RMSE was reduced by about

82%, and the y-position RMSE was reduced by about 28%. This is a significant improvement for target tracking applications. As shown next, further increasing the modeling uncertainty causes the KF-PDA strategy to fail.

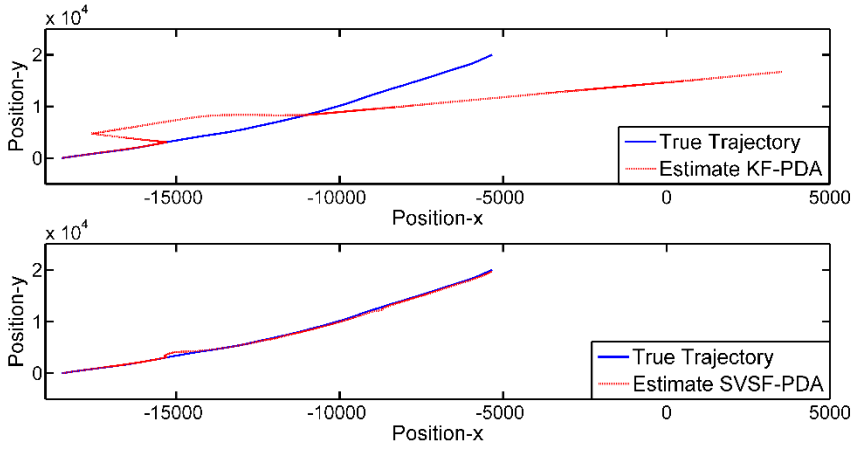

Figure 2.4 KF-PDA and SVSF-PDA results (increased uncertainty).

As shown in the above figure, when the modeling uncertainty was increased further to 4%, the KF-PDA failed to obtain the correct target track. However, due to the unique switching action of the SVSF, the SVSF-PDA method maintained the correct track and was able to provide a good estimate.

2.1.7 Conclusion

The purpose of this paper was to introduce a new target tracking strategy referred to as the SVSF-PDA. A simple target tracking simulation was studied in an effort to compare the popular KF-PDA with the SVSF-PDA. Under normal conditions, both methods were able to provide good target tracking estimates. However, when modeling uncertainty was injected into the simulation, the KF-PDA failed to yield a good target track of the estimate.

Future research will study multi-target tracking scenarios, by implementing the joint probabilistic data association (JPDA) technique.

2.2 Multi-Target Tracking Formulation of the SVSF with JPDA (Conference paper *b*)

2.2.1 Abstract

Target tracking scenarios offer an interesting challenge for state and parameter estimation techniques. This paper studies a situation with multiple targets in the presence of clutter. In this paper, the relatively new smooth variable structure filter (SVSF) is combined with the joint probability data association (JPDA) technique. This new method, referred to as the JPDA-SVSF, is applied on a simple multi-target tracking problem for a proof of concept. The results are compared with the popular Kalman filter (KF).

2.2.2 Introduction

The purpose of multiple target tracking is to maintain true tracks using noisy measurements originated from true targets or the clutter. This environment interpretation has many applications in air traffic control, road vehicle tracking, medical image processing, and biology [1]. A recently investigated area of application for target tracking methods is in automotive industries. The ever increasing interest in intelligent vehicles broadens the use and development of multiple-target tracking algorithms in active automotive safety systems and advanced driver assistance system.

In the situations where the tracking is handled in the presence of measurement origin uncertainty, one of the fundamental parts of target tracking methods is the data association algorithm, which differentiates the received measurements and categorizes them into target-originated and clutter-originated [5]. A comprehensive survey of several data association methods can be found in [1] and [30].

Probabilistic data association (PDA) is a widely used data association and tracking method [29, 4]. PDA is a type of 'all- neighbour' data association methods, which assumes several feasible hypotheses for the measurement to track associations and then calculates the association probabilities for each of them [5]. However, PDA is a formulization for tracking single target in clutter and to use it for multiple targets, simply multiple copies of a similar filter are employed [5]. Moreover, PDA is derived with assumption that the tracks are initialized and, consequently, there should be some other algorithms taking care of track initiation [1]. In [28] integrated probabilistic data association (IPDA) is proposed, which is basically a re-derivation of PDA without the assumption of initialized tracks and therefore, provides both the data association and track existence probabilities. An extension of PDA for multi-target tracking, where the targets are interfering, is the joint probabilistic data association (JPDA) [31]. In JPDA, the targets are clustered and then the association probabilities are calculated in a jointly manner across the targets in a cluster [4, 31]. A similar extension of IPDA for multiple targets, named joint integrated probabilistic data association (JIPDA), is suggested in [53].

The aforementioned association methods provide an association probability for each feasible hypothesis which is used to construct a combined innovation term. The combined innovation term substitutes the innovation term in Kalman filtering structure of these algorithms [4].

Kalman filter (KF) is the most well-known filtering strategy because of its optimal estimation properties for linear systems [7, 8]. Since its introduction in the 1960's, there were some modifications to extent the formulation of KF for nonlinear systems and to cope with the issues of uncertainty and instability [50, 11]. In 2007, a recursive predictor-corrector filtering strategy based on the sliding mode concept [17], named smooth variable structure filter (SVSF) was proposed [15]. Basically, the SVSF owes its stability to selecting a corrective gain in a way that in each step decreases the error in the estimated states [15]. In order to achieve this, a hyper-plane as a projection of true state trajectory is introduced and applying the corrective gain, the estimations are forced to go toward this region, and then remain in between [15]. The main characteristic of SVSF, which suggests it as a useful filter in systems with modeling uncertainty, is its robustness against this type of uncertainties [15].

Employing SVSF as the filtering strategy in target tracking algorithms is firstly proposed in [54] for single target tracking in clutter. This paper is an extension of that work for multiple targets in combination with JPDA algorithm.

In section 2.2.3, KF and SVSF filtering algorithms are briefly overviewed. The basic formulation of JPDA algorithm is provided in section 2.2.4. Section 2.2.5 introduces the JPDA-SVSF tracking algorithm. In section 2.1.6 a simple multiple-target tracking example is studied to get a comparison between JPDA-KF and JPDA-SVSF. The paper is concluded in section 2.2.7.

2.2.3 Estimation Strategies

The Kalman filter is the best estimator in MMSE sense [6]. Indeed, KF minimizes the trace of state covariance matrix [51, 17]. In its original form, KF is based on two models: system

model (2.42) which describes the evolution of the states, and measurement model (2.43) which relates the measurements to states.

$$x(k+1) = Ax(k) + Bu(k) + v(k) \tag{2.42}$$

$$z(k) = Cx(k) + w(k) \tag{2.43}$$

where $v(k)$ and $w(k)$ are respectively zero mean white Gaussian process and measurement noises with covariance matrices $Q(k)$ and $R(k)$. The KF algorithm is based on recursive prediction and updating the estimated states and their corresponding error covariance. The prediction consists of the following steps:

$$\hat{x}(k+1|k) = A\hat{x}(k|k) + Bu(k) \tag{2.44}$$

$$P(k+1|k) = AP(k|k)A^T + Q(k) \tag{2.45}$$

The Kalman gain $K(k+1)$ is calculated and then used to obtain the updated states and covariance, as follows:

$$K(k+1) = P(k+1|k)C^T[CP(k+1|k)C^T + R(k+1)]^{-1} \tag{2.46}$$

$$\hat{x}(k+1|k+1) = \hat{x}(k+1|k) + K(k+1)[z(k+1) - C\hat{x}(k+1|k)] \tag{2.47}$$

$$P(k+1|k+1) = [I - K(k+1)C]P(k+1|k) \tag{2.48}$$

The Kalman filter in the above form is only applicable on linear systems. A very popular extension of KF for nonlinear systems is Extended KF, which linearizes the nonlinear function using the Jacobian matrix and then uses the same algorithm as KF [11, 10].

The smooth variable structure filter (SVSF) is a relatively new state and parameter estimation technique based on sliding mode concepts [17]. The basic concept is shown in the following figure.

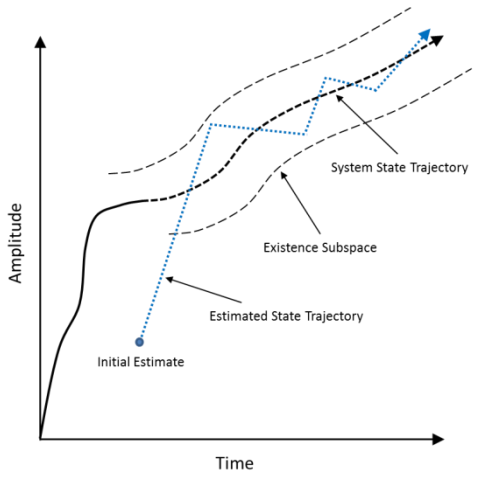

Figure 2.5 SVSF estimation concept [17].

The prediction stage of the SVSF is similar to the KF, and may be summarized by the following sets of equations:

$$\hat{x}(k+1|k) = A\hat{x}(k|k) + Bu(k) \tag{2.49}$$

$$P(k+1|k) = AP(k|k)A^T + Q(k) \tag{2.50}$$

Note that the SVSF may also be formulated to handle nonlinear system and measurement functions [17]. The a priori or predicted measurement error is also calculated as follows:

$$e_z(k+1|k) = z(k+1) - \hat{z}(k+1|k) \tag{2.51}$$

The SVSF gain is calculated as follows [17]:

$$K_{SVSF} = C^{+} diag\left[(|e_z(k+1|k)|_{Abs} + \gamma|e_z(k|k)|_{Abs}) \circ sat\left(\frac{e_z(k+1|k)}{\psi_i}\right)\right]\left[diag\left(e_z(k+1|k)\right)\right]^{-1} \quad (2.52)$$

As described in [17], the SVSF gain is a function of: the a priori and a posteriori measurement error vectors $e_{z,k+1|k}$ and $e_{z,k|k}$; the smoothing boundary layer widths ψ_i where i refers to the i^{th} width; the 'SVSF' memory or convergence rate γ with elements $0 < \gamma_{ii} \leq 1$; and the linear measurement matrix C. However, for numerical stability, it is important to ensure that one does not divide by zero in (2.52). This can be accomplished using a simple if statement with a very small threshold (i.e. 1×10^{-12}) [17].

The SVSF update equations are also very similar to the KF, and may be defined as follows:

$$\hat{x}(k+1|k+1) = \hat{x}(k+1|k) + K_{SVSF} e_z(k+1|k) \quad (2.53)$$

$$P(k+1|k+1) = [I - K(k+1)C]P(k+1|k) \quad (2.54)$$

However, note that the a posteriori or updated measurement error needs to be calculated as per (2.55). This value is used in the next time step.

$$e_z(k+1|k+1) = z(k+1) - \hat{z}(k+1|k+1) \quad (2.55)$$

2.2.4 Joint Probabilistic Data Association Principles

Originally, PDAF was formulated for tracking single targets in clutter. In PDAF, it is assumed that all the non-target originated received measurements are from clutter and are of a uniform distribution in the validation gate [29]. This assumption is violated in the presence of interfering targets [5]. The extension of PDAF to tackle this issue in tracking

multiple targets in clutter is JPDAF [5]. In JPDAF, it is assumed that the number of initialized tracks is known and the density of state vector conditioned on past data is approximated by a Gaussian distribution as [31]:

$$p[x(k)|Z^{k-1}] = \mathcal{N}[x(k); \hat{x}(k|k-1), P(k|k-1)] \tag{2.56}$$

The JPDA and PDA algorithms utilize the same estimation equations. The difference is on the way the association probabilities are calculated [5, 31]. The association probabilities in PDA are calculated separately for each target, whereas in JPDA these probabilities are calculated in a jointly manner across the targets in a cluster [5]. In this sense, in JPDA algorithm the conditional probabilities of the following joint events are evaluated [5]:

$$\mathcal{H}(k) = \bigcap_{j=1}^{m(k)} \mathcal{H}_{jt_j}(k) \tag{2.57}$$

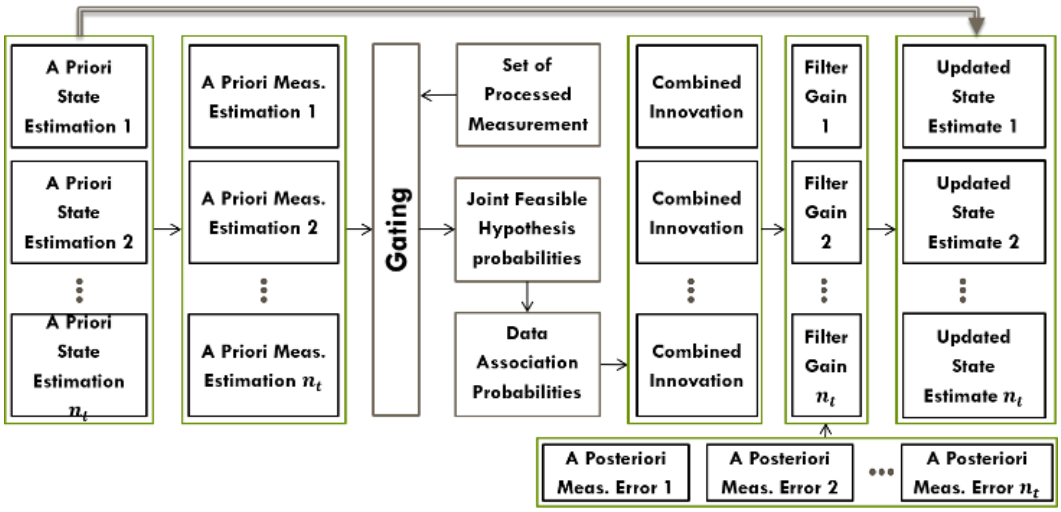

Figure 2.6 Schematic representation of JPDA-SVSF algorithm

where $\mathcal{H}_{jt_j}(k)$ is the hypothesis that measurement j is originated from target t, $0 \leq j \leq m(k)$, $0 \leq t \leq T$, k is the time index, t_j is the target that measurement j is associated with, m_k is the number of measurements, and T is the number of targets [31]. The measurements at time k are named as z^j. Thus, the total available measurements at time k are $Z^k = \{z^1, \dots, z^{n_m}\} \cup Z^{k-1}$. Assuming the number of false measurements being from a Poisson distribution with spatial density λ, the joint association probabilities are calculated as below [5]:

$$P\{\mathcal{H}|Z^k\} = c \prod_j \left\{\lambda^{-1}\mathcal{L}_{t_j}\left[z_j(k)\right]\right\}^{\tau_j} \prod_t (P_D^t)^{\delta_t}(1-P_D)^{1-\delta_t} \tag{2.58}$$

where

$$\mathcal{L}_{t_j}\left[z_j(k)\right] = \mathcal{N}\left[z_j(k); \hat{z}^{t_j}(k|k-1), S^{t_j}(k)\right] \tag{2.59}$$

and P_D^t is the detection probability of target t, τ_j and δ_t are respectively, the target detection and measurement association indicators [31].

To carry out the estimation, the marginal association probabilities are needed. These probabilities are obtained from joint probabilities (2.58) by summing over all joint hypotheses in which the marginal hypothesis of interest happens as below [5]:

$$\beta_{jt}(k) = P\left\{\mathcal{H}_{jt}(k)\middle|Z^k\right\} = \sum_{\mathcal{H}:\mathcal{H}_{jt}\in\mathcal{H}} P\{\mathcal{H}(k)|Z^k\} \tag{2.60}$$

These probabilities are used to make the combined innovation for each target.

2.2.5 Formulation of the JPDA-SVSF

This section is a generalization of the method introduced in [54]. Here, we propose a novel formulation of SVSF for multi-target tracking in clutter based on JPDA method. Figure 2.6 illustrates a schematic presentation of the method, referred to as SVSF-JPDA. The JPDA-SVSF algorithm is outlined as follows.

A. Gating Step

A validation gate is constructed around the predicted measurement of each track, based on the statistical distance, as follows [5]:

$$\mathcal{V}_t(k,\gamma) = \{z: [z - \hat{z}_t(k|k-1)]' S_t(k)^{-1} [z - \hat{z}_t(k|k-1)] \leq \gamma\} \tag{2.61}$$

where γ is the gate threshold corresponding to the gate probability, and $S_t(k)$ is the covariance of the innovation for each track. Then, the feasible hypotheses are determined and target detection and measurement association indicators are obtained [31].

B. Prediction Step

This step provides the prediction of states and measurements.

$$\hat{x}_t(k|k-1) = A_t(k-1)\hat{x}_t(k-1|k-1) \tag{2.62}$$

$$P_t(k|k-1) = A_t(k-1)P_t(k-1|k-1)A_t(k-1)' + Q_t(k-1) \tag{2.63}$$

$$z_t(k|k-1) = C_t(k-1)\hat{x}_t(k|k-1) \tag{2.64}$$

The marginal association probabilities of (2.60) are used to calculate the combined innovation for each track as:

$$\tilde{z}_t(k) = \sum_{i=1}^{m(k)} \beta_{it}(k)\tilde{z}_{it}(k) \tag{2.65}$$

The a priori measurement error of each track is set to be equal to the corresponding combined innovation:

$$e_{zt}(k|k-1) = \tilde{z}_t(k) \tag{2.66}$$

C. State Update Step

In this step, the SVSF gain is calculated for each track and is used to update the states [17].

$$\hat{x}_t(k|k-1) = A_t(k-1)\hat{x}_t(k-1|k-1) \tag{2.67}$$

$$\hat{x}_t(k|k) = \hat{x}_t(k|k-1) + K_t(k)e_{zt}(k|k-1) \tag{2.68}$$

$$K_t(k) = C_t^+ diag[(|e_{zt}(k|k-1)|_{Abs} + \gamma_t|e_{zt}(k-1|k-1)|_{Abs}) \circ sat\left(\frac{e_{zt}(k|k-1)}{\psi_t}\right)][diag(e_{zt}(k|k-1))]^{-1} \tag{2.69}$$

The updated state covariance associated with each track is calculated as below [17]:

$$P_t(k|k) = \beta_{0t}(k)P_t(k|k-1) + [1-\beta_{0t}(k)]P_t^*(k|k) + \tilde{P}_t(k) \tag{2.70}$$

where $P_t^*(k|k)$ is the SVSF covariance matrix computed as below [17]:

$$P_t^*(k|k) = [I - K_t(k)C_t(k)]P_t(k|k-1)[I - K_t(k)C_t(k)]' + K_t(k)R_t(k)K_t'(k) \tag{2.71}$$

and $\tilde{P}(k)$ is an added uncertainty because of the associations uncertainties, as follows [29]:

$$\tilde{P}_t(k) = K_t(k)\left[\sum_{i=1}^{m(k)} \beta_{it}(k)\tilde{z}_{it}(k)\tilde{z}_{it}(k)' - \tilde{z}_t(k)\tilde{z}_t(k)'\right]K_t(k) \tag{2.72}$$

A posteriori measurement error for each track is calculated as follows:

$$e_{zt}(k|k) = [I - C_t(k)K_t(k)]e_{zt}(k|k-1) \tag{2.73}$$

2.2.6 Simulation Problem and Results

A. Problem Setup

A simple near constant velocity model is implemented as per [24]. There are four states in total, related to the target's position and velocity (x and y directions), defined as follows: $x = [\xi\ \eta\ \dot{\xi}\ \dot{\eta}]$. Note that ξ and η are the position in two Cartesian directions, and $\dot{\xi}$ and $\dot{\eta}$ are the corresponding velocities. This model assumes that the accelerations of the target between two sequential samples are constant and are drawn from a discrete-time zero mean white noise. The near constant velocity model is defined as follows:

$$x(k+1) = Ax(k) + Bv(k) \tag{2.74}$$

where the system and process noise gain matrices are defined by:

$$A = \begin{bmatrix} 1 & 0 & T_s & 0 \\ 0 & 1 & 0 & T_s \\ 0 & 0 & 1 & 0 \\ 0 & 0 & 0 & 1 \end{bmatrix} \tag{2.75}$$

$$B = \begin{bmatrix} T_s^2/2 & 0 \\ 0 & T_s^2/2 \\ T_s & 0 \\ 0 & T_s \end{bmatrix} \tag{2.76}$$

The white acceleration noise is defined as follows:

$$Q = cov\{v(k)\} = \begin{bmatrix} \sigma_v^2 & 0 \\ 0 & \sigma_v^2 \end{bmatrix} \tag{2.77}$$

The measurement function, matrix, and noise covariance are defined respectively as follows:

$$z(k) = Cx(k) + w(k) \tag{2.78}$$

$$C = \begin{bmatrix} 1 & 0 & 0 & 0 \\ 0 & 1 & 0 & 0 \end{bmatrix} \tag{2.79}$$

$$R = cov\{w(k)\} = \begin{bmatrix} \sigma_w^2 & 0 \\ 0 & \sigma_w^2 \end{bmatrix} \tag{2.80}$$

The JPDA-KF and JPDA-SVSF algorithms were implemented on two scenarios, with three targets under the presence of clutter. The parameter values used for the simulations are $T_s = 0.5\ s$ and $P_D = 0.9$. The clutter is assumed to have a spatial uniform distribution, and the number of cluttered measurements is generated by a Poisson's distribution of $\lambda = 10^{-4}$. The process noise variance is $\sigma_v^2 = 1^2$, and the measurement noise variance is $\sigma_w^2 = 3^2$.

B. Estimation Results

For the normal scenario, three targets are tracked and clutter occurs at $T = 229\ sec$ and $T = 294\ sec$. The total simulation length is $300\ s$ec. For a well-defined smoothing boundary layer (i.e., implementing the time-varying boundary layer presented in [17]), the JPDA-SVSF is able to match the performance of the JPDA-KF. This is shown in the following figures.

The RMSE errors for this scenario were computed across the three targets and are shown in the following table. Note that, for this case, the two filters yielded the same results.

Table 2.4. RMSE Estimation Results – Normal Case

	Car #1		Car #2		Car #3	
	JPDA KF	JPDA SVSF	JPDA KF	JPDA SVSF	JPDA KF	JPDA SVSF
ξ	10.09	10.31	9.92	10.15	12.38	12.57
η	10.16	10.39	10.33	10.55	5.70	6.08
$\dot{\xi}$	4.57	5.21	4.57	5.12	4.61	5.17
$\dot{\eta}$	4.59	5.13	4.60	5.02	4.55	5.11

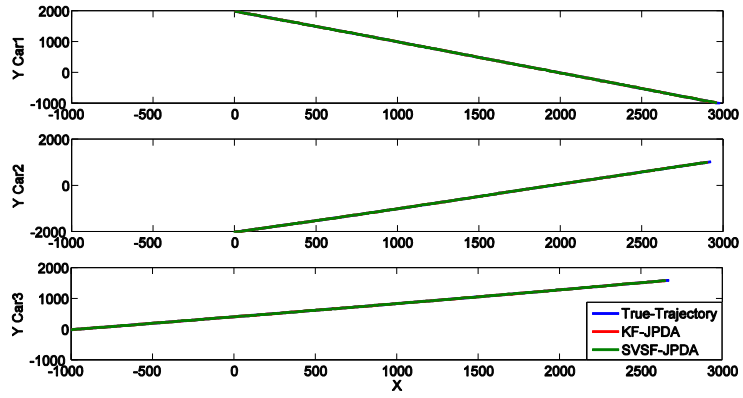

Figure 2.7 JPDA-KF and JPDA-SVSF estimation results: normal case

The second scenario looked at the case of modeling errors or uncertainties. To further investigate the robustness of the proposed JPDA-SVSF strategy, modeling uncertainty is injected at $t = 75S$ for a duration of 10 sampling times into the simulation in the form of changes in the state transition matrix of the model. Figure 2.8 shows the simulation results for the level of modeling uncertainty of 3% ($A_{unc} = 1.03A$), where JPDA-SVSF provides a more stable estimate, as the results did not diverge from the true state trajectory.

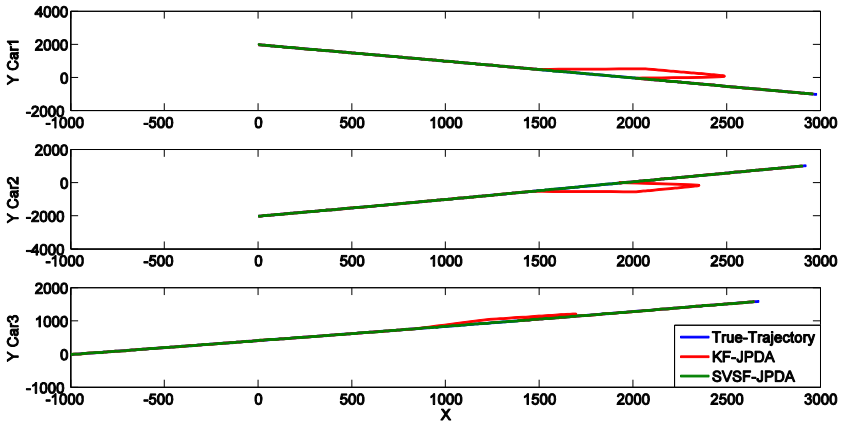

Figure 2.8 JPDA-KF and JPDA-SVSF estimation results (error case)

The RMSE under this scenario was recalculated, and is shown in the following table. The position RMSEs of JPDA-SVSF method are considerably smaller than of JPDA-KF method.

Table 2.5. RMSE Estimation Results –uncertainty of 3%

	Car #1		Car #2		Car #3	
	JPDA KF	JPDA SVSF	JPDA KF	JPDA SVSF	JPDA KF	JPDA SVSF
ξ	86.88	10.31	75.21	10.23	25.79	12.49
η	21.03	10.29	28.65	10.57	18.45	6.24
$\dot{\xi}$	5.88	5.91	5.43	5.41	5.61	5.77
$\dot{\eta}$	5.46	5.55	4.98	5.01	5.49	5.61

Furthermore, increasing the modeling uncertainty causes the JPDA-KF strategy to fail. While due to the unique switching action of the SVSF, the JPDA-SVSF method maintained its tracking capability and was able to provide a good estimate with up to 8% uncertainty in the system matrix.

2.2.7 Conclusion

This paper introduced a new multi-target tracking strategy referred to as the JPDA-SVSF. A multi target tracking simulation was studied to compare the well-studied JPDA-KF algorithm with the JPDA-SVSF. Both methods were able to perform a good target tracking in normal cases. However, the proposed JPDA-SVSF outperforms JPDA-KF in the case of modeling uncertainty in the system matrix, and yielded a more robust estimation method. Future work will build upon the results of this paper, and will study more challenging multi-target tracking scenarios, including interfering targets. Also, some unique characteristics of SVSF method, such as extra indicators of performance will be formulated to improve the data association probabilities.

2.3 Automotive Tracking Technique Using a New IMM based PDA-SVSF (Conference paper *c*)

2.3.1 Abstract

Car tracking algorithms are important for a number of applications, including self-driving cars and vehicle safety systems. The probabilistic data association (PDA) algorithm, in conjunction with Kalman Filter (KF), and interacting multiple model (IMM) are well studied, specifically in the aero-tracking applications. This paper studies single targets while performing maneuvers in the presence of clutter, which is a common scenario for road vehicle tracking applications. The relatively new smooth variable structure filter (SVSF) is demonstrated to be robust and stable filtering strategy under the presence of

modeling uncertainties. In this paper, SVSF based PDA technique is combined with IMM method. The new method, referred to as IMM-PDA-SVSF is simulated under several possible car motion scenarios. Also, the algorithm is tested on a real experimental data acquired by GPS device.

2.3.2 Introduction

The key challenge in the advanced driver assistance systems is the detection of the object of interest on the road as well as estimation of its quantities of interest such as position and velocity. Tracking a maneuvering target in the presence of clutter is a challenging part of these systems. However, generally clutter originated measurements are not easily distinguished from target originated measurements. A number of data association methods have been proposed to deal with this problem [1, 4]. These techniques range from the probabilistic data association (PDA) [5] to more computationally demanding multiple hypothesis tracking (MHT) [55, 1, 32]. The PDA, as an all neighbour association algorithm, considers all feasible measurement-to-track association events to calculate the association probability of each track [5]. In the derivation of PDA, the tracks are assumed to have already been initialized and thus another algorithm is used for track initialization [1, 56]. A derivation of the PDA without this assumption, referred to as the integrated probabilistic data association (IPDA) algorithm, is proposed in [28]. The extensions of PDA and IPDA methods for multiple-target tracking are respectively referred to as the joint probabilistic data association (JPDA) [31] and the joint integrated probabilistic data association (JIPDA) [53]. These methods calculate the association probabilities in a jointly manner across all the neighbouring targets. Once the measurement-to-track association is completed, the tracks are updated with KF [17] strategy. For each hypothesis, an association probability is calculated, which is used to construct a combined innovation term to be used by the KF [4]. The KF and its variants are the most popular estimation methods

[7, 8]. Another estimation strategy referred to as the smooth variable structure filter (SVSF) was proposed in [15]. SVSF is a recursive predictor-corrector filter based on the sliding mode concept [17]. Robustness, multiple indicators of performance (innovation vector and chattering term), and the ability to identify the source of uncertainty are some of the characteristics of the SVSF [15]. In particular, due to its inherent robustness to modeling uncertainties and disturbances, the SVSF is an appropriate candidate for target tracking in clutter problems. In [54] a formulation of SVSF based PDA, namely PDA-SVSF, is proposed for single target tracking in the presence of measurement origin uncertainty. An extension of the method for multiple-target tracking is proposed in [57].

Typical targets can maneuver; therefore beside data association, target trajectory estimation can be a challenge. The tracking filter should be able to accurately estimate the maneuvers. The interacting multiple model (IMM) algorithm is a computationally efficient method which is extensively used for tracking maneuvering targets [20]. There are a number of dynamic models in the IMM algorithm which together can describe the behaviour of the target in time [6]. A number of methods have been proposed to track maneuvering targets in clutter. These algorithms typically use a combination of the IMM and the PDA or one of its extensions [56, 58, 23] . In this paper, a new SVSF based maneuvering target tracking in clutter is presented. The IMM-SVSF method has been proposed in [17] and demonstrated to be efficient in a fault detection application in [59]. The proposed method of this paper, uses the new formulation of SVSF which considers the data association uncertainty as well as the target maneuver.

In section 2.3.3 the SVSF based data association algorithm is summarized. The proposed IMM-PDA-SVSF method is derived in section 2.3.4. The method is evaluated using a scenario designed to include different car motion patterns and also a set of experimental GPS data in section 2.3.5. The paper is summarized and concluded in section 2.3.6.

2.3.3 PDA-SVSF

It is assumed that the system can be described based on two models: system model (2.81) which describes the evolution of the states, and measurement model (2.82) which relates the measurements to states.

$$x_{k+1} = Ax_k + Bu_k + v_k \tag{2.81}$$

$$z_k = Hx_k + w_k \tag{2.82}$$

Where x_k is the state vector, A is the system matrix, B is the input matrix, z_k is the measurement vector, H is the measurement matrix, v_k and w_k are zero mean white Gaussian process and measurement noises and their corresponding covariance matrices are Q_k and R_k. The smooth variable structure filter (SVSF) is a relatively new state and parameter estimation technique [17]. The stability of the SVSF is achieved by selecting a corrective gain in a way that in each step the error in the estimated states decreases [15]. By introduction of a hyper-plane, which is a projection of true state trajectory, and application of the corrective gain the estimations are forced to go toward this region, and then remain in between [15]. The basic concept is shown in the following figure.

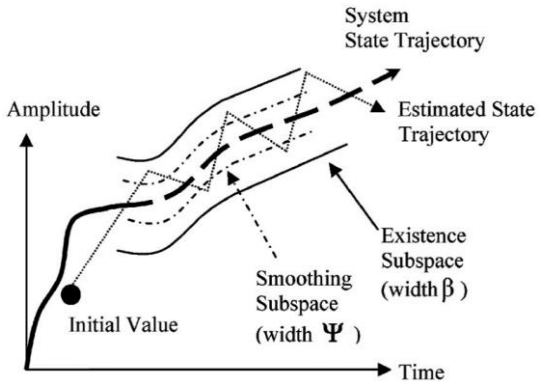

Figure 2.9. SVSF estimation concept [17]

The SVSF estimation consists of the prediction stage ((2.83) to (2.87)) and update stage ((2.88) to (2.90)) [17]. The a priori state vector, covariance matrix and measurement vector are respectively calculated as follows.

$$\hat{x}_{k|k-1} = A\hat{x}_{k-1|k-1} + Bu_k \tag{2.83}$$

$$P_{k|k-1} = AP_{k-1|k-1}A^T + Q_k \tag{2.84}$$

$$\hat{z}_{k|k-1} = H\hat{x}_{k|k-1} \tag{2.85}$$

The a priori or predicted measurement error is also calculated as below.

$$e_{z,k|k-1} = z_k - \hat{z}_{k|k-1} \tag{2.86}$$

The SVSF gain is calculated as follows [17]:

$$\begin{aligned} K_k^{SVSF} = H^+ diag\Big[\Big(\big|e_{z,k|k-1}\big|_{Abs} + \gamma\big|e_{z,k-1,k-1}\big|_{Abs}\Big) \\ \circ sat\Big(\frac{e_{z,k|k-1}}{\Psi}\Big)\Big]\big[diag\big(e_{z,k|k-1}\big)\big]^{-1} \end{aligned} \tag{2.87}$$

The SVSF gain is a function of the a priori and a posteriori measurement error vectors $e_{z,k|k-1}$ and $e_{z,k-1|k-1}$, the smoothing boundary layer widths Ψ, the 'SVSF' memory or convergence rate γ with elements $0 < \gamma_{ii} \leq 1$, and the linear measurement matrix H [17].

The SVSF state vector and covariance matrix are updated as follows:

$$\hat{x}_{k|k} = \hat{x}_{k|k-1} + K_k^{SVSF} e_{z,k|k-1} \tag{2.88}$$

$$P_{k|k} = [I - K_k^{SVSF} H]P_{k|k-1} \tag{2.89}$$

However, note that the a posteriori measurement error needs to be calculated as per (2.90). This value is used in the next time step for gain calculation.

$$e_{z,k|k} = z_k - \hat{z}_{k|k} \tag{2.90}$$

To deal with the data association uncertainty, the formulation of the PDA-SVSF is presented [54]. The PDA-SVSF is basically formulated for tracking single target in clutter. A number of measurements around the predicted measurement ((2.85)) of the track are validated based on an elliptical region defined for stochastic distance to the predicted measurements as follows [5].

$$\mathcal{V}_{k,\vartheta} = \left\{z: \left[z - \hat{z}_{k|k-1}\right]' S_k^{-1} \left[z - \hat{z}_{k|k-1}\right] \leq \vartheta\right\} \tag{2.91}$$

where ϑ is the gate threshold corresponding to the gate probability with which the actual measurement lies within the gate (if detected), and S_k is the covariance of the innovation corresponding to the actual measurement.

Then a priori state estimate, a priori state covariance, and the SVSF gain are respectively calculated using equations (2.83), (2.84) and (2.87). To calculate the a priori measurement error, the following procedure is used.

The n_m candidate measurements at time k are named as $z^i, i = 1, \dots, n_m$. Therefore, one can define $n_{m,k} + 1$ distinct association hypotheses at the time k for these candidate measurements as follows [1, 54]:

$$\mathcal{H}_k^i = \left\{z^i \; is \; target \; originated \; \right\} \tag{2.92}$$

$$\mathcal{H}_k^0 = \{none \; are \; target \; originated\} \tag{2.93}$$

Then the estimate can be written as follows:

$$\hat{x}_{k|k} = \sum_{i=0}^{n_{m,k}} \hat{x}_{k|k}^{i} \beta_k^i \tag{2.94}$$

where $\hat{x}_{k|k}^{\mathrm{i}}$ is the updated state given that the ith hypothesis is correct and β_k^{i} is the corresponding association probability and calculated as follows [5, 4, 54].

$$\beta_k^i = \begin{cases} \dfrac{1 - P_D P_G}{1 - P_D P_G + \sum_{i=1}^{n_m(k)} \mathcal{L}_k^i}, & i = 0 \\ \dfrac{\mathcal{L}_i(k)}{1 - P_D P_G + \sum_{i=1}^{n_m(k)} \mathcal{L}_k^i}, & i = 1, \dots, n_{m,k} \end{cases} \tag{2.95}$$

where P_G is the gate probability [4], P_D is the target detection probability and $\mathcal{L}_k^i$ is the likelihood ratio of the measurement z_k^i, if it is originated from the target, which is calculated as follows.

$$\mathcal{L}_k^i = \frac{\mathcal{N}\left[\tilde{z}_k^i; \hat{z}_{k|k-1}, S_k\right] P_D}{\lambda} \tag{2.96}$$

where λ is the spatial density of the Poisson distribution describing the number of clutter measurements and $\tilde{z}_k^i = z_k^i - \hat{z}_{k|k-1}$ [5]. The combined innovation, which is used as a priori measurement error, is calculated as a weighted sum of $n_{m,k}$ validated measurements:

$$\tilde{z}_k = \sum_{i=1}^{n_{m,k}} \beta_k^i \tilde{z}_k^i \tag{2.97}$$

Then, the states are estimated using (2.88), where $e_{z,k|k-1} = \tilde{z}_k$. The updated covariance is calculated as follows [5].

$$P_{k|k} = \beta_k^0 P_{k|k-1} + [1 - \beta_k^0] P_{k|k}^* + \tilde{P}_k \tag{2.98}$$

Note that $P_{k|k}^*$ is calculated by (2.89) and $\tilde{P}_k$ is an increment as an effect of uncertain associations and is computed by [5]:

$$\tilde{P}_k = K_k^{SVSF} [\sum_{i=1}^{n_m(k)} \beta_k^i \tilde{z}_k^i \tilde{z}_k^{i\prime} - \tilde{z}_k \tilde{z}_k{}'] K_k^{SVSF} \tag{2.99}$$

As described in [54], the a posteriori measurement error is calculated as follows.

$$e_{z,k|k} = [I - H_k K_k^{SVSF}] e_{z,k|k-1} \tag{2.100}$$

2.3.4 IMM-PDA-SVSF

The fundamental assumption of IMM-based tracking methods is that the target trajectory can be explained at any time by one of a finite number of models. Each of these models yields a covariance, or estimated state error which is the basis for the estimator to select a model [6]. The interacting multiple model (IMM) estimator is demonstrated to be an efficient and computationally acceptable method, in which there is a filter for each of the models. Each filter is initialized based on the probability that its corresponding model is in effect [6]. The second assumption of the IMM is that the dynamic model evolves as a Morkov chain with given transition probabilities [6].

The IMM algorithm in its original form does not consider the problem of measurement origin uncertainty, i.e. in the derivation of IMM, it is assumed that there is only one

measurement received and that measurement is originated from the target. To consider the clutter originated measurements, it has been proposed in this paper to replace each of the model matched filters in IMM configuration by a PDA-SVSF. The resulting algorithm will be referred to as the IMM-PDA-SVSF algorithm. Although the IMM-PDA-SVSF algorithm is obtained by combining the IMM and the PDA-SVSF methods, some considerations should be taken into account which do not arise in either the IMM or in the PDA-SVSF.

Assuming that the PDA-SVSF track is formed and there are r imbedded models, the IMM-PDA-SVSF algorithm includes the following steps [1, 54]:

1. Computation of the mixed initial conditions for the model matched filter i:

$$\hat{x}_{k-1|k-1}^{0i} = \sum_{j=1}^{r} \hat{x}_{k-1|k-1}^{j} \mu_{k-1|k-1}^{j|i} \quad i = 1, \dots, r \tag{2.101}$$

where $\mu_{k-1|k-1}^{j|i} = \frac{p_{ji}\mu_{k-1}^{j}}{\sum_{j=1}^{r} p_{ji}\mu_{k-1}^{j}}$,$p_{ji}$ are model switching probabilities and μ_{k-1}^{j} are the model probabilities at the time $k-1$.

$$P_{k-1|k-1}^{0i} = \sum_{j=1}^{r} \mu_{k-1|k-1}^{j|i} \{P_{k-1|k-1}^{j} + (\hat{x}_{k-1|k-1}^{j} - \hat{x}_{k-1|k-1}^{0i})(\hat{x}_{k-1|k-1}^{j} - \hat{x}_{k-1|k-1}^{0i})'\} \tag{2.102}$$

2. Calculation of likelihood function for each of model-matched filters in parallel and independently (This step is one of the key differences between IMM-SVSF and IMM-PDA-SVSF algorithms):

$$\Lambda_k^i = \lambda(1 - P_D P_G) + \sum_{j=1}^{n_m(k)} \mathcal{N}\left[\tilde{z}_k^i; \hat{z}_{k|k-1}, S_k\right] P_D \tag{2.103}$$

3. Calculation of association probabilities as per (2.95), combined innovation as per (2.97), and updating each PDA-SVSF using (2.88) and (2.98) yielding $\hat{x}_{k|k}^i$ and $P_{k|k}^i$.

4. Updating the model probabilities:

$$\mu_k^i = \frac{\Lambda_k^i \sum_{j=1}^r p_{ji} \mu_{k-1}^j}{\sum_{i=1}^r \Lambda_k^i \sum_{j=1}^r p_{ji} \mu_{k-1}^j} \tag{2.104}$$

5. Calculation of combined model-conditioned state estimate and covariance (for output purposes):

$$\mu_k^i = \frac{\Lambda_k^i \sum_{j=1}^r p_{ji} \mu_{k-1}^j}{\sum_{i=1}^r \Lambda_k^i \sum_{j=1}^r p_{ji} \mu_{k-1}^j} \tag{2.105}$$

$$P_{k|k} = \sum_{i=1}^r \mu_k^i \{P_{k|k}^i + (\hat{x}_{k|k}^i - \hat{x}_{k|k})(\hat{x}_{k|k}^i - \hat{x}_{k|k})'\} \tag{2.106}$$

2.3.5 Simulation and Results

Generally, car motion models can be divided into two categories:

The near constant velocity model [6, 40] describes the uniform motion and captures both constant velocity and constant acceleration motions. There are four states, related to the target position and velocity defined as $x = [\xi \ \eta \ \dot{\xi} \ \dot{\eta}]'$. Note that ξ and η are the position in two Cartesian directions, and $\dot{\xi}$ and $\dot{\eta}$ are the corresponding velocities. This model assumes that the accelerations of the target between two sequential samples are constant and are

drawn from a discrete-time zero mean white Gaussian noise. The motion model is defined as follows:

$$x(k+1) = Ax(k) + Bv(k) \tag{2.107}$$

where the system and process noise gain matrices are defined by:

$$A = \begin{bmatrix} 1 & 0 & T_s & 0 \\ 0 & 1 & 0 & T_s \\ 0 & 0 & 1 & 0 \\ 0 & 0 & 0 & 1 \end{bmatrix} \quad , \quad B = \begin{bmatrix} T_s^2/2 & 0 \\ 0 & T_s^2/2 \\ T_s & 0 \\ 0 & T_s \end{bmatrix} \tag{2.108}$$

The white acceleration noise is defined as follows:

$$Q = cov\{v(k)\} = \begin{bmatrix} \sigma_v^2 & 0 \\ 0 & \sigma_v^2 \end{bmatrix} \tag{2.109}$$

The near constant speed turn model [6, 40] describes maneuvering car moving at a constant turn rate. The state vector is $x = [\xi\ \eta\ \dot{\xi}\ \dot{\eta}\ \omega]$. Note that ξ and η are the position in two Cartesian directions, and $\dot{\xi}$ and $\dot{\eta}$ are the corresponding velocities and ω is the angular velocity. The motion model is defined as follows:

$$x(k+1) = Ax(k) + Bv(k) \tag{2.110}$$

where the system and process noise gain matrices are defined by:

$$A=\begin{bmatrix} 1 & 0 & \frac{\sin\omega_k T_s}{\omega_k} & -\frac{1-\cos\omega_k T_s}{\omega_k} & 0 \\ 0 & 1 & \frac{1-\cos\omega_k T_s}{\omega_k} & \frac{\sin\omega_k T_s}{\omega_k} & 0 \\ 0 & 0 & \cos\omega_k T_s & -\sin\omega_k T_s & 0 \\ 0 & 0 & \sin\omega_k T_s & \cos\omega_k T_s & 0 \\ 0 & 0 & 0 & 0 & 1 \end{bmatrix} \tag{2.111}$$

$$B=\begin{bmatrix} T_s^2/2 & 0 & 0 \\ 0 & T_s^2/2 & 0 \\ T_s & 0 & 0 \\ 0 & T_s & 0 \\ 0 & 0 & T_s \end{bmatrix}$$

The remaining equations are the same as the near constant velocity model.

The various driving patterns of a vehicle on a road, as depicted in Figure 1.8, include straight line and curve, cut-in-out, U-turn and interchange [40].

For the purpose of using the IMM method, the hybrid system will use the near constant velocity model for uniform motion, and the near constant speed turn model for maneuvering motion [6, 40]. To track a maneuvering target in the presence of clutter, the proposed IMM-PDA-SVSF method has been used. The SVSF is used for uniform motion model, while the EK-SVSF [17] is used for the maneuvering model.

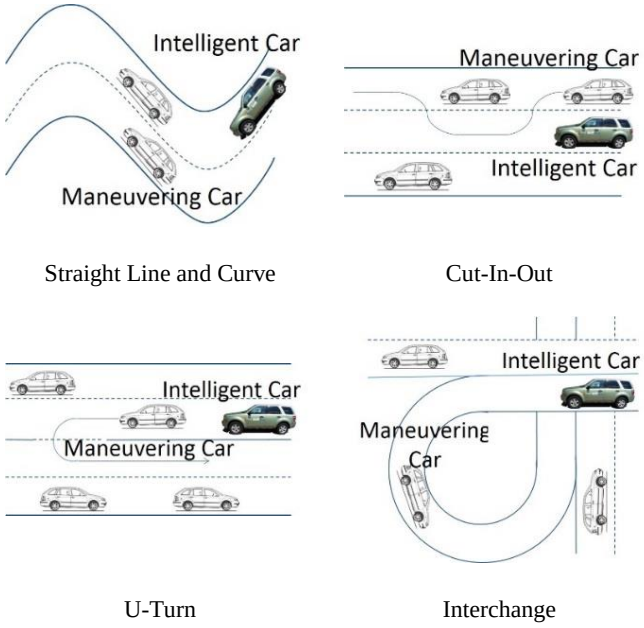

Figure 2.10 Various driving patterns of a vehicle [40]

The simulation scenario is designed based on four aforementioned driving patterns as follows:

The car's initial state is $[\xi_0 = -1000\,m\,, \eta_0 = 0\,, \dot{\xi}_0 = 33\,m/s\,, \dot{\eta}_0 = 0]$. It performs a non-maneuvering near constant velocity motion between $0\,s$ and $115\,s$, a "straight line and curve" maneuver between $116\,s$ and $155\,s$, a non-maneuvering near constant velocity motion between $156\,s$ and $237\,s$, a "cut-in-out" maneuver between $238\,s$ and $283\,s$, a non-maneuvering near constant velocity motion between $284\,s$ and $343\,s$, an "interchange" maneuver between $344\,s$ and $378\,s$, a "straight line and curve" maneuver between $379\,s$ and $399\,s$, a non-maneuvering near constant velocity motion between $400\,s$ and $543\,s$, a "U-turn" maneuver between $544\,s$ and $559\,s$, and a non-maneuvering near constant velocity motion between $560\,s$ and $800\,s$. Also, the parameters' values used for this set of simulations are $T_s = 1\,s$ and $P_D = 0.95$. The clutter is assumed to have a spatial

uniform distribution, and the number of cluttered measurements is generated by a Poisson's distribution with parameter of $\lambda = 10^{-4}$. The process noise variance is set to be $\sigma_v^2 = 2^2$, and the measurement noise variance is $\sigma_w^2 = 3^2$.

Figure 2.11, Figure 2.12, and Figure 2.13 respectively illustrate estimated trajectories of the cars, estimated state variables, and uniform motion mode probabilities for the scenario. The simulation results compared the IMM-PDA-KF method and the IMM-PDA-SVSF in terms of the RMS of state estimation error (See Table 2.6).

The IMM-PDA-SVSF provided a stable estimate, as the results did not diverge from the true state trajectory. Furthermore, when compared with the IMM-PDA-KF, the x-position RMSE of the IMM-PDA-SVSF was reduced by about 12.5%, and the y-position RMSE was reduced by about 16%. This is due to the strict assumptions of the KF that the system is known, while SVSF does not have this assumption and therefore is a more robust filtering strategy against the modeling uncertainties.

The stability of the SVSF method comes from the special switching gain of the SVSF algorithm that is designed in a way that reduces the absolute value of the estimation error at each step.

Table 2.6. RMS of state estimation error for simulation scenario comparing IMM-PDA-KF and IMM-PDA-SVSF

State	IMM-PDA-KF	IMM-PDA-SVSF
x	36.57	32.00
y	10.24	8.58
v_x	5.05	4.38
v_y	3.57	4.04

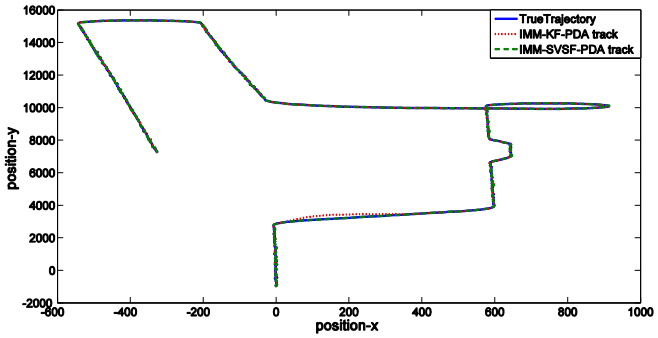

Figure 2.11 The estimated trajectories for the IMM-PDA-KF and the IMM-PDA-SVSF

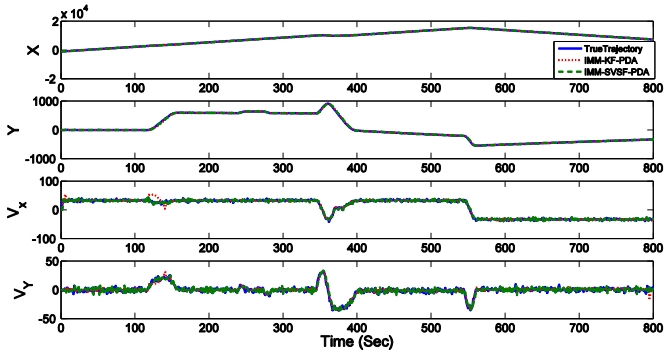

Figure 2.12 The estimated states for the IMM-PDA-KF and the IMM-PDA-SVSF

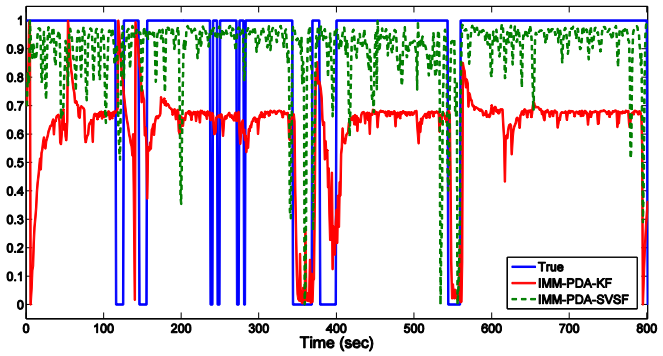

Figure 2.13 The uniform motion mode probabilities for the IMM-PDA-KF and the IMM-PDA-SVSF

To further demonstrate the efficiency of the method, the algorithm is applied on a GPS data gathered from a path starting from McMaster University to the east Hamilton with the sample rate of 1 second (see Figure 2.14). This path resulted in a number of uniform motions and maneuvers [17]. Also, the clutter is artificially added to the data with a spatial uniform distribution, and the number of cluttered measurements is generated by a Poisson's distribution of $\lambda = 10^{-4}$. Figure 2.15, Figure 2.16, and Figure 2.17 respectively illustrate the trajectories, states, and mode probabilities comparing both the IMM-PDA-KF and the IMM-PDA-SVSF. The RMS of state estimation errors are presented in Table 2.7. The simulation results indicated that both algorithms have a reliable performance to track a maneuvering target. Furthermore, the IMM-PDA-SVSF when compared with the IMM-PDA-KF, has slightly reduced the x-position RMSE and the y-position RMSE because of the robustness of the filtering method against the modeling uncertainties.

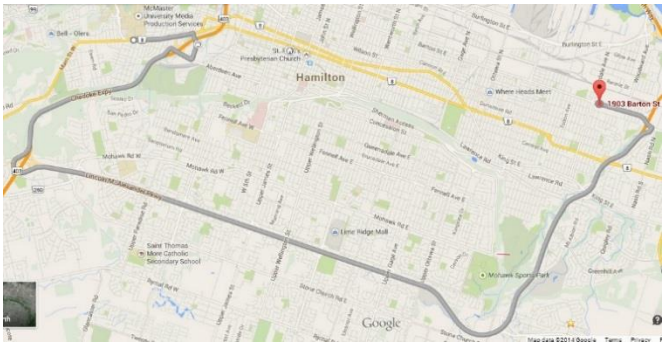

Figure 2.14 The path where the GPS data is gathered

Table 2.7. RMS of state estimation error for GPS data for IMM-PDA-KF and IMM-PDA-SVSF

State	IMM-PDA-KF	IMM-PDA-SVSF
x	10.65	10.04
y	21.13	19.51
v_x	3.90	4.11
v_y	4.46	4.27

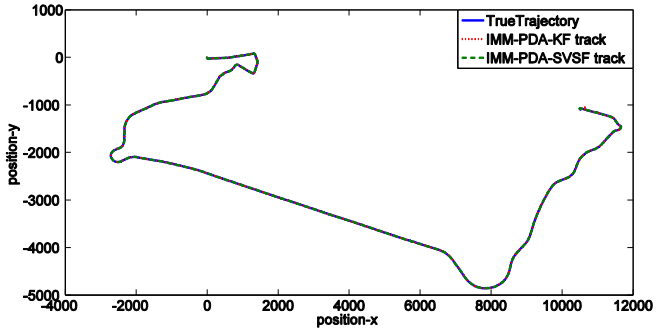

Figure 2.15 The estimated trajectories of GPS data for IMM-PDA-KF and IMM-PDA-SVSF

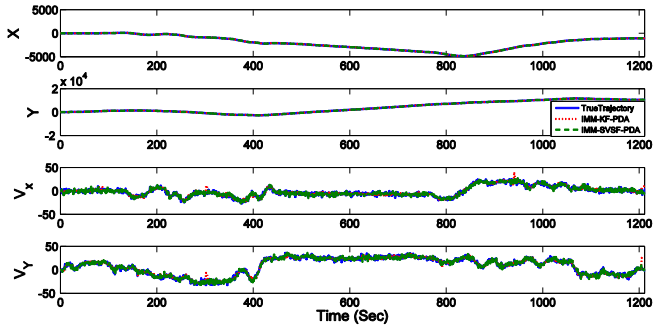

Figure 2.16 The estimated states of GPS data for IMM-PDA-KF and IMM-PDA-SVSF

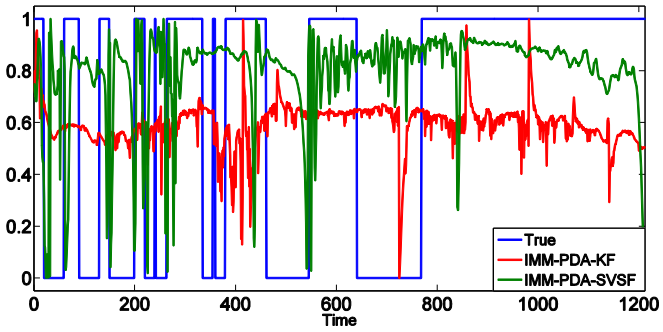

Figure 2.17 The uniform motion mode probabilities of IMM-PDA-KF and IMM-PDA-SVSF for GPS data

2.3.6 Conclusion

This paper introduced new formulation for the smooth variable structure filter (SVSF) for tracking the maneuvering target in the presence of clutter. The IMM-PDA-SVSF algorithm was introduced and described, and applied on a designed simulation problem consisted of several driving pattern, as well as an acquired GPS data. The results were compared with the popular KF based IMM-PDA strategy. It was determined that the SVSF-based target tracking strategies provided better results in terms of RMS error of the states. This is due to the inherent stability present in the SVSF caused by the switching effect of the gain. The future work will include the extension of the work for multiple maneuvering target tracking in clutter.

Chapter 3

Generalized Covariance SVSF for Target Tracking in Clutter

3.1 Abstract

An important area of study for aerospace and electronic systems involves target tracking applications. To successfully track a target, state and parameter estimation strategies are used in conjunction with data association techniques. Even after 50 years, the Kalman filter (KF) remains the most popular and well-studied estimation strategy in the field. However, the KF adheres to a number of strict assumptions that leads to instabilities in some cases. The smooth variable structure filter (SVSF) is a relatively new method which is becoming increasingly popular due to its robustness to disturbances and uncertainties. This paper presents a new formulation of the SVSF. The probabilistic and joint probabilistic data association (PDA, JPDA) techniques are combined with the SVSF and applied on multi-target tracking scenarios. In addition, a new covariance formulation of the SVSF is presented based on improving the estimation results of non-measured states. The results are compared and discussed with the popular KF method.

3.2 Introduction

Target tracking algorithms have been used in a wide-variety of applications; ranging from air traffic control and monitoring, to data processing of medical images [1]. Most recently, target tracking systems are growing in popularity in the area of automotive research. For example, intelligent and cognitive vehicles make use of target tracking algorithms for active safety systems and advanced driver assistance systems (ADAS) [60, 61, 2, 3]. In surveillance and monitoring systems, the fundamental role of tracking algorithms is to interpret the surrounding environment, which typically consists of noise and other disturbances, using sensor information in an effort to form target tracks and estimates [1, 30].

Data association algorithms are an important component in multi-target tracking (MTT) scenarios, especially when handling measurements with uncertain or complex origins. Data association algorithms categorize measurements from various sources into target-originated and clutter-originated classifications. The algorithms differentiate measurements belonging to different targets of interest [5]. A comprehensive survey of several data association methods can be found in [1] and [30].

There are a number of different data association algorithms. The standard nearest neighbour filter (SNN), which uses statistical distance to predict and associate measurements to tracks, is considered one of the simplest algorithm [4]. One of the most popular technique is the probabilistic data association filter (PDA) [5]. The PDA also has a number of extensions, like the joint probabilistic data association filter (JPDA) [31]. The PDA is a type of all-neighbour data association method. It considers all feasible measurement-to-track association hypotheses, and calculates the association probabilities for each track [5, 29]. In deriving the PDA, it is assumed that the tracks have already been initialized. Hence,

another algorithm must be used to initialize the tracks [1, 56]. A derivation of the PDA without track initialization was proposed in [28]. This method, referred to as the integrated probabilistic data association (IPDA) technique, provides the data association probabilities as well as track existence probabilities. The PDA was originally formulated for single-target tracking in the presence of clutter. A number of PDA's may be utilized in parallel for multiple-target tracking [5]. Joint probabilistic data association (JPDA) is an extension of PDA for multiple-target tracking. It has improved performance when target trajectories are interfering, thereby increasing the tracking complexity [31]. The main difference between PDA and JPDA is the calculation procedure of association probabilities. In JPDA, the association probabilities are jointly calculated across the previously clustered targets in a cluster [31]. For multiple targets, the IPDA has been extended and is referred to as the joint integrated probabilistic data association (JIPDA) [53].

A multiple hypothesis tracker (MHT) was presented in 1979 [32]. In this strategy, the received measurements of each frame are assigned to the initialized targets, new targets, or false alarms. This algorithm relies on the enumeration of all measurement-to-track assignments, and then pruning and gating to limit the set of feasible associations. There is a risk of elimination of the correct measurement sequences [62]. In probabilistic multiple hypothesis tracking (PMHT), the measurements are not assigned to specific tracks; the probability of each measurement belonging to each track is calculated using a Bayesian approach [33]. The PMHT estimates the target states and measurement-to-track association probabilities in a jointly manner; this way, PMHT avoids hard measurement to track assignment decisions [33]. The PMHT is implemented for maneuvering target tracking in [63] on the basis of hidden Markov chain model-switch. Also, a thorough review of the advances in PMHT and a generalized version of it is presented in [34].

An alternative approach (to MHT, JPDAF, and PMHT) is a method based on random finite set concepts. In this approach, the multiple targets and observations are treated as a set-valued state and a set-valued observation, respectively. The so-called probability hypothesis density (PHD) filter is a successful marriage of such approaches with finite set statistics (FISST) [64]. Several approximations of the PHD recursion are presented such as the sequential Monte Carlo PHD (SMCPHD) filter [35], the Gaussian mixture PHD (GMPHD) filter [37], and the Cardinalized PHD (CPHD) filter [36].

Once the measurement-to-track association is completed, the tracks are updated with an estimation strategy. The most common method employed is the Kalman filter (KF) and its variants [17]. In the case of maneuvering targets, an interacting multiple model (IMM) approach is used [20], which uses several filters in parallel for a finite number of target maneuvers [23, 65, 4]. For each hypothesis, an association probability is calculated which is used to construct a combined innovation term. This term is a weighted sum of all the innovations, and is used by the KF [4].

The KF was initially introduced in the 1960s, and remains one of the most popular estimation methods. It provides a statistically optimal solution for linear estimation problems [7, 8]. In [50, 11], the KF was modified in an effort to handle nonlinear systems and measurements, as well as to overcome modeling uncertainties and instability. In [15], another estimation strategy referred to as the smooth variable structure filter (SVSF) was proposed. It is a recursive predictor-corrector filter based on the sliding mode concept [17]. In the SVSF concept, the true trajectory of a system is projected as a hyper-plane, and to within an existence subspace. A corrective gain forces the estimated states towards the existence subspace. The estimates remain within this subspace by the use of a switching gain, which causes the estimates to chatter or go back-and-forth across the actual state trajectory [15]. Some interesting characteristics of the SVSF are its robustness, multiple

indicators of performance (innovation vector and chattering term), and the ability to identify the source of uncertainty [15]. In particular, due to its inherent robustness to modeling uncertainties and disturbances, the SVSF was applied to target tracking problems with the presence of clutter [54, 57]. The SVSF covariance formulation of [17] was implemented, and was shown to work well when each state has a corresponding measurement. Since the state error covariance matrix plays a pivotal role in data association procedures, a new SVSF state error covariance matrix that is a generalization for the cases when the number of measurements is less than the number of states, is presented in this paper. The new SVSF formulation, called covariance modified SVSF (CM-SVSF) was combined with the PDA and JPDA techniques, and are referred to as the CM-PDA-SVSF and CM-JPDA-SVSF, respectively. The simulation results are compared with the KF-based methods. Note that it is possible to make the KF more robust by implementing methods such as estimating the system matrix, or modeling the unknown system matrix as multiplicative noise to capture the modeling uncertainties. However, these approaches are equivalently applicable to the SVSF-based filtering. Furthermore, a comparison of the robustness of the SVSF to Kalman filter has been made in [66, 67, 68]. Therefore, in this paper, the original form of the KF is compared to the basic form of the CM-SVSF.

In section 3.3, the KF and SVSF estimation strategies are summarized. Data association principles are discussed in Section 3.4. Section 3.5 introduces the proposed PDA-SVSF and JPDA-SVSF tracking algorithms, including the corresponding covariance derivations. In Section 3.6, a number of target tracking cases are studied. The estimation and tracking results are discussed and compared with the popular KF method. The paper is then summarized and concluded.

3.3 Estimation Strategies

3.3.1 Kalman Filter

The Kalman filter (KF) is an optimal estimation strategy and yields the minimum mean square error solution [6]. The KF accomplishes this task as it is formulated based on minimizing the trace of the state covariance matrix [51, 17]. Most estimation methods are based on a system and measurement model, described as follows:

$$x_{k+1} = Ax_k + Bu_k + v_k \tag{3.1}$$

$$z_k = Cx_k + w_k \tag{3.2}$$

where v_k and w_k are zero mean white Gaussian process and measurement noises, with covariance matrices Q_k and R_k, respectively.

The KF is a recursive predictor-corrector strategy, based on two main steps. The first step is referred to as the prediction step, and consists of the following equations:

$$\hat{x}_{k+1|k} = A\hat{x}_{k|k} + Bu_k \tag{3.3}$$

$$P_{k+1|k} = AP_{k|k}A^T + Q_k \tag{3.4}$$

The state estimates are first predicted in (3.3), and the corresponding state error covariance is calculated as per (3.4). These values are then used in the prediction or updated step, which consists of the following equations:

$$K_{k+1} = P_{k+1|k}C^T\left[CP_{k+1|k}C^T + R_{k+1}\right]^{-1} \tag{3.5}$$

$$\hat{x}_{k+1|k+1} = \hat{x}_{k+1|k} + K_{k+1}\left[z_{k+1} - C\hat{x}_{k+1|k}\right] \tag{3.6}$$

$$P_{k+1|k+1} = [I - K_{k+1}C]P_{k+1|k} \tag{3.7}$$

Equations (3.3)-(3.7) summarize the KF solution for linear estimation problems. The process is repeated iteratively. For nonlinear estimation problems, many variations of the KF have been presented in literature [6, 10]. The most popular and simplest strategy is the extended KF (EKF), which linearizes the nonlinearities using a Jacobian matrix [11, 10].

3.3.2 Smooth Variable Structure Filter

The smooth variable structure filter was first presented in 2007, and is a state and parameter estimation technique based on sliding mode concepts formulated in a predictor-corrector fashion [17, 15]. The basic concept is shown in the following figure.

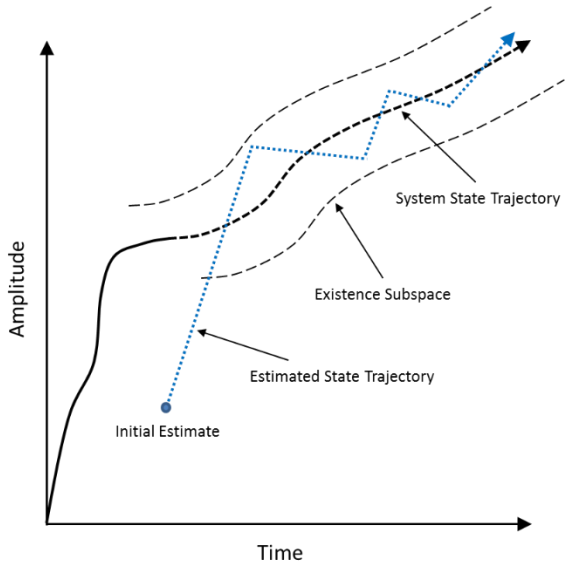

Figure 3.1 SVSF estimation concept [17].

Similar to the KF strategy, the SVSF consists of two main steps: prediction and update. However, the main difference lies in how the SVSF gain is formulated. The prediction stage begins as follows:

$$\hat{x}_{k+1|k} = A\hat{x}_{k|k} + Bu_k \tag{3.8}$$

$$P_{k+1|k} = AP_{k|k}A^T + Q_k \tag{3.9}$$

The SVSF may also be formulated to handle nonlinear system and measurement functions [17]. The a priori or predicted measurement error is calculated by the following:

$$e_{z,k+1|k} = z_{k+1} - \hat{z}_{k+1|k} \tag{3.10}$$

The SVSF gain is calculated next, as follows [17]:

$$\begin{aligned} K_{SVSF} = C^{+} diag\left[\left(\left|e_{z,k+1|k}\right|_{Abs} + \gamma\left|e_{z,k|k}\right|_{Abs}\right)\right. \\ \left.\circ\, sat\left(e_{z,k+1|k}, \psi\right)\right]\left[diag\left(e_{z,k+1|k}\right)\right]^{-1} \end{aligned} \tag{3.11}$$

where $|.|_{Abs}$ is the element-wise absolute value of the vector; the operator $\circ$ is the Schur product [69]; $e_{z,k+1|k}$ and $e_{z,k|k}$ are the a priori and the a posteriori measurement error vectors; γ is the 'SVSF' memory or convergence rate in the form of a diagonal matrix with elements $0 < \gamma_{ii} \leq 1$; and C the measurement matrix. The elements of the function $sat(vec, \psi)$ are defined as

$$sat_i(vec, \psi) = \begin{cases} vec_i/\psi_i & ; \quad |vec_i/\psi_i| \leq 1 \\ sign(vec_i/\psi_i); & |vec_i/\psi_i| > 1 \end{cases} \tag{3.12}$$

where ψ_i is the smoothing boundary layer widths in which i refers to the i^{th} width. For numerical stability, it is important to ensure that one does not divide by zero in (3.11). This can be accomplished using a simple if statement with a very small threshold [17].

The update step is summarized by the following equations:

$$\hat{x}_{k+1|k+1} = \hat{x}_{k+1|k} + K_{SVSF} e_{z,k+1|k} \tag{3.13}$$

$$P_{k+1|k+1} = (I - K_{SVSF} C) P_{k+1|k} (I - K_{SVSF} C)^T + K_{SVSF} R_{k+1} K_{SVSF} \tag{3.14}$$

The a posteriori or updated measurement error needs to be calculated as per (3.15). This value is used in the next time step, and the process is repeated iteratively.

$$e_{z,k+1|k+1} = z_{k+1} - \hat{z}_{k+1|k+1} \tag{3.15}$$

The SVSF concept may be further described by the following two figures. The chattering effect shown in Figure 3.2 (a) allows the SVSF estimates to be robust to modeling uncertainties and disturbances. Essentially, given some initial estimate, by use of the SVSF corrective gain, the SVSF converges the estimated state trajectory to within an existence subspace around the true trajectory. The width of the existence subspace is a function of uncertain dynamics due to uncertainties. Once the estimated states are in that subspace, they switch back and forth across the true trajectory and will remaining within this subspace [15]. This is similar to the sliding mode concept, however it has been formulated in a predictor-correction fashion for state and parameter estimation.

The smoothing boundary layer is a common strategy used in sliding mode control to reduce or remove chattering effects due to discontinuous corrective action, such as used in the SVSF. Here a boundary layer is introduced around the switching hyperplane such that discontinuous corrective action is made linearly variable with respect to the distance from

the switching hyperplane; while outside the boundary layer the full magnitude of the discontinuous action is applied. If the size of the smoothing boundary layer is greater than the existence subspace, then the chattering effects are removed as shown in Figure 3.2 (b) [15]. However, the smoothing boundary layer is effective by removing chattering but at the expense of robust performance.

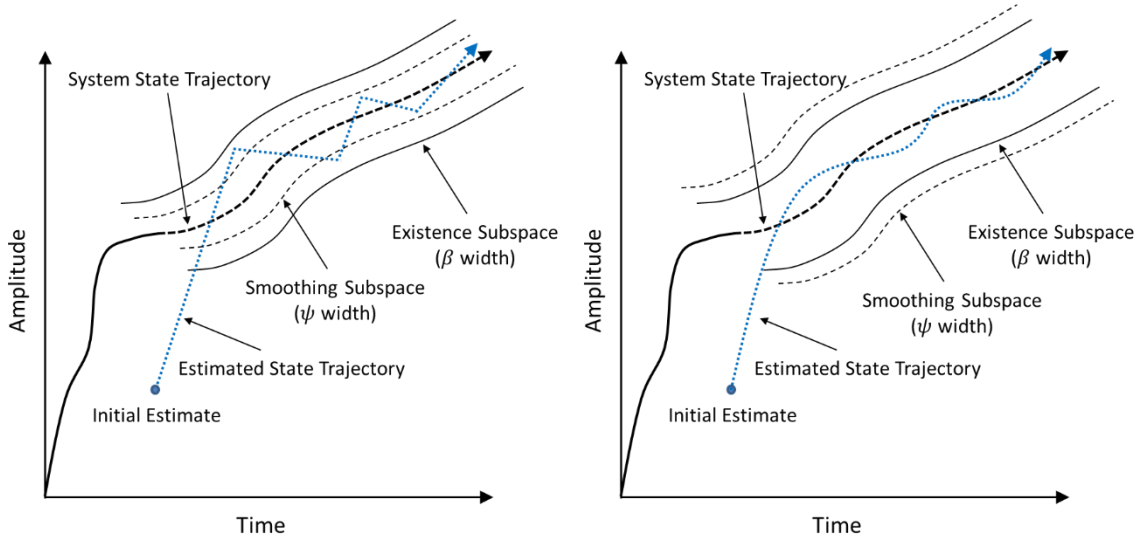

Figure 3.2 (a) Chattering effect of the SVSF gain, and (b) Smoothed estimated state trajectory [59].

3.4 Data Association Principles

In target tracking scenarios, there are often more than one measurements associated with one target. This is due to the presence of false measurements of targets. Data association methods assign measurements to targets based on probabilities. The first step, in an effort to improve the computational efficiency, is to select the portion of the measurements that

are over a probability threshold. This is referred to as gating the measurements. The gate is defined as a region in which the associated measurement is highly probable to fall within. For the gated measurements, a decision is made in order to assign the measurement to a corresponding target. The simplest approach to assign gated measurements to targets is the standard nearest neighbour filter [4]. Other variations of this strategy include the global nearest neighbour filter, probabilistic nearest neighbour, and distributed sequential nearest neighbour [4, 1]

The nearest neighbour filter associates the measurement with the smallest normalized distance squared among the validated measurements to the corresponding target [4]. The main drawback of this filter is that the nearest neighbour measurement may be based on clutter which are unwanted measurements. This problem may be overcome by implementing a probabilistic approach for data association, such as the probabilistic data association filter (PDAF) [29, 5]. The PDAF has several extensions, such as the joint probabilistic data association filter (JPDAF) for multiple target tracking, and the integrated PDAF (IPDAF) and integrated JPDAF (IJPDAF) which resolves track initiation and termination issues [31, 28, 53] .

The PDAF is typically formulated for single target tracking in the presence of clutter based on the KF. Consider the following. Assume that the target track has been initialized. Also, define past information through time $k-1$ about the target trajectory in the form of a normal distribution as follows [5]:

$$p[x_k|Z^{k-1}] = \mathcal{N}[x_k; \hat{x}_{k|k-1}, P_{k|k-1}] \tag{3.16}$$

It is also assumed that if the target is detected, then, there is only one target originated measurement within the validation gate, and the remaining measurements are clutter

originated. The number of validated false measurements is Poisson distributed with spatial density λ and their spatial distribution is modeled as i.i.d.(independent and identically distributed) uniform [5]. The m_k candidate measurements at time k are named as $z^i, i = 1, \dots, m_k$. The set of available measurements at time k are defined as $Z^k = \{z^1, \dots, z^{m_k}\} \cup Z^{k-1}$. For m_k validated measurements in time k, one can describe $m_k + 1$ distinct association hypotheses as [1]:

$$\mathcal{H}_k^i = \{z^i \; is \; target \; originated \;\} \tag{3.17}$$

$$\mathcal{H}_k^0 = \{none \; are \; target \; originated\} \tag{3.18}$$

where $i = 1, \dots, m_k$. Since these hypothesis are mutually exclusive and exhaustive, the use of the total probability theorem is allowed [5, 6]. The minimum variance estimate is written as follows:

$$\hat{x}_{k|k} = \mathbb{E}\{x_k|Z^k\} = \sum_{i=0}^{m_k} \mathbb{E}\{x_k|\mathcal{H}_k^i, Z^k\} P\{\mathcal{H}_k^i|Z^k\} = \sum_{i=0}^{m_k} \hat{x}_{k|k}^i \beta_k^i \tag{3.19}$$

where $\hat{x}_{k|k}^i$ is the updated state given that the ith hypothesis is correct and β_k^i is named association probability which is the conditioned probability of the ith hypothesis [29, 1]. These association probabilities are computed as follows [5, 4] :

$$\beta_k^i = \begin{cases} \dfrac{1 - P_D P_G}{1 - P_D P_G + \sum_{i=1}^{m_k} \mathcal{L}_k^i}, & i = 0 \\ \dfrac{\mathcal{L}_k^i}{1 - P_D P_G + \sum_{i=1}^{m_k} \mathcal{L}_k^i}, & i = 1, \dots, m_k \end{cases} \tag{3.20}$$

where $i = 0$ is association probability of the hypothesis when none of the validated measurements is target originated, P_G is gate probability [4], and P_D is the target detection probability. In addition:

$$\mathcal{L}_k^i = \frac{\mathcal{N}\left[z_k^i; \hat{z}_{k|k-1}, S_k\right] P_D}{\lambda} \tag{3.21}$$

which is the likelihood ratio of the measurement z_k^i, assuming that it is target originated [5] . The combined innovation to be used in the filter update is calculated as a weighted sum of m_k validated measurements, as follows:

$$\tilde{z}_k = \sum_{i=1}^{m_k} \beta_k^i e_{z,k+1|k}^i \tag{3.22}$$

where $e_{z,k+1|k}^i = z_k^i - Cx_{k|k-1}$ [30]. The states are updated with the standard KF estimation strategy. To update the covariance, the following equation is used:

$$P_{k|k} = \beta_k^0 P_{k|k-1} + [1 - \beta_k^0] P_{k|k}^* + \tilde{P}_k \tag{3.23}$$

where $P_{k|k}^*$ is the standard KF covariance matrix and $\tilde{P}_k$ accounts for uncertainty increment due to association uncertainty. It is computed as follows [29]:

$$\tilde{P}_k = K_k \left[\sum_{i=1}^{m_k} \beta_k^i e_{z,k+1|k}^i {e_{z,k+1|k}^i}' - \tilde{z}_k \tilde{z}_k' \right] {K_k}' \tag{3.24}$$

The PDAF is formulated for tracking single targets in the presence of clutter. In a multi-target tracking scenario, a number of PDAFs may be used in parallel for several targets. However, in the presence of multiple interfering targets that share measurements, the

assumption of uniform distribution for all measurements which are not originated from the target is violated [5] [29]. To tackle this problem, the PDAF has been extended to a joint probabilistic data association (JPDA) formulation, which considers joint association hypotheses. PDAF and JPDAF algorithms utilize similar prediction and update equations. The main difference occurs in the calculation of association probabilities [5, 31]. In PDAF, the association probabilities are calculated separately for each target; whereas in the JPDAF, these probabilities are calculated jointly across all of the targets which share some validated measurements [5]. The conditional probabilities of the following joint events are evaluated as follows [5]:

$$\mathcal{H}_k = \bigcap_{i=1}^{m_k} \mathcal{H}_k^{ji} \tag{3.25}$$

where $\mathcal{H}_k^{it_i}$ is the hypothesis that measurement j originated from target t, $0 \leq i \leq m_k$, $0 \leq t \leq T$, k is the time index, t_j is the target that measurement j is associated with, m_k is the number of measurements, and T is the number of targets [31]. The joint association probabilities are calculated as follows [5]:

$$P\{\mathcal{H}_k|Z^k\} = c \prod_i \left\{\lambda^{-1}\mathcal{L}_k^{t_i}\right\}^{\tau_i} \prod_t (P_D^t)^{\delta_t}(1 - P_D^t)^{1-\delta_t} \tag{3.26}$$

where P_D^t is the detection probability of target t; and τ_i and δ_t are the target detection and measurement association indicators, respectively [31]. In addition:

$$\mathcal{L}_k^{t_i} = \mathcal{N}[z_k^i; \hat{z}_{k|k-1}^{t_i}, S_k^{t_i}] \tag{3.27}$$

The state estimation is carried out separately for each target using the marginal association probabilities [5, 31]. These probabilities are obtained from joint probabilities (1.31) by summing the joint hypotheses in which the marginal hypothesis of interest is included, as follows [5]:

$$\beta_k^{it} = P\{\mathcal{H}_k^{it}|Z^k\} = \sum_{\mathcal{H}:\mathcal{H}^{it}\in\mathcal{H}} P\{\mathcal{H}_k|Z^k\} \tag{3.28}$$

These probabilities are used to create the combined innovation for each target, which is used during the filter update stage.

3.5 Proposed Strategies

In this section, novel approaches for simultaneous data association and filtering are investigated and presented. The approaches are based on a robust filter known as the SVSF [15]. This filter is based on sliding mode concepts and formulated in a predictor-corrector fashion, and is demonstrated to be robust to modeling errors and uncertainties [17, 15]. This section describes the so called PDA-SVSF for single target tracking in the presence of data association uncertainty [54]. In addition, its extension known as the JPDA-SVSF which handles multiple target tracking is presented [57]. The main difference between these data association filters with previously published versions is in the extraction of a new state covariance when handling fewer measurements than states. In [15], a similar strategy to Luenberger's reduced order observer is used to estimate the non-measured states. In [17], a state covariance matrix is formulated for the SVSF for the case when there is full measurement matrix ((3.14)). However, to handle the cases when the number of measurements are fewer that the number of states, a generalized form of the SVSF

covariance was needed. Particularly, the covariance matrix plays a key role in the data association procedure. Therefore, a new strategy for calculating the state covariance matrix is formulated and presented in this paper based on the SVSF formulation for fewer measurements than states.

3.5.1 Covariance Modified PDA-SVSF (CM-PDA-SVSF)

Consider system and measurement models (equations (3.1) and (3.2)) where the measurement matrix H is of dimension $m \times n$, and $m < n$ is the number of measured states, n is the rank of the system, and also:

$$C = [C_1 \quad C_2] \tag{3.29}$$

where C_1 is of dimension $m \times m$ and C_2 is a null matrix of dimension $m \times (n - m)$.

The state space representation of the system can be partitioned, or if necessary transformed, into two parts as follows:

$$x_k = \begin{bmatrix} x_{u_k} \\ x_{l_k} \end{bmatrix} = \begin{bmatrix} x_{1_k} \\ \vdots \\ x_{m_k} \\ x_{m+1_k} \\ \vdots \\ x_{n_k} \end{bmatrix} \tag{3.30}$$

The segment x_{u_k} is directly linked to the measurements and the related corrective gain is defined as per [17, 15]:

$$K_{u_{k+1}} = C_1^{-1} diag\left[\left(\left|e_{z,k+1|k}\right| + \gamma\left|e_{z,k|k}\right|\right) \circ sat\left(\frac{e_{z,k+1|k}}{\psi_z}\right)\right]\left[diag(e_{z,k+1|k})\right]^{-1} \tag{3.31}$$

where γ is an $m \times m$ diagonal matrix with elements such that $0 \leq \gamma_{ii} < 1$.

If the system model is completely observable and completely controllable, then a reduced order estimator is constructed for x_{l_k}. The state vector is transformed into a partitioned form so that the upper portion has an identity relationship with the measurement vector.

$$Tx_k = \begin{bmatrix} y_{u_k} \\ y_{l_k} \end{bmatrix} \tag{3.32}$$

where T is a transformation matrix, then:

$$z_k = Iy_{u_k} + v_k \tag{3.33}$$

A revised state vector is defined such that:

$$y_k = \begin{bmatrix} z_k \\ y_{l_k} \end{bmatrix} \tag{3.34}$$

The system model or equation can be restated in a partitioned form as follows:

$$\begin{bmatrix} z_{k+1} \\ y_{l_{k+1}} \end{bmatrix} = \begin{bmatrix} \Phi_{11} & \Phi_{12} \\ \Phi_{21} & \Phi_{22} \end{bmatrix} \begin{bmatrix} z_k \\ y_{l_k} \end{bmatrix} + \begin{bmatrix} \overline{w}_{1_k} \\ \overline{w}_{2_k} \end{bmatrix} \tag{3.35}$$

where $\Phi = \mathrm{T}^{-1}AT = \begin{bmatrix} \Phi_{11} & \Phi_{12} \\ \Phi_{21} & \Phi_{22} \end{bmatrix}$, and $\overline{w}_k = T^{-1}w_k - \begin{bmatrix} \Phi_{11} \\ \Phi_{21} \end{bmatrix} v_k = \begin{bmatrix} \overline{w}_{1_k} \\ \overline{w}_{2_k} \end{bmatrix}$. In this case, the corresponding output matrix is an identity matrix. As demonstrated in [15], the following equations may be obtained for the a posteriori and a priori errors of y_{l_k}:

$$e_{y_{l_{k|k}}} = \Phi_{12}^{-1} e_{z,k+1|k} - \Phi_{12}^{-1} \overline{w}_{1_k} \tag{3.36}$$

$$e_{y_{l_{k+1|k}}} = \Phi_{22}\Phi_{12}^{-1}e_{z,k+1|k} - \Phi_{22}\Phi_{12}^{-1}\overline{w}_{1_k} + \overline{w}_{2_k} \tag{3.37}$$

Using the proven corrective gain for the lower portion of the state vector as per [15], and the modified version of the gain as per [17], consider the following proposed corrective gain used to update the lower portion of the state vector:

$$\begin{aligned} K_{L_{k+1}} = \; & diag\left[\left(\left|\Phi_{22}\Phi_{12}^{-1}e_{z,k+1|k}\right| + \gamma\left|\Phi_{12}^{-1}e_{z,k+1|k}\right|\right)\right. \\ & \left.\circ\, sat\left(\frac{\Phi_{22}\Phi_{12}^{-1}e_{z,k+1|k}}{\psi_y}\right)\right]\left[diag(\Phi_{22}\Phi_{12}^{-1}e_{z,k+1|k})\right]^{-1} \end{aligned} \tag{3.38}$$

The new SVSF state update equation is therefore defined as follows:

$$x_k = \begin{bmatrix} x_{u_{k+1|k+1}} \\ x_{l_{k+1|k+1}} \end{bmatrix} = \begin{bmatrix} x_{u_{k+1|k}} \\ x_{l_{k+1|k}} \end{bmatrix} + \begin{bmatrix} K_{u_{k+1}} & 0 \\ 0 & K_{l_{k+1}} \end{bmatrix} \begin{bmatrix} e_{z,k+1|k} \\ \Phi_{22}\Phi_{12}^{-1}e_{z,k+1|k} \end{bmatrix} \tag{3.39}$$

Rearranging (3.39), gives the following simplified new SVSF state update equation:

$$x_k = \begin{bmatrix} x_{u_{k+1|k+1}} \\ x_{l_{k+1|k+1}} \end{bmatrix} = \begin{bmatrix} x_{u_{k+1|k}} \\ x_{l_{k+1|k}} \end{bmatrix} + \begin{bmatrix} K_{u_{k+1}} \\ K_{l_{k+1}} \end{bmatrix} e_{z,k+1|k} \tag{3.40}$$

where $K_{l_{k+1}} = K_{L_{k+1}}\Phi_{22}\Phi_{12}^{-1}$.

The following presents the derivation of the complete a priori and a posteriori state error covariance equations for the SVSF with fewer measurements than states. In most cases, the system and measurement matrices are assumed to be known and time invariant. However, this assumption is not critical for the derivation of the SVSF [15]. The a priori state error covariance matrix is defined as follows:

$$P_{k+1|k} = E\{\tilde{x}_{k+1|k}\tilde{x}_{k+1|k}^T\} \tag{3.41}$$

where $\tilde{x}_{k+1|k} = A\tilde{x}_{k+1|k} + w_k$. Based on this, the a priori state error covariance matrix is defined by:

$$P_{k+1|k} = \begin{bmatrix} P_{k+1|k}^{11} & P_{k+1|k}^{12} \\ P_{k+1|k}^{21} & P_{k+1|k}^{22} \end{bmatrix} = AP_{k|k}A^T + Q_k \tag{3.42}$$

Note that (3.42) is identical to the formulation in [17]. The a posteriori state error covariance matrix is defined as follows:

$$P_{k+1|k+1} = E\{\tilde{x}_{k+1|k+1}\tilde{x}_{k+1|k+1}^T\} \tag{3.43}$$

where $\tilde{x}_{k+1|k+1} = x_{k+1} - \hat{x}_{k+1|k+1}$. Manipulation of (3.40) with knowledge of the measurement, measurement errors, and measurement model yields:

$$\begin{bmatrix} \tilde{x}_{u_{k+1|k+1}} \\ \tilde{x}_{l_{k+1|k+1}} \end{bmatrix} = \begin{bmatrix} \tilde{x}_{u_{k+1|k}} \\ \tilde{x}_{l_{k+1|k}} \end{bmatrix} - \begin{bmatrix} K_{u_{k+1}} \\ K_{l_{k+1}} \end{bmatrix} (C_1\tilde{x}_{u_{k+1|k}} + v_{k+1}) \tag{3.44}$$

The a posteriori state covariance matrix is defined by:

$$\begin{aligned} P_{k+1|k+1} &= \begin{bmatrix} P_{k+1|k+1}^{11} & P_{k+1|k+1}^{12} \\ P_{k+1|k+1}^{21} & P_{k+1|k+1}^{22} \end{bmatrix} \\ &= \begin{bmatrix} E\{\tilde{x}_{u_{k+1|k+1}}\tilde{x}_{u_{k+1|k+1}}^T\} & E\{\tilde{x}_{u_{k+1|k+1}}\tilde{x}_{l_{k+1|k+1}}^T\} \\ E\{\tilde{x}_{l_{k+1|k+1}}\tilde{x}_{u_{k+1|k+1}}^T\} & E\{\tilde{x}_{l_{k+1|k+1}}\tilde{x}_{l_{k+1|k+1}}^T\} \end{bmatrix} \end{aligned} \tag{3.45}$$

The elements of the new a posteriori state error covariance are calculated as follows:

$$P_{k+1|k+1}^{11} = P_{k+1|k}^{11} - K_{u_{k+1}} C_1 P_{k+1|k}^{11} - P_{k+1|k}^{11} C_1^T K_{u_{k+1}}^T + K_{u_{k+1}} S_{k+1} K_{u_{k+1}}^T \quad (3.46)$$

$$P_{k+1|k+1}^{12} = P_{k+1|k}^{12} - K_{u_{k+1}} C_1 P_{k+1|k}^{12} - P_{k+1|k}^{11} C_1^T K_{l_{k+1}}^T + K_{u_{k+1}} S_{k+1} K_{l_{k+1}}^T \quad (3.47)$$

$$P_{k+1|k+1}^{21} = P_{k+1|k}^{21} - K_{l_{k+1}} C_1 P_{k+1|k}^{11} - P_{k+1|k}^{21} C_1^T K_{u_{k+1}}^T + K_{l_{k+1}} S_{k+1} K_{u_{k+1}}^T \quad (3.48)$$

$$P_{k+1|k+1}^{22} = P_{k+1|k}^{22} - K_{l_{k+1}} C_1 P_{k+1|k}^{21} - P_{k+1|k}^{12} C_1^T K_{l_{k+1}}^T + K_{l_{k+1}} S_{k+1} K_{l_{k+1}}^T \quad (3.49)$$

where $S_{k+1} = C_1 P_{k+1|k}^{11} C_1^T + R$. The proposed formulation of the a posteriori state error covariance ((3.46)-(3.49)) includes the uncertainties of all measured and non-measured states. This is an essential step in applying data association methods in the context of smooth variable structure filtering.

The following assumptions are used to formulate PDA-SVSF algorithm:

- The target of interest has been initialized.
- If the target-originated measurement falls within the validation gate, then at most one of the validated measurements is originated from the target, and the remaining are originated from any existing clutter.
- The past information through time $k-1$ about the target state is approximated by a normal distribution.
- The stochastic portion of the estimation error is bounded, which is a required condition of stability for the SVSF [15].

The proposed PDA-SVSF algorithm is summarized by three steps: prediction, gating, and update. In the prediction step, the state estimates and measurements are predicted using the system (or motion) and measurement models, and the a priori state error covariance is calculated.

$$\hat{x}_{k+1|k} = A\hat{x}_{k|k} \tag{3.50}$$

$$P_{k+1|k} = \begin{bmatrix} P^{11}_{k+1|k} & P^{12}_{k+1|k} \\ P^{21}_{k+1|k} & P^{22}_{k+1|k} \end{bmatrix} = AP_{k|k}A^T + Q_k \tag{3.51}$$

$$z_{k+1|k} = C\hat{x}_{k+1|k} \tag{3.52}$$

$$S_{k+1} = CP_{k+1|k}C^T + R_{k+1} \tag{3.53}$$

The association probabilities and the combined innovation are calculated using (3.20) and (3.22), respectively. The a priori measurement error is calculated to be equal to the combined innovation, and based on this, the a priori measurement error for the unmeasured states is calculated from (3.37).

$$e_{z_{k+1|k}} = \tilde{z}_k \tag{3.54}$$

The gating step is described next. The received measurements are validated based on the assumptions made earlier. The validation region is an elliptical region defined as a stochastic distance to the predicted measurements, as follows [5] (see the following figure):

$$\mathcal{V}(k+1,\gamma) = \left\{ z : \left[z_{k+1} - \hat{z}_{k+1|k} \right]^T S^T_{k+1} \left[z_{k+1} - \hat{z}_{k+1|k} \right] \leq \gamma \right\} \tag{3.55}$$

where γ is the gate threshold or probability. This value corresponds to the measurement that falls within the gate, if detected.

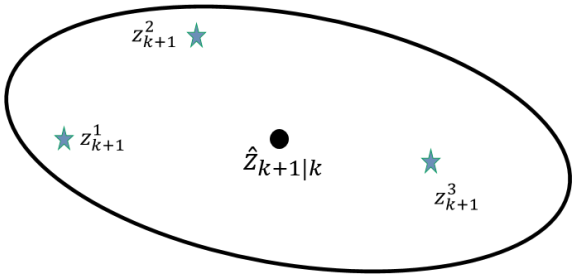

Figure 3.3 Several measurements z_{k+1}^i in the validation region of a single target: an ellipse centered at the predicted measurement $\hat{z}_{k+1|k}$.

Finally, as per state and parameter estimation, the SVSF correction gain is calculated and the states are updated as follows:

$$K_{k+1} = \begin{bmatrix} K_{u_{k+1}} \\ K_{l_{k+1}} \end{bmatrix} \tag{3.56}$$

$$\hat{x}_{k+1|k+1} = \hat{x}_{k+1|k} + K_{k+1} e_{z_{k+1|k}} \tag{3.57}$$

where:

$$K_{u_{k+1}} = H_1^{-1} diag\left[\left(\left|e_{z,k+1|k}\right| + \gamma\left|e_{z,k|k}\right|\right) \circ sat\left(e_{z,k+1|k}, \psi_z\right)\right]\left[diag\left(e_{z,k+1|k}\right)\right]^{-1} \tag{3.58}$$

$$K_{l_{k+1}} = diag\left[\left(\left|\Phi_{22}\Phi_{12}^{-1} e_{z,k+1|k}\right| + \gamma\left|\Phi_{12}^{-1} e_{z,k+1|k}\right|\right) \circ sat\left(\Phi_{22}\Phi_{12}^{-1} e_{z,k+1|k}, \psi_y\right)\right]\left[diag\left(e_{z,k+1|k}\right)\right]^{-1} \tag{3.59}$$

The covariance associated with the updated states is then calculated by (3.8). Note that $P^*(k|k)$ is the SVSF covariance matrix, and is computed by (3.45)-(3.49). Furthermore, $\tilde{P}(k)$ is calculated by (3.24). Note that an a posteriori measurement error is needed in

(3.57). In the typical SVSF scenario, the a posteriori measurement error is calculated as follows:

$$e_{z_{k|k}} = z_k - C\hat{x}_{k|k} \tag{3.60}$$

However, in a target tracking scenario with the presence of clutter, there may be more than one available measurement. To handle this issue, a direct relation between the a posteriori measurement error and the a priori measurement error (which is calculated as a combined innovation of all validated measurements) is required. The a priori measurement error can be interpreted as the innovation of a projected real measurement and the predicted measurement, as follows:

$$e_{z_{k|k-1}} = z_k^h - \hat{z}_{k|k-1} \tag{3.61}$$

therefore:

$$z_k^h = e_{z_{k|k-1}} + \hat{z}_{k|k-1} \tag{3.62}$$

$$z_k^h = e_{z_{k|k-1}} + C\hat{x}_{k|k-1} \tag{3.63}$$

Substitution of the projected real measurement from (3.63) into (3.60), yields the following equation:

$$e_{z_{k|k}} = e_{z_{k|k-1}} + C\hat{x}_{k|k-1} - C\hat{x}_{k|k} \tag{3.64}$$

Simplification of the above equations yields a direct relation between the a posteriori and a priori measurement errors, as follows:

$$e_{z_{k|k}} = [I - CK_k]e_{z_{k|k-1}} \tag{3.65}$$

Equation (3.65) is used to update the a posteriori measurement error in the CM-PDA-SVSF process. The above three steps are repeated recursively.

3.5.2 Covariance Modified JPDA-SVSF (CM-JPDA-SVSF)

The joint probabilistic data association smooth variable structure filter (JPDA-SVSF) is an extension of the PDA-SVSF, described earlier. The JPDA-SVSF enables tracking multiple targets with the presence of clutter [57]. In the JPDA-SVSF algorithm, the association probabilities are calculated jointly across the targets; while in the PDA-SVSF, different filters are used for each target. The following figure illustrates a schematic representation of the JPDA-SVSF process [57].

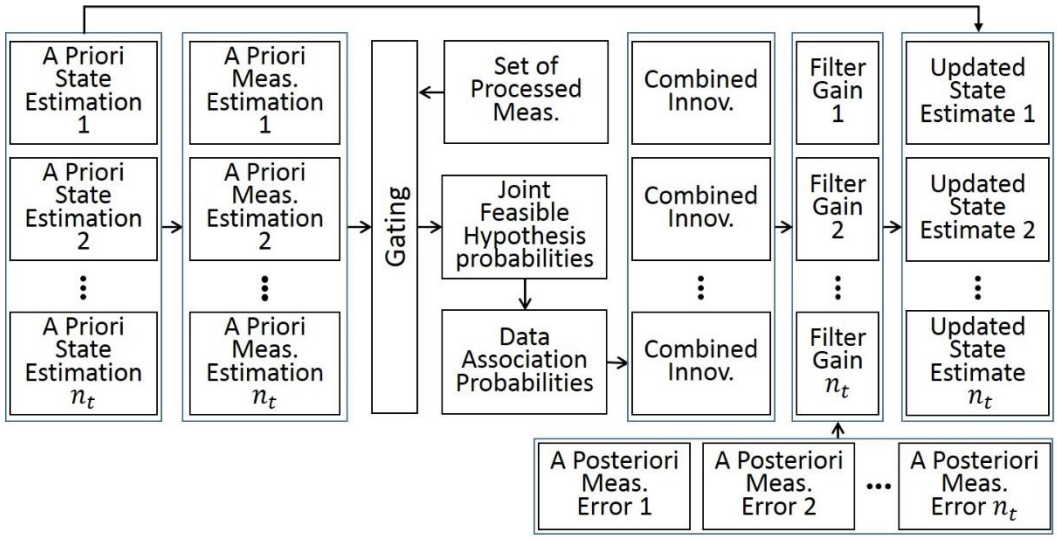

Figure 3.4 Flowchart of the proposed JPDA-SVSF algorithm [57]

Similar to the PDA-SVSF, the JPDA-SVSF algorithm consists of three main steps: state prediction, gating, and state update. However, in the prediction step, the association

probabilities are calculated using all of the feasible association hypotheses, as per (3.26). The marginal association probabilities defined by (3.28) are used to calculate the combined innovation for each track:

$$\tilde{z}_k^t = \sum_{i=1}^{m_k} \beta_k^{it} e_{z,k+1|k}^{it} \tag{3.66}$$

The update step is performed separately for each track, and the state error covariance is calculated by (3.45)-(3.49). Furthermore, note that the new covariance formulation presented in this paper improves both the gating and data association steps of the method.

3.6 Target Tracking Cases and Results

This section describes the results of a number of target tracking scenarios. The first case compares the results of applying the PDA-KF and the PDA-SVSF to a single target tracking scenario. The second compares the results when the methods are applied to a multiple target tracking problem.

3.6.1 Single Target Tracking with Clutter

This scenario studies the results of a single target tracking scenario with clutter. There are two parts to this problem: presence of no modeling uncertainty, and presence of modeling uncertainty. A simple two-dimensional discrete, constant velocity model is implemented as per [6]. The PDA-KF, the PDA-SVSF, and CM-PDA-SVSF are applied for the purposes of target tracking and the results are compared. Note that the PDA-SVSF refers to the standard covariance matrix as per [17], whereas the CM-PDA-SVSF refers to the modified

covariance formulation presented earlier in Section 3.5 ((3.45)-(3.49)). The state vector is defined as $\boldsymbol{x} = [x\ y\ v_x\ v_y]$, where x and y are the position in two Cartesian directions, and v_x and v_y are the corresponding velocities. In this model, the accelerations of the target between two sequential samples are assumed to be constant with discrete-time zero mean white Gaussian noise. The system or motion model is defined as follows:

$$x(k+1) = Ax(k) + Gv(k) \tag{3.67}$$

where the system and process noise gain matrices are defined by:

$$A = \begin{bmatrix} 1 & 0 & T_s & 0 \\ 0 & 1 & 0 & T_s \\ 0 & 0 & 1 & 0 \\ 0 & 0 & 0 & 1 \end{bmatrix} \tag{3.68}$$

$$G = \begin{bmatrix} T_s^2/2 & 0 \\ 0 & T_s^2/2 \\ T_s & 0 \\ 0 & T_s \end{bmatrix} \tag{3.69}$$

The white acceleration noise is defined as follows:

$$Q = cov\{v(k)\} = \begin{bmatrix} \sigma_v^2 & 0 \\ 0 & \sigma_v^2 \end{bmatrix} \tag{3.70}$$

The measurement function, matrix, and noise covariance are defined respectively as follows:

$$z(k) = Cx(k) + w(k) \tag{3.71}$$

$$H = \begin{bmatrix} 1 & 0 & 0 & 0 \\ 0 & 1 & 0 & 0 \end{bmatrix} \tag{3.72}$$

$$R = cov\{w(k)\} = \begin{bmatrix} \sigma_w^2 & 0 \\ 0 & \sigma_w^2 \end{bmatrix} \tag{3.73}$$

Simulations are run for the PDA-KF, PDA-SVSF, and CM-PDA-SVSF algorithms. The parameter values used for the simulations are $T_s = 0.5\,s$ and $P_D = 0.95$. The clutter is assumed to have a spatial uniform distribution, and the number of cluttered measurements is generated by a Poisson's distribution of $\lambda = 10^{-2}$. The process noise variance is $\sigma_v^2 = 1^2$, and the measurement noise variance is $\sigma_w^2 = 4^2$.

The RMSE errors for the four states of the system are computed for 250 Monte-Carlo runs and shown in Table 3.1. Note that all three strategies have an acceptable level of performance. In terms of RMSE, the KF-PDA performed slightly better than the SVSF-based PDAs. Figure 3.5 illustrates the trace of the covariance matrix for the strategies. The proposed covariance of this paper, described in Section 3.5, improved the efficiency of the estimator in terms of the trace of the covariance matrix or state estimation errors.

Table 3.1 RMSE Results for Single Target Tracking Case (No Uncertainty)

	PDA-KF	PDA-SVSF	CM-PDA-SVSF
x	1.26	2.23	2.02
y	1.25	2.12	1.99
v_x	0.98	5.92	1.62
v_y	0.95	5.13	1.46

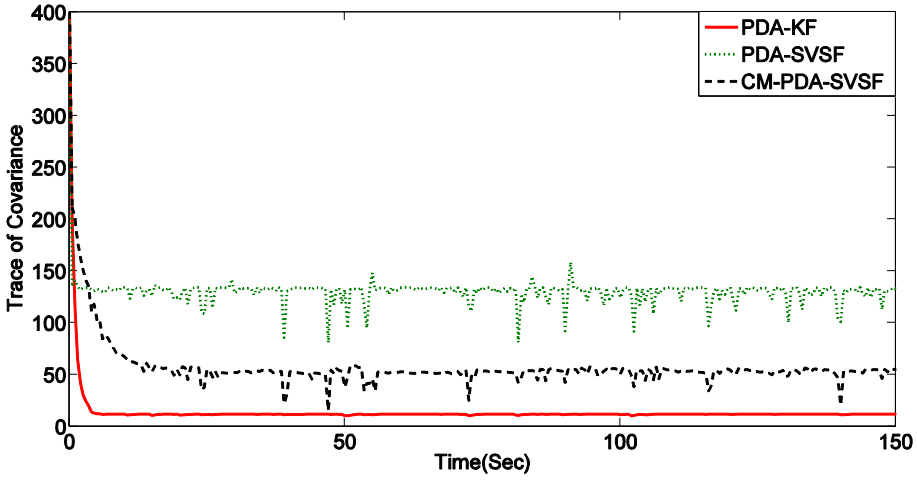

Figure 3.5 Trace of the covariance matrix for the three strategies (no uncertainty)

The consistency of the proposed estimation algorithm is also examined. The examination is based on normalized estimation error squared (NEES) [6]. The results for CM-PDA-SVSF algorithm are shown in Figure 3.6 for 250 Monte-Carlo runs. The one-sided 95% probability interval was used. The results show that the CM-PDA-SVSF is a pessimistic filtering approach.

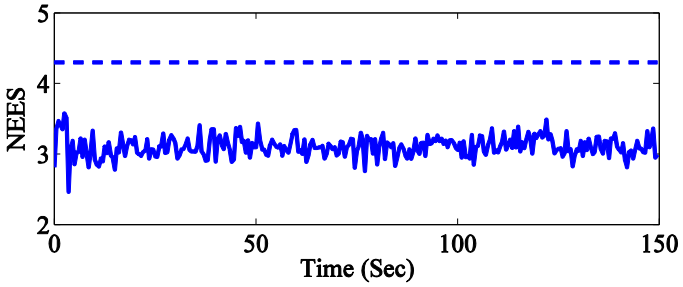

Figure 3.6 NEES (normalized estimation error squared) for CM-PDA-SVSF compared to upper bound of 95% probability interval

To further investigate the robustness of the proposed SVSF-based methods, modeling uncertainty of 4% was injected into the simulation between $t = 50s$ and $t = 60s$. The uncertainty is an incremental change of two elements of the state transition matrix (3.68) in the form of increasing the sampling time T_s by a specified percentage ε, as follows.

$$A = \begin{bmatrix} 1 & 0 & T_s(1+\varepsilon) & 0 \\ 0 & 1 & 0 & T_s(1+\varepsilon) \\ 0 & 0 & 1 & 0 \\ 0 & 0 & 0 & 1 \end{bmatrix} \tag{3.74}$$

The tracking success rate for three algorithms for two scenarios with injected uncertainty under 100 Monte-Carlo runs is shown in the following table.

Table 3.2 Tracking success rate for single target tracking case

Injected Uncertainty	PDA-KF	PDA-SVSF	CM-PDA-SVSF
2%	43%	93%	99%
4%	9%	54%	81%

As the higher tracking success rate indicates, the SVSF-based PDAs and more specifically CM-PDA-SVSF provided more stable estimate. The following figure, illustrates a sample scenario of injecting modeling uncertainty into the estimation process which causes the PDA-KF to fail. These results are due to the strict assumptions of the KF.

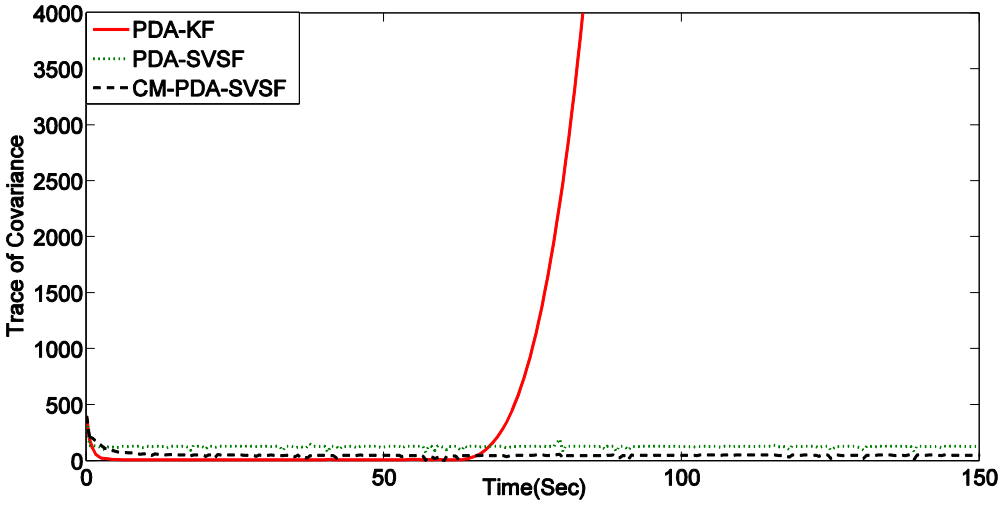

Figure 3.7 Trace of the covariance matrix for the three strategies (uncertainty case)

3.6.2 Multiple Target Tracking with Clutter

This target tracking scenario consists of three maneuvering cars, described as follows (Figure 3.8).

Car #1. The initial state is ($x_0 = 200\,m,\ y_0 = 50,\ v_{x_0} = 28\,m/s,\ v_{y_0} = 1$). It performs a non-maneuvering constant velocity motion between $0\,s$ and $93s$, a "straight line and curve" maneuver between $94\,s$ and $138\,s$, and a non-maneuvering constant velocity motion between $139\,s$ and $500\,s$.

Car #2. The initial state is ($x_0 = -1000\,m, y_0 = 25, v_{x_0} = 33\,m/s, v_{y_0} = 1$). It performs a non-maneuvering constant velocity motion between $0\,s$ and $115\,s$, a "straight line and curve" maneuver between $116\,s$ and $157\,s$, a non-maneuvering constant velocity

motion between 158 s and 236 s, a "cut-in-out" maneuver between 237 s and 312 s, and a non-maneuvering constant velocity motion between 305 s and 500 s.

Car #3. The initial state is ($x_0 = -2000\,m,\ y_0 = 0,\ v_{x_0} = 34\,m/s,\ v_{y_0} = 1$). It performs a non-maneuvering constant velocity motion between 0 s and 139 s, a "straight line and curve" maneuver between 140 s and 180 s, a non-maneuvering constant velocity motion between 181 s and 357 s, a "cut-in-out" maneuver between 358 s and 407 s, and a non-maneuvering constant velocity motion between 407 s and 500 .

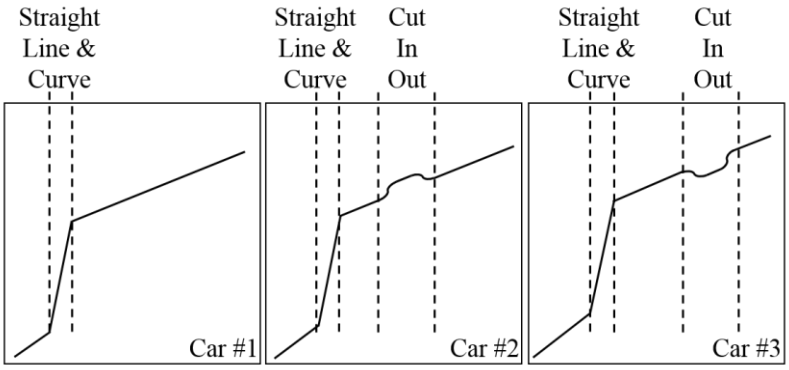

Figure 3.8 Vehicle trajectories illustrating their maneuvers

Although the cars experience maneuvering behaviours, the three algorithms (JPDA-KF, JPDA-SVSF and CM-JPDA-SVSF) will only use the near-constant velocity model as the motion model: in addition to dealing with measurements from interfering vehicles and clutter, the algorithms will also have to overcome modeling uncertainty. The following figure shows the true trajectories for the three cars, as well as the estimated trajectories. All of the methods overcame the uncertainties, and were able to track the trajectories. The following table provides the RMSE of the states for the three vehicles.

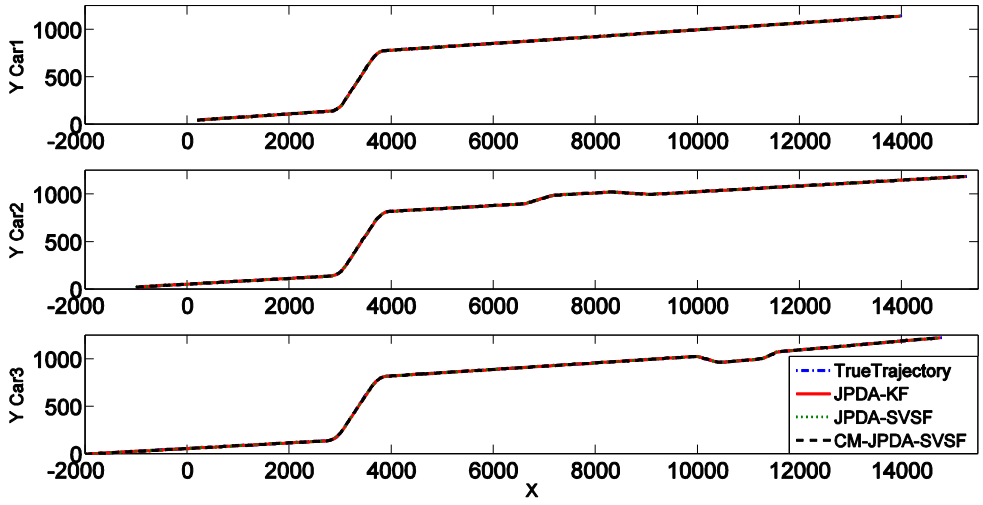

Figure 3.9 Vehicle trajectories with corresponding estimates

(all three performed similarly)

Table 3.3 RMSE Results for Multiple Target Tracking Case (First Case)

	Car #1			Car #2			Car #3		
	JPDA-KF	JPDA-SVSF	CM-JPDA-SVSF	JPDA-KF	JPDA-SVSF	CM-JPDA-SVSF	JPDA-KF	JPDA-SVSF	CM-JPDA-SVSF
x	27.55	27.60	27.58	32.57	32.57	32.57	33.55	33.55	33.54
y	4.83	4.84	4.86	5.25	5.29	5.27	5.46	5.49	5.50
v_x	1.99	2.01	1.92	1.84	2.13	1.74	1.79	2.02	1.97
v_y	1.23	1.51	1.15	1.65	1.61	1.28	1.69	1.52	1.38

To increase the complexity of this scenario, the car trajectories were made to infer with each other. Car #1 and Car #2 were brought as close as 6.49 meters at $t = 240\ s$ during which Car #2 performs a cut-in-out maneuver. Also, Car #1 and Car #3 were as close as 8 meters at $t = 375\ s$, during which Car #3 performs a cut-in-out maneuver (Figure 3.10).

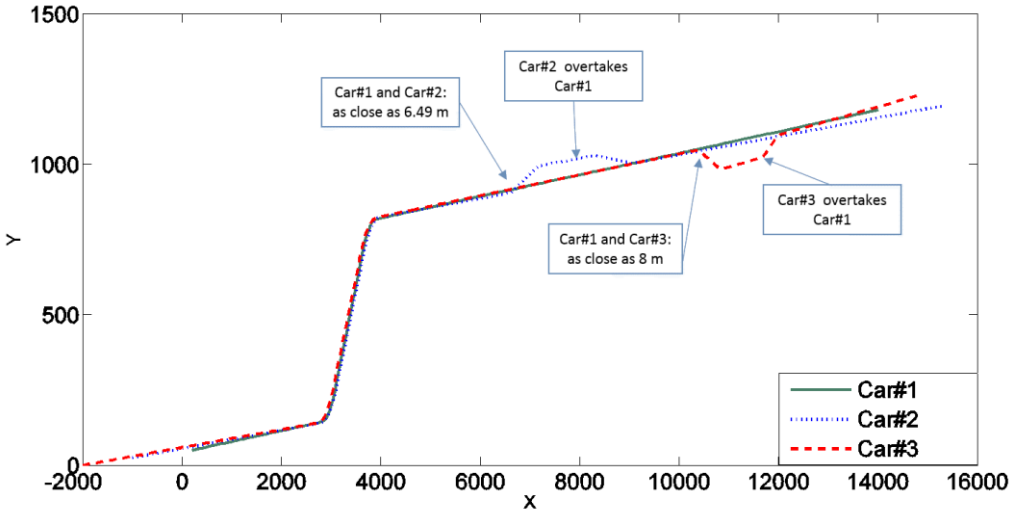

Figure 3.10 Interfering car trajectories

The performance of the three algorithms is illustrated in the following figure. Since the SVSF-based methods are more robust against modeling uncertainties, they were expected to handle the interfering trajectories.

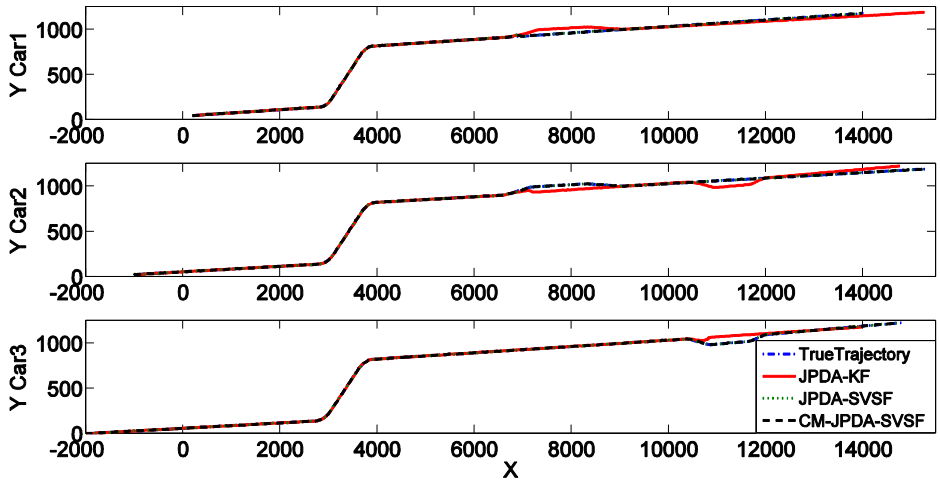

Figure 3.11 Interfering vehicle trajectories with corresponding estimates.

The proposed CM-JPDA-SVSF and JPDA-SVSF successfully handled the interfering car trajectories, whereas the JPDA-KF failed to track the correct vehicle trajectories. These results further demonstrate the robustness of the SVSF filtering strategy, which is inherently stable due to the switching nature of the corrective gain. The following figure shows the trace of the covariance over time.

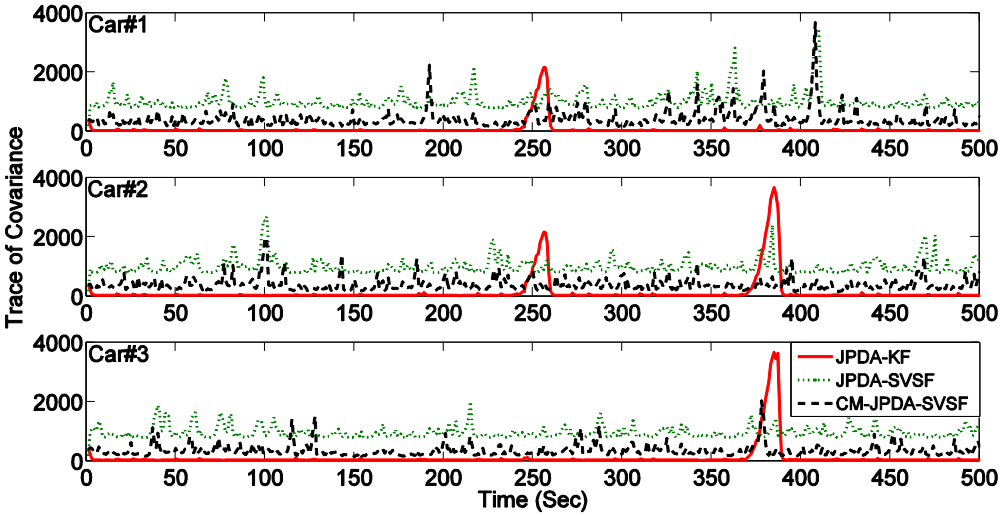

Figure 3.12 Trace of the covariance matrix for the interfering vehicle trajectories.

Furthermore, note that 100 Monte Carlo runs were performed to ensure an average result. The RMSE for the estimated states provided by the JPDA-SVSF and CM-JPDA-SVSF are shown in the following table. Note that the results were similar for the states that have corresponding measurements. However, the CM-JPDA-SVSF method significantly improves the non-measured estimates.

Table 3.4 RMSE Results for interfering Multiple Target Tracking case (JPDA-SVSF and CM-JPDA-SVSF)

	Car #1		Car #2		Car #3	
	JPDA-SVSF	CM-JPDA-SVSF	JPDA-SVSF	CM-JPDA-SVSF	JPDA-SVSF	CM-JPDA-SVSF
$\boldsymbol{x}$	27.48	27.30	32.65	32.65	33.71	33.97
$\boldsymbol{y}$	5.03	5.12	5.56	5.57	5.60	5.81
$\boldsymbol{v_x}$	2.07	1.89	2.25	1.74	2.19	1.97
$\boldsymbol{v_y}$	1.47	1.06	1.55	1.28	1.56	1.38

3.7 Conclusions

This paper introduced new formulations for the smooth variable structure filter (SVSF) for target tracking scenarios. The PDA-SVSF and JPDA-SVSF algorithms were introduced and described, and applied on a series of target tracking problems. The results were compared with the popular Kalman filter (KF) based strategies. It was determined that the SVSF-based target tracking strategies were more robust to the presence of modeling uncertainty and interfering targets. This is due to the inherent stability present in the SVSF caused by the switching effect of the gain. In addition, a new covariance formulation based on the Luenberger observer was formulated and the CM-SVSF was presented. The CM-SVSF was found to outperform the SVSF in terms of estimating non-measured states.

The main contribution of this paper is based on the proposed estimation strategy used in the context of data association methods. Future work may include implementation with other data association trackers.

Chapter 4

An SVSF-Based Generalized VBL-SVSF for Target Tracking in Clutter

4.1 Abstract

Autonomous self-drive requires intelligence and cognition that relies on observations and tracking of the state of motion of surrounding vehicles. This information can be acquired by using sensors; but these are often affected by clutter and noise that in turn introduce the issues of estimation and data origin uncertainty into the tracking system. The most popular methods for estimation and tracking are based on the well-studied Kalman filter (KF). KF is optimal when noise is white and remains so despite uncertainties in the filter model; the robustness and stability of the KF is affected if this condition is not met. The smooth variable structure filter (SVSF) is a relatively new method which is more robust to disturbances and uncertainties. The SVSF ensures stability by using a discontinuous corrective term that maintains estimates to within a subspace of the true state trajectory. The discontinuous corrective term result in chattering that is removed by using a smoothing boundary layer. In this paper, a generalized covariance formulation of the SVSF and a generalized optimal time varying smoothing boundary layer is proposed. The generalized optimal SVSF is then combined with joint probabilistic data association (JPDA) technique

for target tracking. The robustness and accuracy of the new form of filtering and data association is validated and comparatively analyzed by its application to an experimental traffic monitoring system based on LiDAR (LIght Detection And Ranging).

4.2 Introduction

Tracking has numerous applications such as in surveillance, air traffic control, medical imaging, finance, autonomous vehicles, driver assist, and aerospace. Tracking involves recursively estimation of an unknown variable or state over time from indirect, inaccurate and uncertain observations [6]. The unknown variable might be the temperature in a chamber, the position or velocity of a vehicle, stock value in the market, or the movement of a cell in a blood vessel. Tracking is increasingly being used in automotive applications as a consequence of a societal need for autonomous cars or those with advanced driver assist capability [70, 61]. In autonomous vehicles or driver-assist systems applications, tracking requires observations of the position of surrounding vehicles acquired using sensors mounted on the car, such as a radar, a LiDAR, and/or cameras [70, 71]. The sensory observations are often affected by clutter and noise. As such tracking systems requiring filtering and estimation strategies that are robust and capable of dealing with data origin uncertainty, especially when dealing with multiple targets. For the latter problem of data origin uncertainty in multiple target tracking, there are a number of different data association algorithms proposed in the literature [4, 1]. Data association techniques differentiate measurements from different targets of interest [4, 1]. One of the simplest algorithms is the standard nearest neighbor filter (SNNF), which associates the nearest measurement, in the sense of the statistical distance, to each target [4]. The global nearest

neighbour filter is an extension of SNNF that looks for one single most probable association hypothesis [1].

The probabilistic data association filter (PDA) is one of the most commonly used data association methods [27]. The PDA takes all feasible measurement-to-track association hypotheses into consideration, and calculates the association probability for the track [5]. Hence, it is an all-neighbor data association method. Since the PDA assumes that the track has already been initialized, another algorithm is required to handle the track maintenance, such as logic-based track formation [4], or track-score base methods [1]. Also, the integrated probabilistic data association (IPDA) is a derivation of the PDA without the aforementioned assumption, that yields the data association probabilities as well as track existence probabilities [28]. The original derivation of the PDA is for single-target tracking in the presence of clutter. Therefore, for multiple-target tracking, a number of PDA's may be used in parallel [5]. When the target trajectories are interfering, an extension of PDA, named as the joint probabilistic data association (JPDA), is utilized and has improved performance [31]. In JPDA, the association probabilities are calculated in a joint manner across all targets [31].

In 1979 the multiple hypothesis tracker (MHT) is presented [32]. In MHT all the measurement to track assignments are enumerated; then the infeasible assignments are eliminated using pruning and gating methods, which imposes the risk of the elimination of the correct measurement sequences. Unlike the traditional MHT, the probabilistic multi hypothesis tracking (PMHT) is based on the calculation of the probability of each measurement belonging to each track by a Bayesian inference [33]. In PMHT, the hard decision of measurement to track is avoided by a joint estimation of the target states and measurement-to-track association probabilities [33]. A literature review of the advances in PMHT is presented in [34].

Another approach to treat multiple targets and observations is a method based on random finite set concept, named as probability hypothesis density (PHD) filter. Some of the approximations to deal with the PHD recursion are suggested, including Sequential Monte Carlo PHD (SMCPHD) filter [35], Cardinalised PHD (CPHD) filter [36] and Gaussian Mixture PHD (GMPHD) filter [37].

Once the measurement-to-track association is performed, an estimation strategy is required to update the tracks. For each hypothesis, an association probability is calculated which is used to construct a combined innovation term. This term is a weighted sum of all the innovations, and is used by the estimation strategy [4].

The most popular and well-studied model based estimation strategy is the Kalman filter (KF) introduced in late 1950s [6]. The KF is described based on the following motion and measurement models:

$$x_{k+1} = Ax_k + Bu_k + w_k \tag{4.1}$$

$$z_k = Hx_k + v_k \tag{4.2}$$

where x_k and z_k are state and measurement vectors, of dimensions of $(n \times 1)$ and $(m \times 1)$, respectively, and w_k and v_k are zero mean white Gaussian process and measurement noise, with covariance matrices Q_k and R_k, respectively. The KF provides the best solution in the sense of minimum mean square error for linear estimation problems in the presence of Gaussian noise [6]. The KF succeeds this task as its gain is optimized to minimize the a posteriori state covariance matrix [17]. The formulation of the KF consists of two major steps: prediction and update. The prediction step of the KF is governed by (4.3) and (4.4), where the state estimate is predicted in (4.3), and the corresponding state error covariance is calculated as per (4.4).

$$\hat{x}_{k+1|k} = A\hat{x}_{k|k} + Bu_k \tag{4.3}$$

$$P_{k+1|k} = AP_{k|k}A^T + Q_k \tag{4.4}$$

In the next step, the gain is calculated and the a posteriori estimated state and its corresponding covariance are updated as follows:

$$S_{k+1} = HP_{k+1|k}H^T + R_{k+1} \tag{4.5}$$

$$K_{k+1} = P_{k+1|k}H^T S_{k+1}^{-1} \tag{4.6}$$

$$\hat{x}_{k+1|k+1} = \hat{x}_{k+1|k} + K_{k+1}\left[z_{k+1} - H\hat{x}_{k+1|k}\right] \tag{4.7}$$

$$P_{k+1|k+1} = [I - K_{k+1}H]P_{k+1|k} \tag{4.8}$$

Equations (4.3) to (4.8) summarize the KF method for linear estimation problems. For nonlinear estimation problems, the classical KF has been reformulated [6]. The most popular and simplest revised strategy is the Extended KF (EKF), where the system is linearized according to the Jacobian matrix [11]. However, the linearization process introduces some uncertainty to the system that may cause instability [6].

The KF is based on the linear Gaussian (LG) assumption, i.e. the system is known and linear, system noise and measurement noise are zero-mean white Gaussian with known covariance matrices, and the initial state is modeled as Gaussian with known mean and covariance [6]. The KF yields suboptimal results and is prone to instability if these assumptions do not hold [11]. In an effort to reduce the effects of modeling uncertainties, robust Kalman filtering has been suggested [13, 14, 11]. These techniques try to deal with uncertainties in the system and measurement matrices, or noise covariance matrices. When dealing with uncertainties in the system and measurement matrices, the robust estimator is designed such that it gives an upper bound on the error variance for any allowed modeling

uncertainty [13, 14]. When the uncertainties in noise covariance matrices are dealt with, the KF gain is derived to minimize the estimation error covariance as well as its variation due to changes in process and measurement noise covariance matrices. In this way the sensitivity of the estimation error covariance to changes in the process and measurement noise covariances is reduced [11].

The Gaussian assumption for the noise distribution may be relaxed by implementing a Gaussian mixture to approximate the non-Gaussian probability distribution function (pdf), though increasing the computational complexity [11]. Another approach for nonlinear and non-Gaussian systems is the particle filter (PF) [12]. The PF represents the posterior density by a set of random independent identical distribution (i.i.d.) samples (particles) from the pdf.

A recent robust filtering technique that is less sensitive to modeling uncertainties and is computationally efficient is the Smooth Variable Structure Filter (SVSF) [15]. The SVSF is based on concepts that are closely related to sliding mode control, where the stability can be guaranteed given bounded parametric uncertainties [15]. The SVSF uses a discontinuous gain to maintain the estimated states to within a subspace around the true trajectories known as the existence subspace [15]. Modifications to the SVSF have been proposed, including an optimal form in [17]. To deal with the cases when there are fewer measurements that states, Luenberger observer based approach has originally been proposed in [15]. In later modifications of the SVSF, as in [17], however, this approach has not been mathematically derived and justified.

The SVSF has been used in target tracking applications in the presence of clutter [72, 57, 54, 73]. In [54] and [57], the SVSF has been combined with the PDA and the JPDA, and the results indicate a notably improved performance over the original PDA and JPDA

methods. A combination of PDA-SVSF for maneuvering target tracking has been discussed in [72]. A generalized form of SVSF covariance in the context of tracking single and multiple targets in the presence of clutter has been derived and discussed in [73]. In order to get the best use of the SVSF in the target tracking in clutter applications, a generalized optimal form of the SVSF is addressed in this paper. In the previous derivations of the optimal SVSF [15], there was an assumption of a full measurement matrix, which is relaxed by this new derivation providing a generalized form for the case of fewer number of measurements than the number of states. This new formulation is used for multiple target tracking when there is the issue of data origin uncertainty.

Section 4.3 provides a brief overview of data association principles. The SVSF estimation strategy is summarized in Section 4.4. Section 4.5 presents a new methodology for multiple target tracking in the presence of clutter. A new formulation of SVSF covariance and the derivation of a generalized optimal smoothing boundary layer with respect to the generalized state error covariance matrix is presented. In Section 4.6, a tracking simulation problem is described and then the new proposed method is comparatively analyzed in terms of its estimation accuracy and robustness to uncertainties. Furthermore, the method is experimentally evaluated and applied to a LiDAR based automotive tracking system. The conclusions are provided in Section 4.7.

4.3 Probabilistic Data Association Principle

In multiple-target tracking, there are often more than one measurements associated with one target. The reason is the presence of false measurements or clutter. The aim of a data association method is to assign the measurements to the targets in an efficient way. To

avoid searching the entire measurement set for the measurements originated from a specific target, an ellipsoidal gate is set up for each target, and such a gate is called a validation region [5] (Figure 4.1).

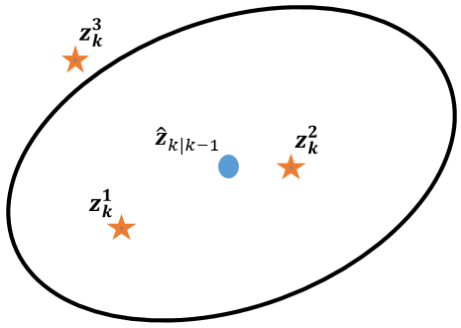

Figure 4.1 The ellipsoidal validation region of a target centered at its predicted measurement $\hat{z}_{k|k-1}$. Two of the three measurements have fallen within the validation region of the target.

The probability with which the target-originated measurement falls within the validation region is called the gate probability [5, 1]. If more than one measurement falls within the gate, then an association uncertainty arises. It is required to decide which measurement is originated form the target and therefore should be used to update the track [4].

The probabilistic data association (PDA) and its extensions are used to handle the problem of data origin uncertainty in multi-target tracking scenarios. The PDA is originally formulated for single target tracking in the presence of clutter.

In PDA, it is assumed that the track of the target has been initialized, and the past information through time $k-1$ about the target trajectory is in the form of a normal distribution [5]:

$$p[x_k|Z^{k-1}] = \mathcal{N}[x_k; \hat{x}_{k|k-1}, P_{k|k-1}] \tag{4.9}$$

Also, if the target is detected, it is also assumed that at most one target originated measurement has fallen within the validation region. The number of false measurements inside the gate is Poisson distributed with parameter λ and their spatial density is modeled as an independent and identically distributed (i.i.d.) uniform distribution [5]. The PDA is a type of all-neighbor association that uses all the validated measurements to update the corresponding track. The idea is to define a weight for each validated measurement z^i , $i = 1, \dots, n_k^m$, in accordance with the probability that it is originated from the associated track [5]. These weights are named as association probabilities. For n_k^m validated measurements at time k, one can form $n_k^m + 1$ distinct association hypotheses as [1]:

$$\mathcal{H}_k^i = \{z^i \; is \; target \; originated \;\} \tag{4.10}$$

$$\mathcal{H}_k^0 = \{none \; are \; target \; originated\} \tag{4.11}$$

The total available measurements at time k are $Z^k = \{z^1, \dots, z^{n_k^m}\} \cup Z^{k-1}$. The association probability, β_k^i is defined as the conditioned probability of the ith hypothesis at time k, as follows [1]:

$$\beta_k^i = P\{\mathcal{H}_k^i | Z^k\} \tag{4.12}$$

These association probabilities for each hypothesis are computed as follows [4, 5]:

$$\beta_k^i = \begin{cases} \dfrac{1 - P_D P_G}{1 - P_D P_G + \sum_{i=1}^{n_k^m} \mathcal{L}_k^i}, & i = 0 \\ \dfrac{\mathcal{L}_k^i}{1 - P_D P_G + \sum_{i=1}^{n_k^m} \mathcal{L}_k^i}, & i = 1, \dots, n_k^m \end{cases} \tag{4.13}$$

where P_G is gate probability [8], and P_D is the target detection probability. In addition:

$$\mathcal{L}_k^i = \frac{\mathcal{N}\left[z_k^i; \hat{z}_{k|k-1}, S_k\right] P_D}{\lambda} \tag{4.14}$$

which is the likelihood ratio of the measurement z_k^i, assuming that it is target originated [5]. The association probabilities are used to calculate a combined innovation to be used in the filter update, as follows:

$$\tilde{z}_k = \sum_{i=1}^{n_k^m} \beta_k^i \tilde{z}_k^i \tag{4.15}$$

where $\tilde{z}_k^i = z_k^i - H x_{k|k}$ is the innovation of measurement i [5]. The states are updated with the standard KF estimation strategy (Equations (4.3) to (4.7)). To update the covariance, the following equation is used:

$$P_{k|k} = \beta_k^0 P_{k|k-1} + [1 - \beta_k^0] P_{k|k}^* + \tilde{P}_k \tag{4.16}$$

where $P_{k|k}^*$ is the standard KF covariance matrix as in equation (4.8) and $\tilde{P}_k$ accounts for uncertainty increment due to association uncertainty. It is computed as follows [4]:

$$\tilde{P}_k = K_k \left[\sum_{i=1}^{n_k^m} \beta_k^i \tilde{z}_k^i \tilde{z}_k^{i\prime} - \tilde{z}_k \tilde{z}_k{}' \right] K_k' \tag{4.17}$$

The PDA has been extended to the Joint Probabilistic Data Association (JPDA) for dealing with the interfering targets in the multiple target tracking problems. The difference between PDA and JPDA is in the way the association probabilities are calculated. The PDA considers the tracks as separate elements and forms the association probabilities separately for each track. However, in the presence of multiple interfering targets that share some measurements, the tracks are no longer acting as separate entities [5]. The JPDA considers joint association hypotheses to calculate the association probabilities, and hence the interfering targets are handled more efficiently by JPDA [31]. The conditional probabilities of the following joint hypotheses are evaluated as follows [5]:

$$\mathcal{H}_k = \bigcap_{j=1}^{m_k} \mathcal{H}_k^{jt_j} \tag{4.18}$$

where $\mathcal{H}_k^{jt}$ is the hypothesis that measurement j originated from target $t, 1 \leq j \leq m_k$, $0 \leq t \leq T$, k is the time index, t_j is the target that measurement j is associated with in the considered hypothesis, m_k is the number of measurements, and T is the number of targets [31]. The joint association probabilities are calculated as follows [5]:

$$P\{\mathcal{H}_k|Z^k\} = c \prod_j \left\{\lambda^{-1}\mathcal{L}_k^{t_j}\right\}^{\tau_j} \prod_t (P_D^t)^{\delta_t}(1 - P_D^t)^{1-\delta_t} \tag{4.19}$$

where λ is the spatial density of the number of false measurements defined from a Poisson distribution, and P_D^t is the detection probability of target t. τ_j and δ_t are the target detection and measurement association indicators, respectively [31] and,

$$\mathcal{L}_k^{t_j} = \mathcal{N}[z_k^j; \hat{z}_{k|k-1}^{t_j}, S_k^{t_j}] \tag{4.20}$$

To carry out the state estimation for each target, the marginal association probabilities are needed [31]. These probabilities are obtained from joint probabilities (4.19) by summing the joint hypotheses in which the marginal hypothesis of interest is included, as follows [5]:

$$\beta_k^{jt} = P\{\mathcal{H}_k^{jt}|Z^k\} = \sum_{\mathcal{H}:\mathcal{H}^{jt}\in\mathcal{H}} P\{\mathcal{H}_k|Z^k\} \tag{4.21}$$

These probabilities are used to create the combined innovation for each target, which is used during the filter update stage.

4.4 Smooth Variable Structure Filter

The smooth variable structure filter (SVSF) is a revised form of the VSF, and was first presented in 2007 [15]. The SVSF is a predictor-corrector state and parameter estimation method based on the sliding mode concept [15, 17]. The SVSF operation is shown in Figure 4.2. Basically, the SVSF uses a switching corrective gain to force the estimated stated to within a boundary around the true state trajectory, named as the existence subspace. The corrective gain is designed based on a Lyapunov based stability theorem [15] such that it makes sure that the estimation error keeps getting smaller by each iteration. This way, it maintains the estimates within this subspace given bounded disturbances [15, 17]. The discontinuous corrective action of the SVSF results in chattering that can be removed by using a smoothing boundary layer.

The SVSF, in its original form [15], did not have a covariance formulation. In [17], an iterative strategy for generating an error covariance matrix was proposed. The error covariance was then used for obtaining a variable and optimal smoothing boundary layer

in [17]. To deal with the cases when there are fewer measurements than states, Luenberger observer based approach has originally been proposed in [15]. In later modifications of the SVSF, as in [17], however, this approach has not been mathematically derived and justified. The SVSF formulation has been modified to a general form to include the case when there are fewer number of measurements than states in [73].

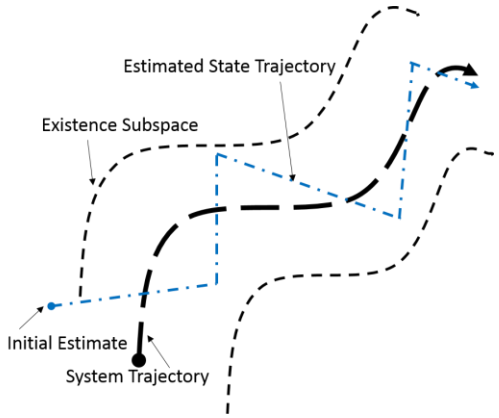

Figure 4.2 SVSF estimation concept [15]

A similar strategy to Luenberger's reduced order observer [15] is adopted, and then the respective modified covariance is derived. The steps of the aforementioned covariance modified SVSF applied to a linear system are considered as follows [73].

Similar to the KF strategy, the SVSF consists of two main steps: prediction and update. However, the main difference lies in how the SVSF gain is formulated. Conceptually, by use of the SVSF corrective gain, the SVSF converges the estimated state trajectory to within an existence subspace around the true trajectory. The width of the existence subspace is a function of uncertain dynamics due to uncertainties. Once the estimated states are in that subspace, they switch back and forth across the true trajectory and will remaining within this subspace [15], as shown in Figure 4.2. To formulate the SVSF approach, consider the

model of equations (4.1) and (4.2) where the measurement matrix H is of dimension $m \times n$, $m < n$ is the number of measured states, n is the rank of the system, and:

$$H = [H_1 \quad H_2] \tag{4.22}$$

where H_1 is of dimension $m \times m$ and H_2 is a null matrix of dimension $m \times (n - m)$. The state vector of the system can be transformed and partitioned into two segments as follows:

$$x_k = \begin{bmatrix} x_{u_k} \\ x_{l_k} \end{bmatrix} = \begin{bmatrix} x_k^1 \\ \vdots \\ x_k^m \\ \hline x_k^{m+1} \\ \vdots \\ x_k^n \end{bmatrix} \tag{4.23}$$

where, x_{u_k} is the measured portion of the states and x_{l_k} is the non-measured portion of the states. This partitioning of states is required to treat the system with an approach similar to the Luenberger's reduced order observer. The SVSF approach uses a switching hyperplane based on the state trajectory to achieve robust stability. The state partitioning of (4.23) allows a projection of switching hyperplane for states that do not have direct measurements associated with them [15]. The prediction step consists of the following equations ((4.24) to (4.26)):

$$\hat{x}_{k+1|k} = A\hat{x}_{k|k} + Bu_k \tag{4.24}$$

The a priori state error covariance matrix is defined as follows:

$$P_{k+1|k} = E\{\tilde{x}_{k+1|k}\tilde{x}_{k+1|k}^T\} \tag{4.25}$$

where $\tilde{x}_{k+1|k} = A\tilde{x}_{k|k} + w_k$. Based on this, the a priori state error covariance matrix is calculated as:

$$P_{k+1|k} = \begin{bmatrix} P^{11}_{k+1|k} & P^{12}_{k+1|k} \\ P^{21}_{k+1|k} & P^{22}_{k+1|k} \end{bmatrix} = AP_{k|k}A^T + Q_k \tag{4.26}$$

The a priori measurement error is calculated by equation (4.28):

$$\hat{z}_{k+1|k} = H\hat{x}_{k+1|k} \tag{4.27}$$

$$e_{z,k+1|k} = z_{k+1} - \hat{z}_{k+1|k} \tag{4.28}$$

The next step is the calculation of the SVSF gain, as follows. The segment x_{u_k} in (4.23) is directly linked to the measurements and the corresponding corrective gain is defined as per [15, 17]:

$$K_{u_{k+1}} = H_1^{-1} diag\big[E_z \circ sat\big(e_{z,k+1|k}, \psi_z\big)\big]\big[diag(e_{z,k+1|k})\big]^{-1} \tag{4.29}$$

where ψ_z is the smoothing boundary layer, and the symbol $\circ$ denotes the Schur product [15]. E_z is an error vector defined as:

$$E_z = \left|e_{z,k+1|k}\right| + \gamma_z \left|e_{z,k|k}\right| \tag{4.30}$$

where γ_z is an $m \times m$ diagonal matrix with elements such that $0 \leq \gamma_{z,ii} < 1$. It is assumed that the motion model is completely observable and completely controllable. Therefore, a reduced order estimator is designed for the segment x_{l_k}. The state vector is transformed into a partitioned form using a transformation matrix, T. The result is such that the upper portion has an identity relationship with the measurement vector.

$$Tx_k = \begin{bmatrix} y_{u_k} \\ y_{l_k} \end{bmatrix} \tag{4.31}$$

Thus, the transformed state transition matrix is as follows:

$$\Phi = TAT^{-1} = \begin{bmatrix} \Phi_{11} & \Phi_{12} \\ \Phi_{21} & \Phi_{22} \end{bmatrix} \tag{4.32}$$

In this case, the corresponding output matrix is an identity matrix. The lower portion corrective gain is as follows [73]:

$$\begin{aligned} K_{l_{k+1}} = \ & diag(E_y) \\ \circ \ & sat\left(\Phi_{22}\Phi_{12}^{-1}e_{z,k+1|k}, \psi_y\right)\left[diag(\Phi_{22}\Phi_{12}^{-1}e_{z,k+1|k})\right]^{-1}\Phi_{22}\Phi_{12}^{-1} \end{aligned} \tag{4.33}$$

where E_y is an error vector defined as:

$$E_y = \left|\Phi_{22}\Phi_{12}^{-1}e_{z,k+1|k}\right| + \gamma_y\left|\Phi_{12}^{-1}e_{z,k+1|k}\right| \tag{4.34}$$

where γ_y is an $(n-m) \times (\mathrm{n}-m)$ diagonal matrix with elements such that $0 \leq \gamma_{y,ii} < 1$. The SVSF state update equation to be used in the algorithm is as follows [73]:

$$\hat{x}_{k+1|k+1} = \begin{bmatrix} \hat{x}_{u_{k+1|k+1}} \\ \hat{x}_{l_{k+1|k+1}} \end{bmatrix} = \begin{bmatrix} \hat{x}_{u_{k+1|k}} \\ \hat{x}_{l_{k+1|k}} \end{bmatrix} + \begin{bmatrix} K_{u_{k+1}} \\ K_{l_{k+1}} \end{bmatrix} e_{z,k+1|k} \tag{4.35}$$

The a posteriori measurement error needs to be calculated as per (4.36). This value is used in the gain calculation of the next time step.

$$e_{z,k+1|k+1} = z_{k+1} - H\hat{x}_{k+1|k+1} \tag{4.36}$$

The last step is the calculation of the generalized a posteriori state error covariance matrix for the SVSF with fewer measurements than states. The a posteriori state error covariance matrix is calculated as follows [73]:

$$P_{k+1|k+1} = P_{k+1|k} - \begin{bmatrix} K_{u_{k+1}} \\ K_{l_{k+1}} \end{bmatrix} H P_{k+1|k} - P_{k+1|k} H^T \begin{bmatrix} K_{u_{k+1}} \\ K_{l_{k+1}} \end{bmatrix}^T + \begin{bmatrix} K_{u_{k+1}} \\ K_{l_{k+1}} \end{bmatrix} S_{k+1} \begin{bmatrix} K_{u_{k+1}} \\ K_{l_{k+1}} \end{bmatrix}^T \tag{4.37}$$

where $S_{k+1} = H_1 P_{k+1|k}^{11} H_1^T + R$. Note that the covariance formulation in (4.37) is similar to the derived covariance in [17]. However, in that derivation, the SVSF gain for non-measured states was not explicitly expressed in the formulation. The proposed formulation of the a posteriori state error covariance (4.37) includes the uncertainties of all measured and non-measured states. This is an essential step in applying data association methods in the context of smooth variable structure filtering.

The SVSF has been demonstrated to be robust against modeling uncertainties [15], however, each benefit comes at a price: for the case of LG assumption, the SVSF is a sub-optimal estimation solution and its covariance matrix does not meet the CRLB (Cramer-Rao lower bound). Therefore, an optimal derivation of the SVSF is required.

The SVSF process has been demonstrated to be stable and converging to the existence subspace if the absolute value of the estimation error keeps getting smaller in each iteration [15]. This condition is satisfied through the design of the corrective gain as discussed. The SVSF gain causes a high frequency switching, called chattering, that is undesirable [15]. As shown in Figure 4.3, a smoothing boundary layer may be used to reduce the magnitude of the chattering and provide a more accurate estimate, while preserving the inherent

robustness in the SVSF process. The smoothing boundary layer is a common strategy used in sliding mode control to reduce or remove chattering effects due to discontinuous corrective action, such as used in the SVSF. Here a boundary layer is introduced around the switching hyperplane such that discontinuous corrective action is made linearly variable with respect to the distance from the switching hyperplane; while outside the boundary layer the full magnitude of the discontinuous action is applied. If the size of the smoothing boundary layer is greater than the existence subspace, then the chattering effects are removed as shown in Figure 4.3. Such smoothing boundary layer in the SVSF switching gain is achieved by using a saturation function instead of a sign function in (4.29) and (4.33). The terms ψ_z and ψ_y represent the width of the smoothing boundary layer. A full description of the use of smoothing boundary layer in SVSF is given in [15].

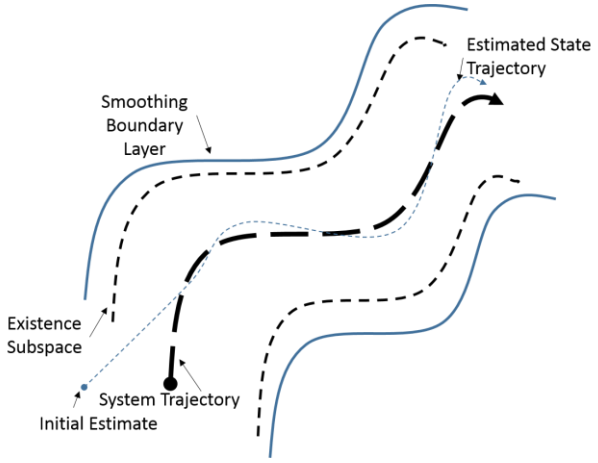

Figure 4.3 Smoothed estimated state trajectory, when the smoothing boundary layer width is bigger than the existence subspace width

4.5 A Novel Approach for Multiple Target Tracking in Clutter

In this section a novel approach for simultaneous data association and filtering is introduced. A generalized variable boundary layer-SVSF (GVBL-SVSF), which has the optimal characteristics of the KF, while maintaining the robustness against modeling uncertainties due to the SVSF, will be derived as a basis for this approach. The proposed generalized formulation includes the uncertainties of all measured and non-measured states and optimizes the smoothing boundary layer accordingly. This is a fundamental step in applying data association in the context of smooth variable structure filtering, while maintaining optimality.

Similarly to a conventional multiple target tracking (MTT) system, the proposed strategy consists of four functions as illustrated in Figure 4.4.

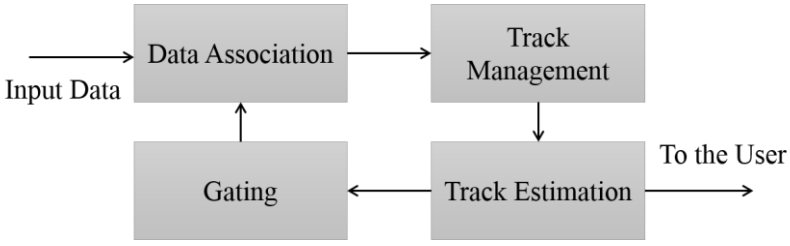

Figure 4.4 Conventional MTT system components

In the gating block of Figure 4.4 elliptical validation regions are constructed around predicted measurements of each track as calculated by (4.27) to reduce the number of possible measurement to track associations (see Figure 4.6). The validation region is defined as a stochastic distance to the predicted measurement, as follows [5].

$$\mathcal{V}_{k+1}^{i}(\alpha) = \left\{ z_{k+1}^{j} : \left[z_{k+1}^{j} - \hat{z}_{k+1|k}^{i} \right]^{T} S_{k+1}^{T} \left[z_{k+1}^{j} - \hat{z}_{k+1|k}^{i} \right] \leq \alpha \right\} \tag{4.38}$$

where α is the gate size [5].

In most investigations of target tracking methods in the presence of data association uncertainty, it is assumed that all tracks have already been initialized and that the number of targets is known. However, this is not a practical assumption. An algorithm is required to carry out the track management in any tracking system. The track management algorithm needs to be responsible for the following [1] (Figure 4.5):

- **Track initiation**: a tentative track is initialized for measurements that are not associated with any of the existing and previously identified targets. An initialized track is named as a tentative track, to which an initial track score is assigned.

- **Track maintenance**: As the new set of observations arrive, the track scores get updated. If a track score exceeds confirmation threshold, the corresponding track gets confirmed and is named a confirmed track. On the other hand, if a track score goes below deletion threshold, the corresponding track gets deleted. If a track score is between two thresholds, then the track remains tentative and the decision is postponed until the arrival of sufficient information.

The track management can be formulized in several ways [4, 1]. In this paper, the track score is calculated and updated based on a recursive likelihood ratio [1]. Figure 4.5 shows the flowchart of the track maintenance algorithm.

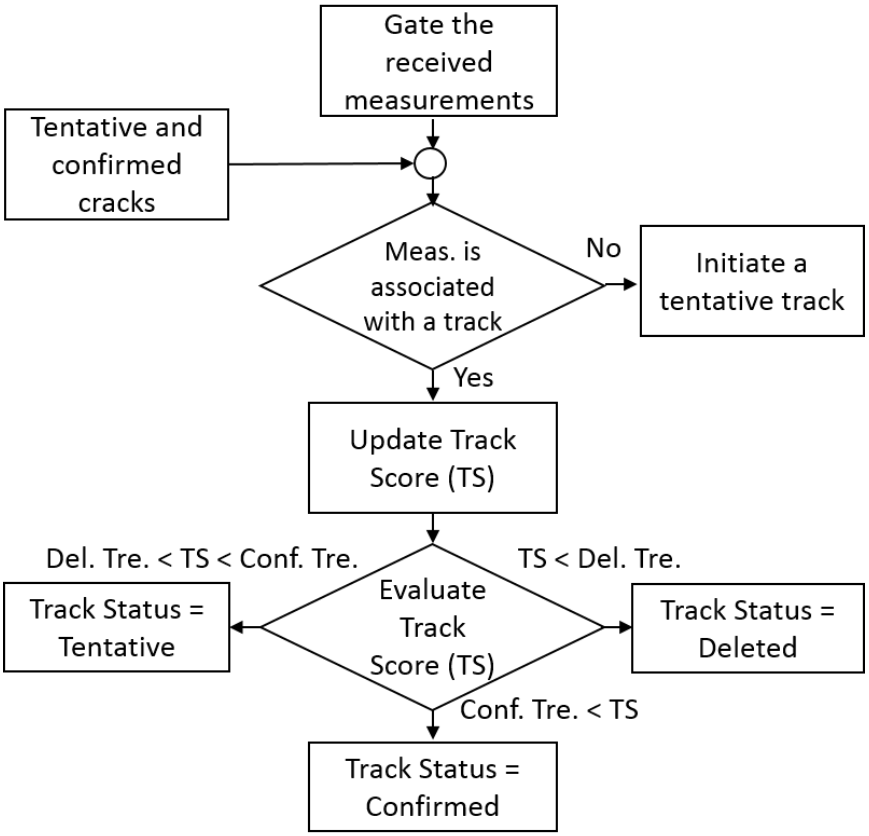

Figure 4.5 The flowchart of the track maintenance algorithm

The data association and estimation functions are handled simultaneously by a novel strategy proposed in this paper, named as JPDA-GVBL-SVSF. This method is proposed for multiple target tracking in the presence of clutter. This method is based on the generalized variable boundary layer- SVSF which is derived in next section.

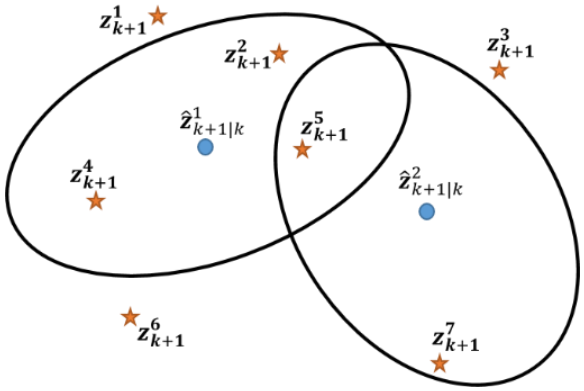

Figure 4.6 Validation regions

Several measurements z^j_{k+1} in the ellipsoidal validation region of two targets centered at their predicted measurements $\hat{z}^i_{k+1|k}$ ($j = 1,..,7$ and $i = 1,2$)

4.5.1 Derivation of a New Generalized Variable Boundary Layer for the SVSF

The width of the smoothing boundary layer ψ reflects the level of uncertainties and the disturbances [15, 17]. The partial derivative of the trace of the generalized a posteriori state covariance with respect to the width of the smoothing boundary layer has been used as a basis for deriving an optimal SVSF. The approach is similar to methodology in [17]. However, unlike the previous derivations, the generalized covariance formulation is utilized, and thus the optimal smoothing boundary layer is generalized for the case when less measurements than states are available. With this derivation, the new SVSF formulation is applicable to observable systems.

In [17], an artificial measurement construction approach is suggested to form a full measurement matrix for when there are fewer measurements than states. However, in this paper, the exact formulation of the generalized covariance matrix and optimal smoothing boundary layer derivation is proposed.

The smoothing boundary layer width ψ, has been considered in a vector form in the original SVSF [15]. A vector form of ψ implies a single smoothing boundary term for each state, and therefore, the terms are assumed independent of each other in the calculation of their corresponding gains. The vector form of ψ prevents an optimal derivation for the smoothing boundary layer. As suggested in [17], a full smoothing boundary layer matrix has been utilized in this paper, where the off-diagonal terms correspond to zero for the original SVSF formulation in [15]. In this full matrix form, the SVSF corrective gain from (4.29) and (4.33) is modified as follows:

$$K_{u_{k+1}} = H_1^{-1} diag(E_z) sat\left(\psi_z^{-1} diag\left(e_{z,k+1|k}\right)\right)\left[diag(e_{z,k+1|k})\right]^{-1} \tag{4.39}$$

$$\begin{aligned} K_{l_{k+1}} = {} & diag\left(E_y\right) sat\left(\psi_y^{-1} diag\left(\Phi_{22}\Phi_{12}^{-1} e_{z,k+1|k}\right)\right) \\ & \left[diag(\Phi_{22}\Phi_{12}^{-1} e_{z,k+1|k})\right]^{-1} \Phi_{22}\Phi_{12}^{-1} \end{aligned} \tag{4.40}$$

where ψ_z is an invertible $m \times m$ matrix, ψ_y is an invertible $(n-m) \times (n-m)$ matrix. In order to solve for an optimal time-varying smoothing boundary layer, the partial derivative of the trace of the generalized a posteriori state covariance (4.37) with respect to the width of the smoothing boundary layers ψ_z and ψ_y is equated to zero, as follows:

$$\begin{cases} \dfrac{\partial\left(trace\left(P_{k+1|k+1}\right)\right)}{\partial \psi_z} = 0 \\ \dfrac{\partial\left(trace\left(P_{k+1|k+1}\right)\right)}{\partial \psi_y} = 0 \end{cases} \tag{4.41}$$

where $P_{k+1|k+1}$ is calculated by using:

$$P^{11}_{k+1|k+1} = P^{11}_{k+1|k} - K_{u_{k+1}} H_1 P^{11}_{k+1|k} - P^{11}_{k+1|k} H_1^T K^T_{u_{k+1}} + K_{u_{k+1}} S_{k+1} K^T_{u_{k+1}} \quad (4.42)$$

$$P^{12}_{k+1|k+1} = P^{12}_{k+1|k} - K_{u_{k+1}} H_1 P^{12}_{k+1|k} - P^{11}_{k+1|k} H_1^T K^T_{l_{k+1}} + K_{u_{k+1}} S_{k+1} K^T_{l_{k+1}} \quad (4.43)$$

$$P^{21}_{k+1|k+1} = P^{21}_{k+1|k} - K_{l_{k+1}} H_1 P^{11}_{k+1|k} - P^{21}_{k+1|k} H_1^T K^T_{u_{k+1}} + K_{l_{k+1}} S_{k+1} K^T_{u_{k+1}} \quad (4.44)$$

$$P^{22}_{k+1|k+1} = P^{22}_{k+1|k} - K_{l_{k+1}} H_1 P^{21}_{k+1|k} - P^{12}_{k+1|k} H_1^T K^T_{l_{k+1}} + K_{l_{k+1}} S_{k+1} K^T_{l_{k+1}} \quad (4.45)$$

One can deduce the following:

$$trace\left(P_{k+1|k+1}\right) = trace\left(P^{11}_{k+1|k+1}\right) + trace\left(P^{22}_{k+1|k+1}\right) \quad (4.46)$$

From (4.46) and given that ψ_z is only an element of $P^{11}_{k+1|k+1}$ and ψ_y is only an element of $P^{22}_{k+1|k+1}$, (4.41) may be specified as below:

$$\frac{\partial\left(trace\left(P^{11}_{k+1|k+1}\right)\right)}{\partial \psi_z} = 0 \quad (4.47)$$

$$\frac{\partial\left(trace\left(P^{22}_{k+1|k+1}\right)\right)}{\partial \psi_y} = 0 \quad (4.48)$$

In an attempt to avoid significant chattering, the solution of (4.47) and (4.48) is considered inside the saturation terms of the SVSF gain (4.39) and (4.40) [17]. With this consideration, the SVSF gain will be as follows:

$$K_{u_{k+1}} = H_1^{-1} diag(E_z) \psi_z^{-1} diag\left(e_{z,k+1|k}\right)\left[diag(e_{z,k+1|k})\right]^{-1} \quad (4.49)$$

$$K_{l_{k+1}} = diag\left(E_y\right) \psi_y^{-1} diag\left(\Phi_{22}\Phi_{12}^{-1} e_{z,k+1|k}\right)\left[diag(\Phi_{22}\Phi_{12}^{-1} e_{z,k+1|k})\right]^{-1} \Phi_{22}\Phi_{12}^{-1} \quad (4.50)$$

Adopting the bar notation $\bar{a}$ to signify a diagonal matrix form of the vector a, the gain (4.49) and (4.50) may be simplified to the following:

$$K_{u_{k+1}} = H_1^{-1}\bar{E}_z\psi_z^{-1} \tag{4.51}$$

$$K_{l_{k+1}} = \bar{E}_y\psi_y^{-1}\Phi_{22}\Phi_{12}^{-1} \tag{4.52}$$

Substituting (4.51) and (4.52) into (4.42) and (4.45) yields

$$\begin{aligned} P_{k+1|k+1}^{11} = P_{k+1|k}^{11} - H_1^{-1}\bar{E}_z\psi_z^{-1}H_1P_{k+1|k}^{11} - P_{k+1|k}^{11}H_1^T(H_1^{-1}\bar{E}_z\psi_z^{-1})^T \\ + H_1^{-1}\bar{E}_z\psi_z^{-1}S_{k+1}(H_1^{-1}\bar{E}_z\psi_z^{-1})^T \end{aligned} \tag{4.53}$$

$$\begin{aligned} P_{k+1|k+1}^{22} = P_{k+1|k}^{22} - \bar{E}_y\psi_y^{-1}\Phi_{22}\Phi_{12}^{-1}H_1P_{k+1|k}^{21} - P_{k+1|k}^{12}H_1^T\left(\bar{E}_y\psi_y^{-1}\Phi_{22}\Phi_{12}^{-1}\right)^T \\ + \bar{E}_y\psi_y^{-1}\Phi_{22}\Phi_{12}^{-1}S_{k+1}\left(\bar{E}_y\psi_y^{-1}\Phi_{22}\Phi_{12}^{-1}\right)^T \end{aligned} \tag{4.54}$$

The next step is to solve for (4.47) and (4.48), considering the individual terms of (4.53) and (4.54) respectively. The procedure for solving (4.47) is as follows [74, 17], where:

$$\frac{\partial\left(trace\left(P_{k+1|k}^{11}\right)\right)}{\partial\psi_z} = 0 \tag{4.55}$$

$$\frac{\partial\left(trace\left(-H_1^{-1}\bar{E}_z\psi_z^{-1}H_1P_{k+1|k}^{11}\right)\right)}{\partial\psi_z} = \psi_z^{-T}\bar{E}_zH_1^{-T}P_{k+1|k}^{11}H_1^T\psi_z^{-T} \tag{4.56}$$

$$\frac{\partial\left(trace\left(-P_{k+1|k}^{11}H_1^T(H_1^{-1}\bar{E}_z\psi_z^{-1})^T\right)\right)}{\partial\psi_z} = \psi_z^{-T}\bar{E}_zH_1^{-T}P_{k+1|k}^{11}H_1^T\psi_z^{-T} \tag{4.57}$$

$$\frac{\partial\left(trace(H_1^{-1}\bar{E}_z\psi_z^{-1}S_{k+1}(H_1^{-1}\bar{E}_z\psi_z^{-1})^T)\right)}{\partial\psi_z} = -2\psi_z^T\bar{E}_zH_1^{-T}H_1^{-1}\bar{E}_z\psi_z^{-1}S_{k+1}\psi_z^{-T} \tag{4.58}$$

Combining (4.55) to (4.58) into (4.47) and (4.53) yields:

$$\begin{aligned}&\frac{\partial\left(trace\left(P_{k+1|k+1}^{11}\right)\right)}{\partial\psi_z}\\&= 2\psi_z^{-T}\bar{E}_z H_1^{-T} P_{k+1|k}^{11} H_1^T \psi_z^{-T} - 2\psi_z^T \bar{E}_z H_1^{-T} H_1^{-1} \bar{E}_z \psi_z^{-1} S_{k+1} \psi_z^{-T}\\&= 0\end{aligned} \tag{4.59}$$

Simplifying (4.59) and solving for the smoothing boundary layer ψ_z results in the following equation:

$$\psi_z^{-1} = \bar{E}_z^{-1} H_1 P_{k+1|k}^{11} H_1^T S_{k+1}^{-1} \tag{4.60}$$

The smoothing boundary layer ψ_z is then obtained as:

$$\psi_z = \left(\bar{E}_z^{-1} H_1 P_{k+1|k}^{11} H_1^T S_{k+1}^{-1}\right)^{-1} \tag{4.61}$$

The matrix ψ_z is an $(m \times m)$ matrix and is invertible if the matrix $\bar{E}_z^{-1} H_1 P_{k+1|k}^{11} H_1^T S_{k+1}$ is nonsingular.

Next, the same procedure is employed to solve for (4.48), considering the individual terms of (4.54), where:

$$\frac{\partial\left(trace\left(P_{k+1|k}^{22}\right)\right)}{\partial\psi_y} = 0 \tag{4.62}$$

$$\frac{\partial\left(trace\left(-\bar{E}_y \psi_y^{-1} \Phi_{22} \Phi_{12}^{-1} H_1 P_{k+1|k}^{21}\right)\right)}{\partial\psi_y} = \psi_y^{-T} \bar{E}_y P_{k+1|k}^{21} H_1^T (\Phi_{22}\Phi_{12}^{-1})^T \psi_y^{-T} \tag{4.63}$$

$$\frac{\partial\left(trace\left(-P_{k+1|k}^{12}H_1^T\Phi_{12}^{-T}\Phi_{22}^T\left(\psi_y^{-T}\bar{E}_y^T\right)^T\right)\right)}{\partial\psi_y} = \psi_y^{-T}\bar{E}_y P_{k+1|k}^{21}H_1^T(\Phi_{22}\Phi_{12}^{-1})^T\psi_y^{-T} \quad (4.64)$$

$$\begin{aligned}&\frac{\partial\left(trace(H_1^{-1}\bar{E}_z\psi_z^{-1}S_{k+1}(H_1^{-1}\bar{E}_z\psi_z^{-1})^T)\right)}{\partial\psi_y}\\ &= -2\psi_y^T\bar{E}_y\bar{E}_y\psi_y^{-1}\Phi_{22}\Phi_{12}^{-1}S_{k+1}(\Phi_{22}\Phi_{12}^{-1})^T\psi_y^{-T}\end{aligned} \quad (4.65)$$

Combining (4.62) to (4.65) into (4.48) and (4.54) yields

$$\begin{aligned}&\frac{\partial\left(trace\left(P_{k+1|k+1}^{22}\right)\right)}{\partial\psi_y}\\ &= 2\psi_y^{-T}\bar{E}_y P_{k+1|k}^{21}H_1^T\Phi_{12}^{-T}\Phi_{22}^T\psi_y^{-T}\\ &- 2\psi_y^T\bar{E}_y\bar{E}_y\psi_y^{-1}\Phi_{22}\Phi_{12}^{-1}S_{k+1}(\Phi_{22}\Phi_{12}^{-1})^T\psi_y^{-T} = 0\end{aligned} \quad (4.66)$$

Simplifying (4.66) and solving for the smoothing boundary layer ψ_y yields the following equation:

$$\psi_y^{-1} = \bar{E}_y^{-1}P_{k+1|k}^{21}H_1^T S_{k+1}^{-1}(\Phi_{22}\Phi_{12}^{-1})^{-1} \quad (4.67)$$

The smoothing boundary layer ψ_y is then obtained as:

$$\psi_y = \left(\bar{E}_y^{-1}P_{k+1|k}^{21}H_1^T S_{k+1}^{-1}(\Phi_{22}\Phi_{12}^{-1})^{-1}\right)^{-1} \quad (4.68)$$

The matrix ψ_y is an $(n-m)\times(n-m)$ matrix and is invertible if the matrix $\bar{E}_y^{-1}P_{k+1|k}^{21}H_1^T S_{k+1}^{-1}(\Phi_{22}\Phi_{12}^{-1})^{-1}$ is nonsingular.

The proposed smoothing boundary layers in (4.61) and (4.68) are directly related to the level of modeling uncertainties (captured by the error terms $\bar{E}_z$ and $\bar{E}_y$) and the estimated

system and measurement noise (by virtue of state and measurement covariance matrices). The optimal width of the smoothing boundary layer for both measured and unmeasured states can now be updated in each time step in accordance with updates in the modeling uncertainty and noise.

As in (4.51) and (4.52), the SVSF gain is dependent on the width of smoothing boundary layer. In an attempt to examine the effects of the optimal smoothing boundary layer (generalized variable boundary layer – GVBL) terms on the SVSF gain, (4.60) and (4.67) are substituted into (4.51) and (4.52) respectively, which yields the following equations.

$$K_{u_{k+1}}^{GVBL} = H_1^{-1}\bar{E}_z(\bar{E}_z^{-1}H_1P_{k+1|k}^{11}H_1^TS_{k+1}^{-1}) \tag{4.69}$$

$$K_{l_{k+1}}^{GVBL} = \bar{E}_y(\bar{E}_y^{-1}P_{k+1|k}^{21}H_1^TS_{k+1}^{-1}(\Phi_{22}\Phi_{12}^{-1})^{-1})\Phi_{22}\Phi_{12}^{-1} \tag{4.70}$$

which is simplified as follows:

$$K_{u_{k+1}}^{GVBL} = P_{k+1|k}^{11}H_1^TS_{k+1}^{-1} \tag{4.71}$$

$$K_{l_{k+1}}^{GVBL} = P_{k+1|k}^{21}H_1^TS_{k+1}^{-1} \tag{4.72}$$

One can arrange the two gains into a matrix form as follows:

$$K^{GVBL} = \begin{bmatrix} K_{u_{k+1}}^{GVBL} \\ K_{l_{k+1}}^{GVBL} \end{bmatrix} = \begin{bmatrix} P_{k+1|k}^{11} & P_{k+1|k}^{12} \\ P_{k+1|k}^{21} & P_{k+1|k}^{22} \end{bmatrix} \begin{bmatrix} H_1^T \\ 0 \end{bmatrix} S_{k+1}^{-1} = P_{k+1|k}H^TS_{k+1}^{-1} \tag{4.73}$$

The SVSF gain of (4.73) is the same as the KF gain (4.6), which is the optimal solution in the MMSE sense for linear Gaussian systems. To preserve the robustness of the SVSF to modeling uncertainties, a generalized combined strategy is proposed, referred to here as GVBL-SVSF. The novel generalized strategy maintains an accurate estimate for both

measured and unmeasured states, using the GVBL calculation, while ensuring the stability of the state estimation by virtue of the standard SVSF gain. A saturation limit, ψ_{max} is imposed on the optimal boundary layer, inside which the optimality of GVBL is maintained and outside which the robustness of standard SVSF is ensured. The calculation process of GVBL-SVSF can be summarized as follows (also see Figure 4.7).

1. The state and covariance are predicted by (4.24) and (4.26) respectively, and the measurement innovation is calculated by (4.28).

2. The GVBL is calculated using (4.61) and (4.68), and its diagonal elements are compared with ψ_{max}; if larger, the corrective gain is calculated by (4.39) and (4.40), if smaller, the corrective gain is obtained from (4.71) and (4.72).

3. The state, the state covariance matrix, and the measurement a posteriori error are updated via (4.35), (4.37) and (4.36) respectively.

4.5.2 Proposed JPDA-GVBL-SVSF for Multiple Target Tracking in Clutter

The following assumptions are used to formulate JPDA-GVBL-SVSF algorithm: *1*. The number of tentative and confirmed tracks is known. *2*. The targets may be interfering, i.e. measurements from one target can fall within the validation gate of a neighboring target. *3*. The past information of the system is approximated by a normal distribution, i.e. the approximate sufficient statistics include approximate conditional means and the covariances for each target. *4*. The stochastic portion of the estimation error is bounded, which is a required condition of stability for the SVSF [15].

The proposed JPDA-GVBL-SVSF algorithm is summarized by three steps:

1- The joint measurement-to-target association probabilities are calculated according to (4.19).

2- The marginal association probabilities for the latest set of measurements are made according to (4.21).

3- The states are estimated with the procedure summarized at the end of Section IV-A, and sequentially according to equations (4.24); (4.26); (4.28); (4.61); (4.68); one of the pairs of (4.39) and (4.40) or (4.71) and (4.72); (4.35);(4.37); and (4.36).

Examples of the JPDA-GVBL-SVSF parameters are provided in 4.6. The number of false measurements is assumed to obey the Poisson distribution with the spatial density λ [4]. Hence, the joint association probabilities are as (4.19). The state estimation of the targets are carried out in a decoupled manner with the assumption that the target states conditioned on the past information are mutually independent [5].

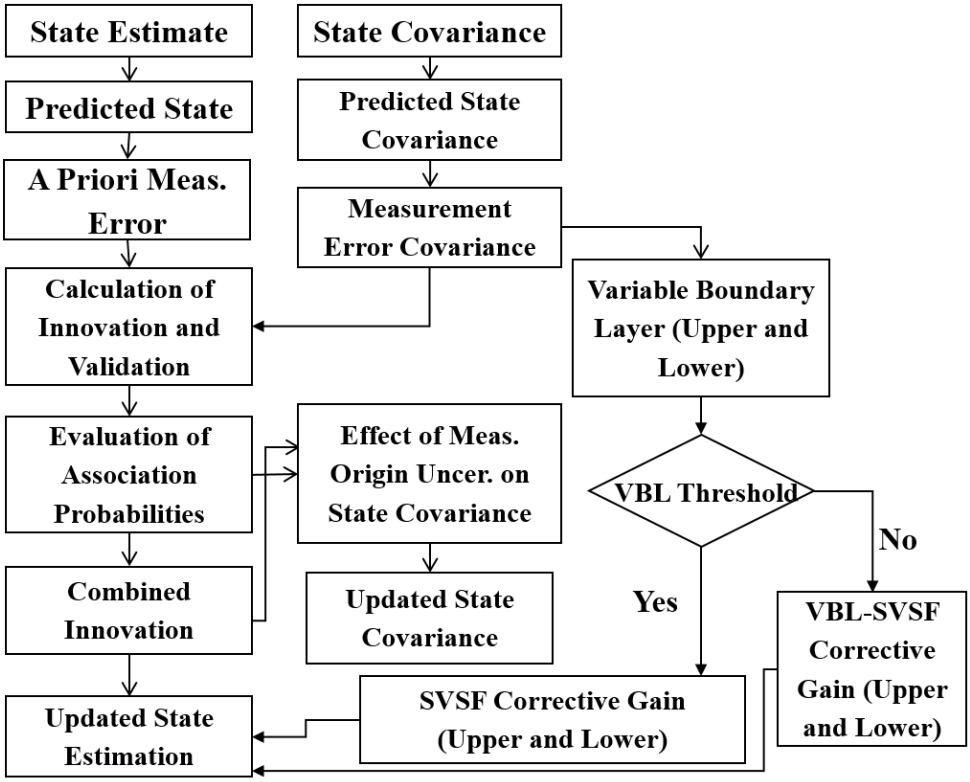

Figure 4.7 The flowchart of the proposed algorithm

With this assumption, the marginal association probabilities are calculated by summing the joint hypotheses in which the marginal hypothesis of interest is included as in (4.21) [4]. Consequently, although the association probabilities for all targets are calculated in a jointly manner, the state estimation procedure is decoupled amongst the targets. The decoupled state estimation avoids the curse of dimensionality as the number of targets increases. Therefore, the computational complexity of the algorithm increases linearly as the number of targets increases.

In the proposed MTT system, the initiation, confirmation and deletion of the tracks is performed using a track-score based track maintenance system. Since the track-score based

track maintenance is not a hard-decision technique, the system is able to tolerate a number of missed detections until the track score falls below a threshold, hence is robust against missed detections for a number of frames.

Employing the proposed JPDA-GVBL-SVSF, the system takes the uncertainties of all measured and non-measured states into account such that the problem of multiple target tracking in the presence of clutter is dealt with in a robust and optimized manner.

4.6 Multiple Target Tracking Cases and Results

This section describes the results of a number of target tracking scenarios. The first case compares the results of applying the JPDA-KF and the JPDA-GVBL-SVSF to a multiple target tracking simulation scenario. The second compares the results when the methods are applied to a LiDAR-based car tracking experimental data.

4.6.1 Multiple Target Tracking with Clutter

The multiple target tracking scenario consists of three maneuvering cars as described by Table 4.1 and Figure 4.8. A simple two-dimensional discrete constant velocity model is implemented as follows [6]. The state vector is defined as $\boldsymbol{x} = [x\ y\ v_x\ v_y]$, where x and y are the position in two Cartesian directions, and v_x and v_y are the corresponding velocities. In this model, the accelerations of the target between two sequential samples are assumed to be constant with discrete-time zero mean white Gaussian noise. The motion model is defined as follows:

$$x(k+1) = Fx(k) + Gv(k) \tag{4.74}$$

where the state transition and process noise gain matrices are defined by:

$$F = \begin{bmatrix} 1 & 0 & T_s & 0 \\ 0 & 1 & 0 & T_s \\ 0 & 0 & 1 & 0 \\ 0 & 0 & 0 & 1 \end{bmatrix}, \qquad G = \begin{bmatrix} T_s^2/2 & 0 \\ 0 & T_s^2/2 \\ T_s & 0 \\ 0 & T_s \end{bmatrix} \tag{4.75}$$

The white acceleration noise covariance matrix is defined as follows:

$$Q = cov\{v(k)\} = \begin{bmatrix} \sigma_v^2 & 0 \\ 0 & \sigma_v^2 \end{bmatrix} \tag{4.76}$$

To emphasize on the performance comparison of the methods, the simulation model is chosen to be a simple kinematic model. From an implementation point of view, the computational complexity of the algorithm should be manageable for real time applications. This limits the complexity of car motion models as the number of targets increase.

The measurement model, matrix, and noise covariance are defined respectively as follows:

$$z(k) = Hx(k) + w(k) \tag{4.77}$$

$$H = \begin{bmatrix} 1 & 0 & 0 & 0 \\ 0 & 1 & 0 & 0 \end{bmatrix} \tag{4.78}$$

$$R = cov\{w(k)\} = \begin{bmatrix} \sigma_w^2 & 0 \\ 0 & \sigma_w^2 \end{bmatrix} \tag{4.79}$$

Table 4.1. Simulation scenario for three cars

Initial State	Maneuver	Duration
Car#1	a near constant velocity motion	0-93s
$x_0 = 200\ m$	a "straight line and curve"	94-139s
$y_0 = 50\ m$ $v_{x_0} = 28\ m/s$ $v_{y_0} = 1\ m/s$	a near constant velocity	140-500s
Car#2	a near const. velocity motion	0-115s
$x_0 = -1000\ m$	a "straight line and curve"	116-156s
$y_0 = 25\ m$	a near constant velocity	157-241s
$v_{x_0} = 33\ m/s$	a "cut-in-out"	242-325s
$v_{y_0} = 1\ m/s$	a near constant velocity motion	326-500s
Car#3	a near constant velocity motion	0-139s
$x_0 = -2000\ m$	a "straight line and curve"	140-179s
$y_0 = 0\ m$	a near constant velocity	180-368s
$v_{x_0} = 34\ m/s$	a "cut-in-out"	368-418s
$v_{y_0} = 1\ m/s$	a near constant velocity motion	419-500s

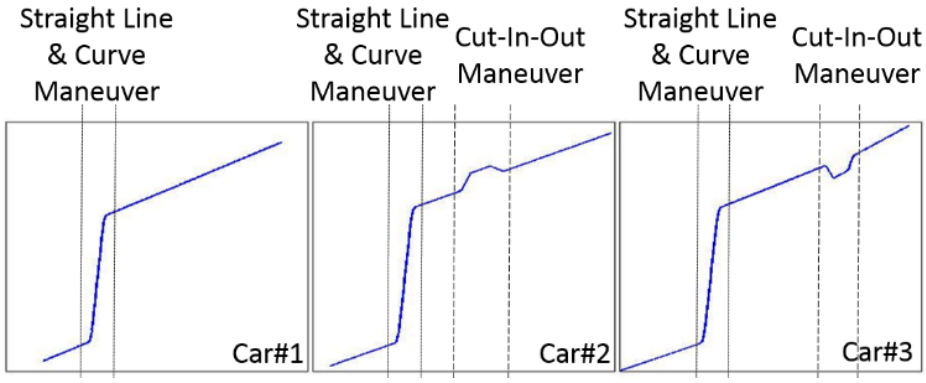

Figure 4.8 Vehicle trajectories illustrating their maneuvers [73]

As the measurement matrix H indicates, the available measurements are the positions in x and y direction, while the state vector includes the position (x and y) as well as the velocity (v_x and v_y) states, i.e. the number of measurements are less than the number of states.

Although the cars have maneuvering behaviors, the two algorithms (JPDA-KF and JPDA-GVL-SVSF) will only use the near-constant velocity model as the motion model, i.e. in addition to dealing with measurements from interfering vehicles and clutter, the algorithms will also have to overcome modeling uncertainty. Both algorithms are tuned for non-maneuvering scenario. Then to check the performance of the algorithms, the maneuvering scenario is simulated for both algorithms without retuning.

The following parameter values are used for the simulations: process and measurement noise covariances are $\sigma_v^2 = 0.5^2$, $\sigma_w^2 = 3^2$ respectively, gate threshold is $\alpha = 16$, gate probability is $P_G = 0.9997$, detection probability is $P_D = 0.9$, spatial density of the number of false alarms is $\lambda = 10^{-2}$, the SVSF gain parameter is $\gamma = 0.1$ and the smoothing boundary layer limit is equal to 20.

The RMSEs of state estimations averaged over 500 Monte Carlo runs for three vehicles are tabulated in Table 4.2. Due to the simultaneous optimal-robust characteristics of GVBL-SVSF, the RMSEs of estimations are considerably decreased using the proposed method. More specifically, in average, there are 9% and 18% decrease in RMSE associated with the position and velocity estimation errors, respectively. The simulation model assumes the near constant velocity motion in both x- and y- directions. However, the scenarios are designed to include a maneuvering motion to represent the modeling uncertainties. The maneuvers are mostly performed in y-direction, hence modeling uncertainty is larger in y-direction. Consequently, the effect of the performance of JPDA-GVBL-SVSF is more vivid in the y-direction.

Table 4.2. RMSE of State Estimations for Multiple Target Tracking Case

States	**Car #1**		**Car #2**		**Car #3**	
	JPDA-KF	JPDA-GVBL-SVSF	JPDA-KF	JPDA-GVBL-SVSF	JPDA-KF	JPDA-GVBL-SVSF
x	1.43	1.37	2.12	2.06	2.33	2.28
y	1.21	0.70	1.39	0.94	1.62	1.26
v_x	0.71	0.71	0.82	0.77	0.83	0.77
v_y	0.99	0.94	1.27	1.04	1.46	1.25

Furthermore, the traces of the covariance matrices for three cars are illustrated in Figure 4.9. Due to the optimized generalized variable boundary layer calculations, the traces of the covariance matrices are decreased to the minimum level of the KF which meets the CRLB condition for the estimator [6]. The modeling uncertainty is imposed on to the system by the choice of model, however, only when the car maneuvers. These cases are detected as an increase in the trace of the covariance matrices in Figure 4.9. The JPDA-GVBL-SVSF benefits from the robustness property of the smooth variable structure filtering strategy and increases the covariance to suppress the effects of modeling uncertainty, which is the reason for the significant improvement in its RMSE in state estimation.

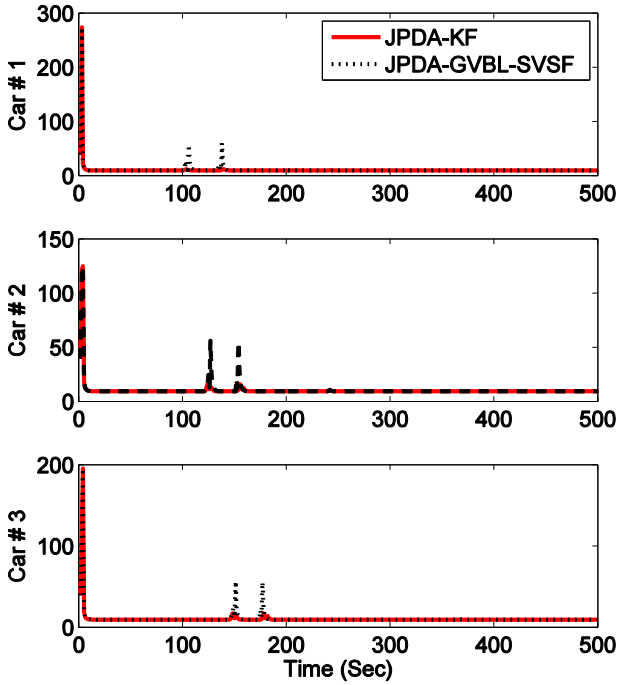

Figure 4.9 Trace of the covariance matrices for three cars, comparing JPDA-KF and JPDA-GVBL-SVSF methods

4.6.2 Experimental Validation: LiDAR-Based Multiple Road Vehicle Tracking

The proposed JPDA-VBL-SVSF algorithm has been tested on a number of processed LiDAR data sets acquired in actual driving in a highway linking two cities (Hamilton and Toronto in Canada along a highway called the Queen Elizabeth Way (QEW)). The proposed method can be used for other types of sensors, including video cameras and radars. However, each sensory data should be processed in order to be fed into the tracking algorithm. The experimental set-up used in this project for data acquisition includes a Ford escape car equipped with a Velodyne HDL32 LiDAR sensor (Figure 4.11). The LiDAR provides a 3D point cloud in each frame with a frame rate of 0.1 second (as shown in

Figure 4.10), which requires to be processed before feeding into tracking algorithm. A concise scheme of the data processing algorithm is as follows:

The data processing algorithm consists of two phases: The first phase is called segmentation which enables the system to distinguish non-ground points from ground points. Since, reducing the computation time plays a critical role in real time implementation, the segmentation step would reduce the computational load of the algorithm by filtering out the false readings. In the second phase, a bounded nearest neighbour based on Euclidean distance is used to make clusters. The clustering from the second phase is to classify the non-ground points into different vehicle-like objects. The clusters are processed to obtain the position of the centre-point of each vehicle-like object and then fed into the tracking algorithm (proposed in Section 4.5) as the input data.

The gating and the track management functions are performed as described in Section IV. The performances of the two algorithms, the JPDA-KF and the JPDA-VBL-SVSF, are summarized and compared in Table 4.3. For the purpose of the calculation of association probabilities it is assumed that the clutter is uniformly distributed and the number of clutter originated measurements abides by a Poisson's distribution with spatial density of $\lambda = 10^{-2}$. The spatial density is roughly obtained by averaging the number of detected clutter objects over the total number of frames of the experimental data.

Note that the table provides the rates of true positive (TP), that is an indicator of the number of correctly tracked targets, and false positive (FP), that is an indicator of the number of falsely tracked objects, attained by the algorithms. The track break-ups rate is a performance index that counts the number of re-labeled targets. The relabeling of targets happens if for any reason the detection system misses a previously confirmed target over a number of frames, and when detected again, it is treated as a new track, with a new label.

From Table 4.3, the proposed algorithm has improved the TP (%) by around 8% and the rate of track break-ups by 6%. Also, the FP (%) indicates that a number of clutter objects are falsely detected and tracked as objects of interest. The proposed algorithm improved this indicator by reducing the FP (%) by around 6%. The performance of the tracking algorithm is limited by the accuracy of the detection algorithm.

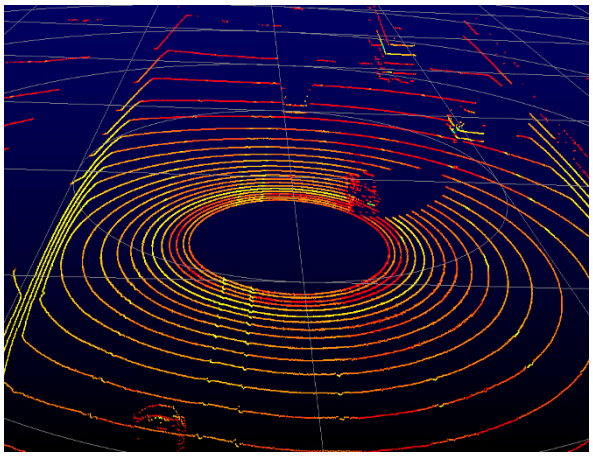

Figure 4.10 One sample frame of raw LiDAR data

Figure 4.11 The car equipped with Velodyne HDL32 LiDAR

Table 4.3. The performance evaluation of multiple car tracking algorithms comparing JPDA-KF and JPDA-GVBL-SVSF

MTT Strategy	# of Cars	Correctly Tracked	Falsely Tracked	TP (%)	FP (%)	Rate of Track Break-ups (%)
JPDA-KF	58	49	9	84.48	15.52	8
JPDA-GVBL-SVSF		53	5	91.38	8.62	2

4.7 Conclusion

In this paper, a new approach for multiple target tracking in the presence of clutter, referred to as JPDA-GVBL-SVSF, is introduced. A generalized form of the SVSF covariance is used to derive the generalized optimal SVSF. This method is then combined with JPDA into the JPDA-GVBL-SVSF strategy. The proposed method has been compared to the JPDA-KF method under a multiple target tracking simulation scenario in terms of estimation accuracy and robustness to uncertainties. The proposed method performed significantly better than the JPDA-KF method due to its combined optimality and robustness to modeling uncertainties. To further investigate the performance of the proposed method, it has been tested on a number of processed LiDAR data sets acquired in actual driving in a highway linking two cities (Hamilton and Toronto in Canada along a highway. The overall performance of the MTT system has been compared for the JPDA-KF and the JPDA-GVBL-SVSF in terms of the TP and FP rates and the rate of track breakups. The proposed algorithm has improved the TP(%), FP(%) and the rate of track break-ups, and made a more reliable tracking algorithm for real car tracking scenarios.

The main contribution of this paper was on the estimation strategy used in the context of data association methods based of probabilistic data association. The proposed estimation

strategy of this paper can be used with other data association methods, and is considered for future work.

Chapter 5

Augmented Probabilistic Data Association Based on SVSF Estimation

5.1 Abstract

In many intelligent car applications, it is required to observe and track the state of motion of surrounding vehicles by use of some sensors. Often, the sensory data is affected by noise and false alarm. The tracking system relies on estimation and data association techniques to resolve these issues. The Kalman filter (KF) is the mostly studied method for estimation and tracking. KF is optimal for a linear-Gaussian assumption. If this assumption is not held, the optimality and stability of KF is affected. The smooth variable structure filter (SVSF) is a relatively new method which is more robust to modeling uncertainties. The SVSF provides extra measures of performance, such as the magnitude of chattering signal. In this paper, a novel data association method has been proposed that extracts extra information of the SVSF in a Bayesian framework. This novel method, named augmented probabilistic data association-SVSF (APDA-SVSF) is presented and analyzed. The robustness and accuracy of the new form of filtering and data association is validated and comparatively analyzed by its application to an experimental traffic monitoring system based on LiDAR (LIght Detection And Ranging).

5.2 Introduction

Tracking techniques are commonly used in surveillance, advanced driver assistance systems (ADAS), air traffic control, medical imaging, finance and autonomous vehicles amongst others. Tracking, by definition is the recursive estimation of the states (position, velocity, etc.) of an unknown target from indirect, inaccurate and uncertain measurements [6]. Data association uncertainty occurs when some of the measurements are not necessarily originated from the targets of interest [5]. In such data association problems, an estimate of the target's states is used to predict the target's state of motion and associated measurement for the next upcoming time step. This prediction is the basis for discriminating and eliminating measurements.

The literature on target tracking in the presence of clutter is extensive [4, 1]. One of the most commonly used data association methods is the probabilistic data association (PDA) filter [5, 27]. In the PDA the association probability for each track is calculated by taking all feasible measurement-to-track association hypotheses into consideration [5, 29]. The PDA assumes that the track has already been initialized [5]. Therefore, in practice, the PDA is used in conjunction with a track maintenance algorithm such as logic-based track formation [4], or a track-score based method [1]. The joint probabilistic data association (JPDA) is an extension of the PDA to handle the problem of multiple interfering targets [31]. In JPDA, the association probabilities are calculated in a joint manner across all targets [31]. Data association techniques may be enhanced by using additional information of measurements from each target. These additional information are referred to as target features or target signatures [75, 76, 4]. The inclusion of a feature or signature information in the hypothesis probability calculation is what makes the difference between signature-aided approaches and the traditional approaches [4].

The data association process provides an association probability for each hypothesis. The association probabilities are used to construct a combined innovation term. This term is a weighted sum of all the innovations, and is used in the estimation algorithm [4]. The most popular model-based estimation strategy is the Kalman filter (KF) which provides the best solution in the minimum mean squared error (MMSE) sense under the linear Gaussian (LG) assumption [6, 8, 7].

The KF is derived for linear systems. Some extensions of KF to work with nonlinear systems are the Extended KF (EKF) [6] and Unscented KF (UKF) [77]. More recently, particle filters (PF) are also being widely used [12]. In EKF, the state probability distribution is approximated with a Gaussian distribution. Then a first order linearization of the system is used to propagate this approximation [6]. However, this process may lead to suboptimal performance or even filter divergence in some cases. In the UKF, the state probability distribution is approximated with a Gaussian distribution that is represented by a set of deterministic sample points. These sample points are then propagated through the nonlinear system [77]. In comparison, for the same order of complexity, the EKF captures the nonlinearities of first order, while the UKF achieves at least 2nd order accuracy [77]. The KF is optimal for linear Gaussian systems. For the case when the Gaussian assumption is breached, one solution is to approximate the non-Gaussian distribution with a Gaussian mixture at the cost of increasing computational complexity [11]. The PF or the sequential Monte Carlo method is proposed for nonlinear non-Gaussian systems [12]. The state probability distribution is approximated by a large number of Monte Carlo independent identical distribution samples, namely particles [12]. The PF is very expensive in implementation, yet powerful in handling difficult problems [12].

A group of robust estimation techniques is the variable structure filter based methods [16]. In these methods, similar to sliding mode concept, the stability of the filter is guaranteed

given bounded parametric uncertainties [16]. The smooth variable structure filter (SVSF) is a type of variable structure filter that uses a discontinuous corrective gain to force the estimated states toward a subspace around the true trajectories, namely the existence subspace. Once the estimated states are within this subspace, they would switch back and forth within its boundaries. This switching effect is referred to as chattering and for a normal operating condition is filtered out by using a smoothing function [15]. The magnitude of the chattering signal is an indicator of modeling uncertainties [15]. Therefore, in addition to conventional filter performance measures, the SVSF provides a unique set of performance indicators that quantify the degree of uncertainty [15].

Some modifications have been proposed to the SVSF from its original form, such as derivation of an optimal form in [78, 17]. Also, a number of SVSF-based methods have been used for target tracking in the presence of data association uncertainty [54, 73, 79, 57, 72]. The SVSF in combination with PDA and JPDA is investigated in [54, 57] and the results indicate an improvement over the original PDA and JPDA approaches. The SVSF-based PDA is used for maneuvering target tracking in conjunction with the interacting multiple model method in [72]. In [73, 79] a generalized version of the SVSF and its optimal form is proposed and examined for automotive tracking applications in the presence of cluttered measurements. In all of the methods proposed in [54, 73, 79, 57, 72] the data association and filtering are performed simultaneously, however, the data association is handled by conventional PDA or JPDA methods. In this paper, an augmented probabilistic data association method is proposed. This proposed method uses the extra source of information that the SVSF provides that is the chattering magnitude signal. Use of chattering is unique to the SVSF concept and has never been implemented before. It is a source of additional information that relates directly to the uncertainty of the filter model. This extra information is used in the Bayesian inference procedure of association

probabilities calculation and can enhance the tracking performance significantly as shown here.

Section 5.3 of this paper provides a brief overview of the SVSF method. The data association principles are summarized in Section 5.4. In Section 5.5 the probability distribution function of the chattering magnitude signal is derived. Then through a Bayesian inference a new augmented set of association probabilities are proposed and discussed. In Section 5.6, a tracking simulation problem is described and then the new proposed method is comparatively analyzed in terms of its estimation accuracy and robustness to uncertainties. Furthermore, the method is experimentally evaluated and applied to a LiDAR based automotive tracking system. The conclusions are provided in Section 5.7.

5.3 Smooth Variable Structure Filter

The smooth variable structure filter (SVSF) is a predictor-corrector model-based estimation strategy which was first presented in 2007 [15]. The operation of the SVSF is shown in Fig 1. Conceptually, the SVSF uses a switching corrective gain to force the estimated states to within a boundary around the true state trajectory, named as the existence subspace. It guarantees the stability through the calculation of the corrective gain using a Lyapunov based stability theorem [15, 17]. The discontinuous corrective action of the SVSF results in chattering that can be suppressed by using a smoothing boundary layer. The filter also allows extraction of a higher degree of information from the measurements through secondary indicators of performance.

The SVSF process has been demonstrated to be stable for bounded uncertainties and converges to a neighborhood of the actual state trajectory referred to as the existence

subspace [15, 17]. Thereafter, the estimates switch back and forth across the true trajectory while remaining within this subspace, as shown in Figure 5.1. The SVSF gain causes a high frequency switching, called chattering, that is undesirable [15, 17]. As shown in [15, 17], a smoothing boundary layer may be used to reduce or remove the magnitude of the chattering at the expense of estimation accuracy, while preserving the inherent robustness in the SVSF process.

The SVSF has been modified and improved since its introduction [79, 17]. In this paper, the generalized variable boundary layer SVSF (GVBL-SVSF) [79] is used.

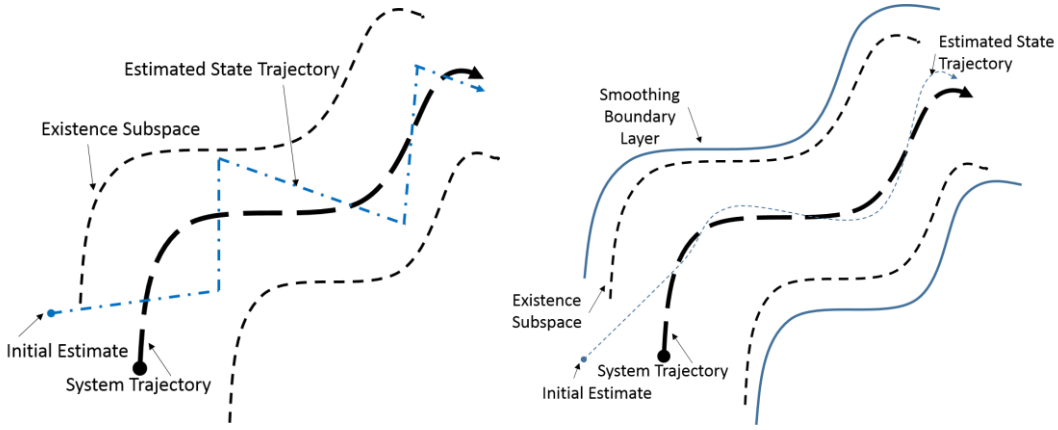

Figure 5.1 SVSF estimation concept [15]

The main steps of the GVBL-SVSF are the prediction and the update as follows. Consider the following state space model:

$$x_{k+1} = Ax_k + w_k \tag{5.1}$$

$$z_k = Hx_k + v_k \tag{5.2}$$

where x_k and z_k are the state and measurement vectors, of dimensions of $(n \times 1)$ and $(m \times 1)$, respectively, and w_k and v_k are zero mean white Gaussian process and measurement

noise, with covariance matrices Q and R, respectively. Also, measurement matrix H is of dimension $m \times n, m < n$ is the number of measured states, n is the rank of the system. The system is assumed to be observable, therefore without loss of generality, the measurement matrix H is of the form:

$$H = [H_{1(m\times m)} \quad H_{2(m\times(n-m))}] \tag{5.3}$$

where H_1 is an identity matrix of dimension $m \times m$ and H_2 is a null matrix of dimension $m \times (n-m)$. In the same way, the state transition matrix is partitioned as follows.

$$A = \begin{bmatrix} A_{11(m\times m)} & A_{12(m\times(n-m))} \\ A_{21((n-m)\times m)} & A_{22((n-m)\times(n-m))} \end{bmatrix} \tag{5.4}$$

The state vector of the system can be transformed and partitioned into two segments as follows, where the states in the upper segment have measurements signals directly associated, and the remaining ones in the lower segment are the non-measured part.

$$x_k = \begin{bmatrix} x_{u_k(m\times 1)} \\ x_{l_k((n-m)\times 1)} \end{bmatrix} \tag{5.5}$$

For target tracking, the prediction step consists of the following equations ((5.6) to (5.9)).

$$\hat{x}_{k+1|k} = A\hat{x}_{k|k} \tag{5.6}$$

The a priori state error covariance matrix is defined as follows.

$$P_{k+1|k} = E\{\tilde{x}_{k+1|k}\tilde{x}_{k+1|k}^T\} = \begin{bmatrix} P_{k+1|k}^{11} & P_{k+1|k}^{12} \\ P_{k+1|k}^{21} & P_{k+1|k}^{22} \end{bmatrix} = AP_{k|k}A^T + Q_k \tag{5.7}$$

where $\tilde{x}_{k+1|k} = A\tilde{x}_{k|k} + w_k$. The a priori measurement error is calculated by equation (5.8) and (5.9).

$$\hat{z}_{k+1|k} = H\hat{x}_{k+1|k} \tag{5.8}$$

$$e_{z,k+1|k} = z_{k+1} - \hat{z}_{k+1|k} \tag{5.9}$$

The innovation covariance matrix is computed as follows.

$$S_{k+1} = H_1 P^{11}_{k+1|k} H_1^T + R \tag{5.10}$$

The next step is the update. The SVSF state update equation is as follows.

$$\hat{x}_{k+1|k+1} = \begin{bmatrix} \hat{x}_{u_{k+1|k+1}} \\ \hat{x}_{l_{k+1|k+1}} \end{bmatrix} = \begin{bmatrix} \hat{x}_{u_{k+1|k}} \\ \hat{x}_{l_{k+1|k}} \end{bmatrix} + \begin{bmatrix} K_{u_{k+1}} \\ K_{l_{k+1}} \end{bmatrix} e_{z,k+1|k} \tag{5.11}$$

The corresponding SVSF corrective gain is calculated as follows [79].

$$K_{u_{k+1}} = H_1^{-1} diag(E_z) sat\left(\Psi^{-1}_{z,k+1} diag\left(e_{z,k+1|k}\right)\right)\left[diag(e_{z,k+1|k})\right]^{-1} \tag{5.12}$$

$$K_{l_{k+1}} = diag(E_y) sat\left(\Psi^{-1}_{y,k+1} diag\left(A_{22}A_{12}^{-1} e_{z,k+1|k}\right)\right) \tag{5.13}$$

$$\left[diag\left(A_{22}A_{12}^{-1} e_{z,k+1|k}\right)\right]^{-1} A_{22}A_{12}^{-1}$$

E_z and E_y are the error vector terms defined as below [79].

$$E_{z,k+1} = \left|e_{z,k+1|k}\right| + \gamma_z \left|e_{z,k|k}\right| \tag{5.14}$$

$$E_{y,k+1} = \left|A_{22}A_{12}^{-1} e_{z,k+1|k}\right| + \gamma_y \left|A_{12}^{-1} e_{z,k+1|k}\right| \tag{5.15}$$

where γ_z and γ_y are $m \times m$ and $(n-m) \times (\mathrm{n}-m)$ diagonal matrices with elements such that $0 \leq \gamma_{z,ii} < 1$ and $0 \leq \gamma_{y,ii} < 1$. Ψ_z and Ψ_y are the smoothing boundary layer matrices of dimensions $m \times m$ and $(n-m) \times (n-m)$ respectively. The diagonal elements of the smoothing boundary layer matrices reflect the level of uncertainties and the disturbances in their corresponding state. The optimal smoothing boundary layers are calculated as follows [79].

$$\Psi_{z,k+1} = \left(diag\left(E_{z,k+1}\right)^{-1} H_1 P_{k+1|k}^{11} H_1^T S_{k+1}^{-1}\right)^{-1} \tag{5.16}$$

$$\Psi_{y,k+1} = \left(diag\left(E_{y,k+1}\right)^{-1} P_{k+1|k}^{21} H_1^T S_{k+1}^{-1} (A_{22}A_{12}^{-1})^{-1}\right)^{-1} \tag{5.17}$$

The smoothing boundary layers in (5.16) and (5.17) are directly related to the level of modeling uncertainties (captured by the error terms E_z and E_y and the estimated system and measurement noises. Substituting (5.16) and (5.17) in the SVSF gain terms (5.12) and (5.13), the following equation is obtained for optimal GVBL-SVSF gain [79].

$$K^{GVBL} = \begin{bmatrix} K_{u_{k+1}}^{GVBL} \\ K_{l_{k+1}}^{GVBL} \end{bmatrix} = \begin{bmatrix} P_{k+1|k}^{11} & P_{k+1|k}^{12} \\ P_{k+1|k}^{21} & P_{k+1|k}^{22} \end{bmatrix} \begin{bmatrix} H_1^T \\ 0 \end{bmatrix} S_{k+1}^{-1} = P_{k+1|k} H^T S_{k+1}^{-1} \tag{5.18}$$

The above GVBL gain calculation maintains an accurate estimate for both measured and unmeasured states, while ensuring the stability of the state estimation by virtue of the standard SVSF gain. To preserve the robustness of the SVSF to modeling uncertainties in the GVBL-SVSF, a saturation limit, ψ_{max} is imposed on the optimal boundary layer, inside which the optimality of GVBL is maintained and outside which the robustness of standard SVSF is ensured. The GVBL is calculated using (5.16) and (5.17), and its diagonal elements are compared with ψ_{max}; if larger, the corrective gain is calculated by using equations (5.12) and (5.13), if smaller, the corrective gain is obtained from (5.18) [79].

The a posteriori measurement error needs to be calculated as per (5.19). This value is used in the gain calculation of the next time step.

$$e_{z,k+1|k+1} = z_{k+1} - H\hat{x}_{k+1|k+1} \tag{5.19}$$

The last step is the calculation of the generalized a posteriori state error covariance matrix for the SVSF with fewer measurements than states. The a posteriori state error covariance matrix is calculated as follows [79, 17].

$$\begin{aligned} P_{k+1|k+1} = P_{k+1|k} - \begin{bmatrix} K_{u_{k+1}} \\ K_{l_{k+1}} \end{bmatrix} H P_{k+1|k} - P_{k+1|k} H^T \begin{bmatrix} K_{u_{k+1}} \\ K_{l_{k+1}} \end{bmatrix}^T \\ + \begin{bmatrix} K_{u_{k+1}} \\ K_{l_{k+1}} \end{bmatrix} S_{k+1} \begin{bmatrix} K_{u_{k+1}} \\ K_{l_{k+1}} \end{bmatrix}^T \end{aligned} \tag{5.20}$$

Figure 5.2 illustrates one cycle of the GVBL-SVSF algorithm.

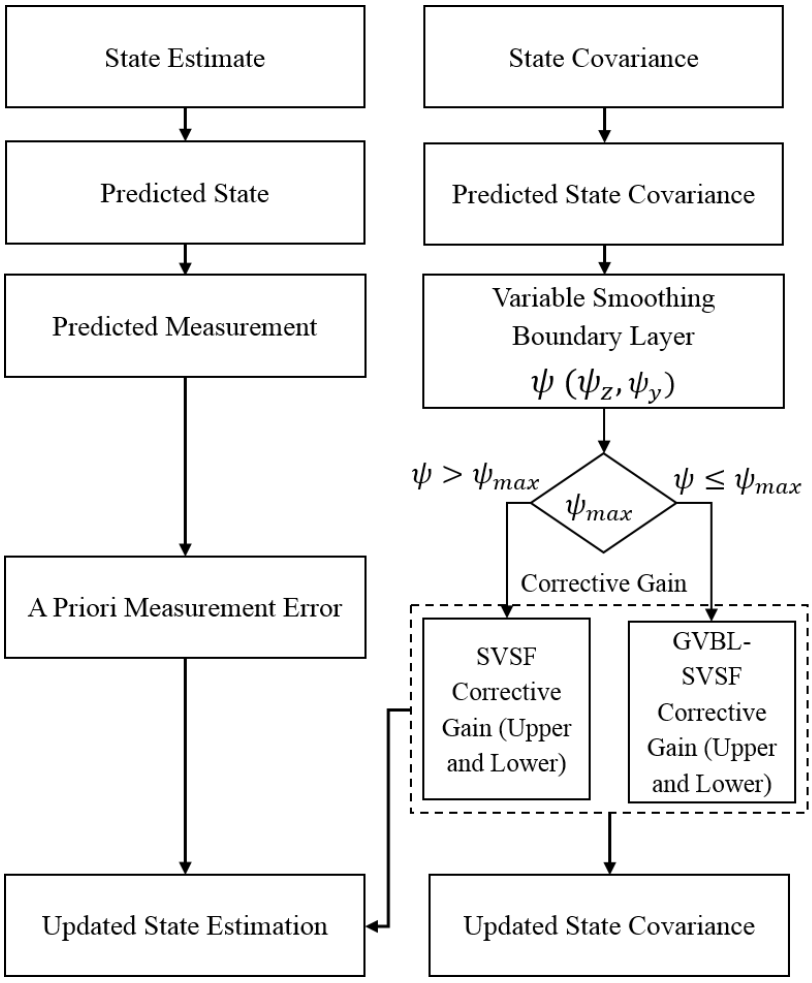

Figure 5.2 One cycle in the GVBL-SVSF estimation

5.4 Data Association Principles

The measurement origin uncertainty often arise in target tracking scenarios. This is due to the presence of clutter and false measurements, which gives more than one measurement for each target. In data association methods, the measurements are associated

to tracks, or sets of observations, based on the likelihood that each measurement could have originated from the track. In probabilistic data association (PDA), it is assumed that the target track has been initialized. Also, the past information through time $k-1$ about the target trajectory is in the form of a normal distribution as follows [5].

$$p[x_{k-1}|Z^{k-1}] = \mathcal{N}[x_{k-1}; \hat{x}_{k-1|k-1}, P_{k-1|k-1}] \tag{5.21}$$

In PDA-based filtering methods, there are three main steps for data association and filtering: state prediction, measurement gating and data association, and state update as follows [79].

State prediction: the system of equations (5.1) and (5.2) is assumed. The state and measurement vectors and the covariance matrix are predicted at time $k+1$ from time k as in GVBL-SVSF by (5.6) to (5.8). The innovation covariance matrix corresponding to the correct measurement is also calculated as (5.10).

Measurement gating and data association: gating refers to selection of a portion of the measurements that are more probable to be originated from the target. The validation gate is defined as an elliptical region around the predicted measurement as follows:

$$G_{k+1,\gamma} = \left\{z: \left[z - \hat{z}_{k+1|k}\right]' S_{k+1}^{-1} \left[z - \hat{z}_{k+1|k}\right] \leq \gamma\right\} \tag{5.22}$$

where γ is the gate threshold corresponding to gate probability P_G [4]. The set of validated measurements according to validation criterion is

$$z_{k+1} = \left\{z_{k+1}^i\right\}_{i=1}^{m_{k+1}} \tag{5.23}$$

There are $m_{k+1}+1$ distinct association hypothesis one can describe for m_{k+1} validated measurements, as below [5].

$$\mathcal{H}_{k+1}^{0} = \{none\ of\ the\ measurements\ are\ target\ originated\} \tag{5.24}$$

$$\mathcal{H}_{k+1}^{i} = \left\{z_{k+1}^{i}\ is\ target\ originated\ \right\} \tag{5.25}$$

The total available measurements at time $k+1$ are $Z^{k+1} = \{z_{k+1}^{1}, \dots, z_{k+1}^{m}\} \cup Z^{k}$. For the parametric PDA, with the Poisson clutter model with spatial density λ, the association probability β_{k+1}^{i} is defined as the conditioned probability of the i^{th} hypothesis at time $k+1$, as (5.26) and computed as (5.27) [4, 1]

$$\beta_{k+1}^{i} = P\{\mathcal{H}_{k+1}^{i} | Z^{k+1}\} \tag{5.26}$$

$$\beta_{k+1}^{i} = \begin{cases} \dfrac{1 - P_D P_G}{1 - P_D P_G + \sum_{i=1}^{m_{k+1}} \mathcal{L}_{k+1}^{i}}, & i = 0 \\ \dfrac{\mathcal{L}_{k}^{i}}{1 - P_D P_G + \sum_{i=1}^{m_{k+1}} \mathcal{L}_{k+1}^{i}}, & i = 1, \dots, m_{k+1} \end{cases} \tag{5.27}$$

where P_D is the target detection probability and, $\mathcal{L}_{k+1}^{i}$ is the likelihood ratio of the measurement z_{k+1}^{i} originating from the target, and computed as follows [5, 4]:

$$\mathcal{L}_{k+1}^{i} = \frac{\mathcal{N}\left[z_{k+1}^{i}; \hat{z}_{k+1|k}, S_{k+1}\right] P_D}{\lambda} \tag{5.28}$$

State update: the states in PDA-GVBL-SVSF are updated according to (5.11), as follows:

$$\hat{x}_{k+1|k+1} = \begin{bmatrix} \hat{x}_{u_{k+1|k+1}} \\ \hat{x}_{l_{k+1|k+1}} \end{bmatrix} = \begin{bmatrix} \hat{x}_{u_{k+1|k}} \\ \hat{x}_{l_{k+1|k}} \end{bmatrix} + \begin{bmatrix} K_{u_{k+1}} \\ K_{l_{k+1}} \end{bmatrix} \vartheta_{k+1} \tag{5.29}$$

where $\vartheta_{k+1|k}$ is the combined innovation term, defined as the weighted sum of the validated measurements' innovation terms as follows [80, 79].

$$\vartheta_{k+1} = \sum_{i=1}^{m_{k+1}} \beta_{k+1}^{i} e_{z,k+1|k}^{i} \tag{5.30}$$

To update the covariance, the following equation is used [80, 79].

$$P_{k+1|k+1} = \beta_{k+1}^{0} P_{k+1|k} + [1 - \beta_{k+1}^{0}] P_{k+1|k+1}^{*} + \tilde{P}_{k+1} \tag{5.31}$$

where $P_{k+1|k+1}^{*}$ is calculated as in (5.20) and $\tilde{P}_{k+1}$ accounts for the spread of innovation terms and is computed as follows [4]:

$$\tilde{P}_{k+1} = \begin{bmatrix} K_{u_{k+1}} \\ K_{l_{k+1}} \end{bmatrix} \left[\sum\nolimits_{i=1}^{m_{k+1}} \beta_{k+1}^{i} e_{z,k+1|k}^{i} {e_{z,k+1|k}^{i}}^{T} - \vartheta_{k+1} \vartheta_{k+1}^{T} \right] \begin{bmatrix} K_{u_{k+1}} \\ K_{l_{k+1}} \end{bmatrix}^{T} \tag{5.32}$$

The PDA-GVBL-SVSF is formulated for tracking single targets. The extension of PDA-GVBL-SVSF for multi-target tracking problems is the joint PDA-GVBL-SVSF (JPDA-GVBL-SVSF) [79]. These two algorithms use similar state prediction and state update approaches. However, the main difference is in the data association and the calculation of association probabilities [5, 79]. In PDA-GVBL-SVSF, the association probabilities are calculated separately for each target, while in the JPDA-GVBL-SVSF, the probabilities are calculated jointly across all the targets which share some validated measurements [5, 79]. The conditional probabilities of the following joint events are evaluated as follows [5, 79].

$$\mathcal{H}_{k+1} = \bigcap_{j=1}^{m_{k+1}} \mathcal{H}_{k+1}^{j,t^{j}} \tag{5.33}$$

where $\mathcal{H}_{k+1}^{j,t^j}$ is the hypothesis that measurement j originated from target t, $j = 1, \dots, m_{k+1}$, $t = 0, \dots, T$ is the time index, t^j is the target that measurement j is associated with, m_{k+1} is the number of measurements, and T is the number of targets [31]. The total available measurements at time $k+1$ are $Z^{k+1} = \{z_{k+1}^1, \dots, z_{k+1}^m\} \cup Z^k$. The joint association probabilities are calculated as follows [5].

$$P\{\mathcal{H}_{k+1}|Z^{k+1}\} = c \prod_j \left\{\lambda^{-1}\mathcal{L}_{k+1}^{t^j}\right\}^{\tau^j} \prod_t (P_D^t)^{\delta^t}(1 - P_D^t)^{1-\delta^t} \tag{5.34}$$

where λ is the spatial density of the number of false measurements defined from a Poisson distribution, and P_D^t is the detection probability of target t. τ^j and δ^t are the target detection and measurement association indicators, respectively [31] and,

$$\mathcal{L}_{k+1}^{t^j} = \mathcal{N}[z_{k+1}^j; \hat{z}_{k+1|k}^{t^j}, S_{k+1}^{t^j}] \tag{5.35}$$

The state estimation is carried out separately for each target using the marginal association probabilities [5, 31]. These probabilities are obtained from joint probabilities (5.34) by summing the joint hypotheses in which the marginal hypothesis of interest is included, as follows [5].

$$\beta_{k+1}^{j,t} = P\{\mathcal{H}_{k+1}^{j,t}|Z^{k+1}\} = \sum_{\mathcal{H}:\mathcal{H}^{j,t} \in \mathcal{H}} P\{\mathcal{H}_{k+1}|Z^{k+1}\} \tag{5.36}$$

These probabilities are used to create the combined innovation for each target, which is used during the filter update stage.

5.5 A Novel Approach for Augmenting Probabilistic Data Association

5.5.1 A. Chattering Magnitude in SVSF and the Information Content

The probabilistic data association (PDA) methods utilize the likelihood that each measurement could have originated from each track to assign the measurements to the various tracks. Using the SVSF in the structure of PDA provides an extra source of information (chattering) that is employed in this section to augment the association probabilities.

The SVSF approach gives two sets of indicators of performance. The primary set of indicators of performance are the estimation errors and the error covariance matrix, which is in common with other filtering strategies like the Kalman filter. The secondary set of indicators of performance are the chattering signals from the application of discontinuous corrective gains, which in a predictor-corrector sense is unique to the SVSF. By use of the smoothing boundary layer, the chattering which is inherently an undesirable phenomenon, is eliminated in the normal working condition. However, when modeling uncertainties exist, the chattering will occur and the magnitude of the chattering is an indicator of the severity of the uncertainties. Therefore, the magnitude of the chattering signal carries information that can be exploited.

The magnitude of chattering is equal to the difference between the width of the smoothing boundary layer and the magnitude of the a priori measurement error [15], as follows.

$$C_{k+1|k} = max(0, |e_{z,k+1|k}| - \psi_{z,k+1}) = \begin{cases} |e_{z,k+1|k}| - \psi_{z,k+1}, & |e_{z,k+1|k}| \geq \psi_{z,k+1} \\ 0, & |e_{z,k+1|k}| < \psi_{z,k+1} \end{cases} \quad (5.37)$$

where $\boldsymbol{\psi}_{k+1}$ is a vector consisting of diagonal elements of boundary layer matrix Ψ_{k+1}. The following procedure is used to calculate the probability distribution function of the chattering magnitude signal $C_{k+1|k}$. It is assumed that the measurements are normally distributed as $z_{k+1} \sim \mathcal{N}(z_{k+1}; \hat{z}_{k+1|k}, S_{k+1})$. As a result, the distribution of the a priori measurement error is as follows.

$$e_{z,k+1|k} \sim \mathcal{N}(e_{z,k+1|k}; 0, S_{k+1}) \tag{5.38}$$

The probability distribution of the absolute value of a normally distributed random variable is a half-normal distribution function [81]. The half-normal distribution is a special case of the folded normal distribution when the expected value of the random variable equals zero. A multivariate folded normal distribution is recently formulated in [81]. This formulation represents the multivariate folded normal distribution as the sum of a number of multivariate normal distributions, noted as h_p. Let $\boldsymbol{S}(\boldsymbol{p}) = \{\boldsymbol{s}: \boldsymbol{s} = (s_1, s_2, \dots s_p), with\ s_i = \pm 1, \forall\ 1 \leq i \leq p\}$, where p denotes the order of the random vector. Then the multivariate folded normal distribution is represented as below.

$$f_p(z_1, z_2, \dots, z_p) = \sum_{(s_1, s_2, \dots, s_p) \in \boldsymbol{S}(\boldsymbol{P})} h_p(s_1 z_1, s_2 z_2, \dots, s_p z_p), \quad for\ \forall\ z_i > 0 \tag{5.39}$$

For example, the bivariate half-normal distribution for random vector $\boldsymbol{z} = \begin{bmatrix} z_1 \\ z_2 \end{bmatrix}$ with zero mean and covariance matrix Σ may be shown as follows.

$$\begin{aligned} \mathcal{N}_h(\boldsymbol{z}; 0, \Sigma) = \frac{1}{4\pi\sqrt{|\Sigma|}} \Big\{ exp\left(-\frac{1}{2}\boldsymbol{z}'\Sigma^{-1}\boldsymbol{z}\right) \\ + exp\left(-\frac{1}{2}\boldsymbol{z}'(2diag(diag(\Sigma)) - \Sigma)^{-1}\boldsymbol{z}\right)\Big\};\ \forall\ z_i > 0 \end{aligned} \tag{5.40}$$

The distribution of the absolute value of the a priori measurement error is a half normal distribution of order m, where m is the order of measurement vector. For a 2-dimentional measurement matrix, this distribution is as follows.

$$\begin{aligned}&\mathcal{N}_h\left(\left|e_{z,k+1|k}\right|; 0, S_{k+1}\right)\\&= \frac{1}{4\pi\sqrt{|S_{k+1}|}}\left\{exp\left(-\frac{1}{2}\left|e_{z,k+1|k}\right|' {S_{k+1}}^{-1}\left|e_{z,k+1|k}\right|\right)\right.\\&+ exp\left(-\frac{1}{2}\left|e_{z,k+1|k}\right|'(2diag(diag(S_{k+1}))\right.\\&\left.\left.- S_{k+1})^{-1}\left|e_{z,k+1|k}\right|\right)\right\}; \left|e_{z,k+1|k}\right| \in (0,\infty)\end{aligned} \tag{5.41}$$

From (5.37) and (5.41), and with a simple change of variable the probability distribution function of chattering magnitude signal is as follows, and depicted in Figure 5.3.

$$\begin{aligned}f\left(C_{k+1|k}\right) = \frac{1}{4\pi\sqrt{|S_{k+1}|}}&\left\{exp\left(-\frac{1}{2}\left(C_{k+1|k}\right)' {S_{k+1}}^{-1}\left(C_{k+1|k}\right)\right)\right.\\&+ exp\left(-\frac{1}{2}\left(C_{k+1|k}\right)'(2diag(diag(S_{k+1}))\right.\\&\left.\left.- S_{k+1})^{-1}\left(C_{k+1|k}\right)\right)\right\}; \left(C_{k+1|k}\right) \in (0,\infty)\end{aligned} \tag{5.42}$$

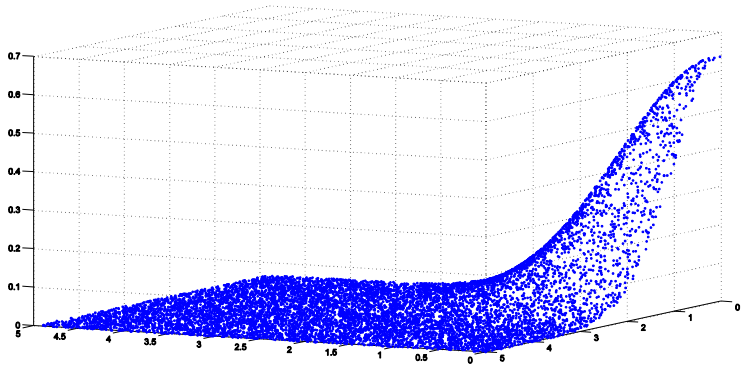

Figure 5.3 Probability distribution function of chattering magnitude signal

Having the probability distribution function of the chattering magnitude signal, provides the required tool to use this information content to improve the data association probabilities. The next section is devoted to deriving the augmented association probabilities.

5.5.2 Derivation of Augmented Association Probabilities

The association probabilities in the probabilistic data association methods are derived by a Bayesian inference. The probability density of each association hypothesis given the prior information is sought to calculate the association probabilities. In its conventional form, PDA uses the current measurement and its history as the prior information, as $P\{\mathcal{H}_k^{\mathrm{i}})|Z^k\}$ [80]. The SVSF-based approaches give an extra source of information which is the chattering information, extracted in the form of chattering magnitude. The total available chattering magnitude signals at time $k+1$ are $C^{k+1} = \{C_{k+1}^1, \dots, C_{k+1}^m\} \cup C^k$. Thus, the new set of conditional hypotheses densities are given as follows.

$$P\{\mathcal{H}_{k+1}^i|Z^{k+1}, C^{k+1}\} = P\{\mathcal{H}_k^i|z_{k+1}, Z^k, C_{k+1}, C^k\} \tag{5.43}$$

Using the Bayesian rule (5.43) is written as follows.

$$P\{\mathcal{H}_{k+1}^{i}|Z^{k+1},C^{k+1}\} = c^{-1}\, p[z_{k+1},C_{k+1}|\mathcal{H}_{k+1}^{i},Z^{k},C^{k}\,]P\{\mathcal{H}_{k+1}^{i}|Z^{k},C^{k}\} \tag{5.44}$$

where $c = p[z_{k+1},C_{k+1}|Z^{k},C^{k}]$ is the normalization constant and is independent of particular hypotheses.

It is required to further break the equation (5.44) into computable probability distribution functions. For this purpose, there are two valid and possible alternatives for applying the conditional probability rule to (5.44). The first alternative is as follows.

$$\begin{aligned} &P\{\mathcal{H}_{k+1}^{i}|Z^{k+1},C^{k+1}\} \\ &= c\; p[C_{k+1}|z_{k+1},\mathcal{H}_{k+1}^{i},Z^{k},C^{k}\,]p[z_{k+1}|\mathcal{H}_{k+1}^{i},Z^{k},C^{k}\,]P\{\mathcal{H}_{k+1}^{i}|Z^{k},C^{k}\} \end{aligned} \tag{5.45}$$

The second alternative is as below.

$$\begin{aligned} &P\{\mathcal{H}_{k+1}^{i}|Z^{k+1},C^{k+1}\} \\ &= c\; p[z_{k+1}|C_{k+1},\mathcal{H}_{k+1}^{i},Z^{k},C^{k}\,]p[C_{k+1}|\mathcal{H}_{k+1}^{i},Z^{k},C^{k}\,]P\{\mathcal{H}_{k+1}^{i}|Z^{k},C^{k}\} \end{aligned} \tag{5.46}$$

Both (5.45) and (5.46) are perfectly valid applications of conditional probability theorem. However, (5.46) is less appropriate for our purposes. The density $p[C_{k+1}|\mathcal{H}_{k+1}^{i},Z^{k},C^{k}\,]$ lacks conditioning on the most recent measurement. Due to the nature of the chattering signal, the most recent chattering is affected by both the recent measurement and the history of measurements. So, the calculation of the second term in (5.46) would be difficult if not impossible. Note that the density of chattering magnitude signal is conditioned on the most recent measurement in (5.45). Therefore, (5.45) is the suitable alternative to continue with.

At this point a discussion of the factors influencing the densities in (5.45) is necessary. In the right hand side of equation (5.45), the density of the most recent chattering signal magnitude is only affected by the most recent measurement, thus in the first term the conditioning on the history of measurement and chattering signal can be disregarded. Also, since the density of the most recent measurement is not affected by the history of the chattering signal, in the second term the condition of z_{k+1} on C^k can be eliminated. Furthermore, without conditioning on the recent information, the density of hypothesis is not affected by the history of information and hence in the third term one can eliminate the conditioning of $\mathcal{H}_{k+1}^i$ on Z^k and C^k. As such (5.45) is updated as follows.

$$P\{\mathcal{H}_{k+1}^i | Z^{k+1}, C^{k+1}\} = c\, p[C_{k+1} | z_{k+1}, \mathcal{H}_{k+1}^i]\, p[z_{k+1} | \mathcal{H}_{k+1}^i, Z^k]\, P\{\mathcal{H}_{k+1}^i\} \quad (5.47)$$

Equation (5.47) gives the relation for new augmented association probabilities that also include the chattering information. Each of the terms in the right hand side of (5.47) will be derived next.

Calculation of $p[z_{k+1} | \mathcal{H}_{k+1}^i, Z^k]$: The probability distribution function of the correct measurement, z_{k+1}^i, with Gaussian assumption that is restricted with gate probability of P_G is as follows.

$$p[z_{k+1}^i | \mathcal{H}_{k+1}^i, Z^k] = P_G^{-1} \mathcal{N}(e_{z,k+1|k}; 0, S_{k+1}) \quad (5.48)$$

Therefore, with the assumption of uniform distribution for clutter, the pdf of $p[z_{k+1} | \mathcal{H}_{k+1}^i, Z^k]$ is as follows [80].

$$p[z_{k+1} | \mathcal{H}_{k+1}^i, Z^k] = \begin{cases} V_{k+1}^{-m_{k+1}+1} P_G^{-1} \mathcal{N}(e_{z,k+1|k}; 0, S_{k+1}), i = 1, \dots, m_{k+1} \\ V_{k+1}^{-m_{k+1}} \quad , i = 0 \end{cases} \quad (5.49)$$

where V_{k+1} is the volume of the validation gate.

Calculation of $P\{\mathcal{H}_{k+1}^{i}\}$: Assuming a Poisson model with spatial density λ, for the number of false alarms, the probabilities of association hypotheses are calculated as below [80].

$$p\{\mathcal{H}_{k+1}^{i}\} = \begin{cases} P_D P_G [P_D P_G m_{k+1} + (1 - P_D P_G)\lambda V_{k+1}]^{-1} & , i = 1, \dots, m_{k+1} \\ (1 - P_D P_G)\lambda V_{k+1} [P_D P_G m_{k+1} + (1 - P_D P_G)\lambda V_{k+1}]^{-1} & , i = 0 \end{cases} \quad (5.50)$$

Calculation of $p\left[C_{k+1} \middle| z_{k+1}, \mathcal{H}_{k+1}^{i}\right]$: The probability distribution function of the chattering magnitude signal for correct measurement, C_{k+1}^{i}, is a multivariate half-Normal distribution as in (5.39) restricted with gate probability of P_G as follows.

$$p\left[C_{k+1}^{i} \middle| \mathcal{H}_{k+1}^{i}, Z^{k}\right] = P_G^{-1} \mathcal{N}_h\left(C_{k+1}^{i}; 0, S_{k+1}\right) \quad (5.51)$$

Therefore, with the assumption of uniform distribution for clutter in the volume outside the smoothing boundary layer's hyper rectangular and inside the gate ellipsoid, the pdf of $p\left[C_{k+1} \middle| \mathcal{H}_{k+1}^{i}, Z^{k}\right]$ is as follows [80].

$$p\left[C_{k+1} \middle| \mathcal{H}_{k+1}^{i}, Z^{k}\right] = \begin{cases} (V_{k+1} - 2^{n_z}\, det(\Psi_{k+1}))^{1-m_{k+1}} P_G^{-1} \mathcal{N}_h\left(C_{k+1}^{i}; 0, S_{k+1}\right), i = 1, \dots, m_{k+1} \\ (V_{k+1} - det(\Psi_{k+1}))^{-m_{k+1}} \qquad , i = 0 \end{cases} \quad (5.52)$$

where the volume of the smoothing boundary layer hyper rectangular is calculated by $2^{n_z} \det(\Psi_{k+1})$, in which n_z is the dimension of measurement vector.

Calculation of the augmented association probability $P\{\mathcal{H}_{k+1}^{i}|Z^{k+1}, C^{k+1}\}$: Substitution of (5.49), (5.50) and (5.52) into (5.47) gives the new set of association probabilities as follows.

$$\beta_i = \begin{cases} \dfrac{f_i}{a + \sum_{i=1}^{m_{k+1}} f_i} & , i = 1, \dots, m_{k+1} \\ \dfrac{a}{a + \sum_{i=1}^{m_{k+1}} f_i} & , i = 0 \end{cases} \tag{5.53}$$

where

$$a \triangleq \frac{\lambda P_G (1 - P_D P_G)}{V_{k+1} - 2^{m_{k+1}}\, det(\Psi_{k+1})}$$
$$f_i \triangleq \mathcal{N}(e_{z,k+1|k}; 0, S_{k+1}) \mathcal{N}_h\left(C_{k+1}^{i}; 0, S_{k+1}\right) \tag{5.54}$$

5.5.3 Chattering Signal Magnitude and Size of Validation Gate

In this section the relation between the magnitude of chattering signal and the validation gate is investigated. In the process of estimation and data association, a multi-dimensional gate is set up to validated the more probable measurements. This approach avoids the search for the candidate measurements in the entire measurement space, and only considers the measurements within the validation gate. The equation of the gate ellipsoid from (5.22) is as follows.

$$\left[z - \hat{z}_{k+1|k}\right]' S_{k+1}^{-1} \left[z - \hat{z}_{k+1|k}\right] = \gamma \tag{5.55}$$

which is an ellipsoid centered at $\hat{z}_{k+1|k}$. This ellipse is defined by the solutions of z to (5.55) where S_{k+1}^{-1} is a positive definite matrix and γ is the gate threshold. One can write (5.55) as below:

$$\left[z - \hat{z}_{k+1|k}\right]' \gamma^{-1} S_{k+1}^{-1} \left[z - \hat{z}_{k+1|k}\right] = 1 \tag{5.56}$$

The eigenvalues of $\gamma^{-1} S_{k+1}^{-1}$ are the reciprocals of the squares of the semi-axes of the gate ellipsoid [82]. Assume that the eigenvalues of S_k are $\lambda_{S_1}, \dots, \lambda_{S_m}$. Then the axes of the gate ellipsoid will be $\sqrt{\gamma}\sqrt{\lambda_{S_1}}, \dots, \sqrt{\gamma}\sqrt{\lambda_{S_m}}$.

A number of measurements fall within the validation gate. These are the most probable candidates for target-originated measurements. Among the validated measurements, some of them, however, may fall outside the smoothing boundary layer. These measurements will cause a chattering signal. Figure 5.4 is a 2-dimensional illustration of this situation. In Figure 5.4 $\hat{z}_{k+1|k}$ is the predicted measurement. Three measurements are received. z_{k+1}^3 is out of the validation gate and is disregarded. z_{k+1}^1 and z_{k+1}^2 are inside the gate and considered for further processing. However, z_{k+1}^1 is outside the smoothing boundary layer rectangular and causes a chattering signal.

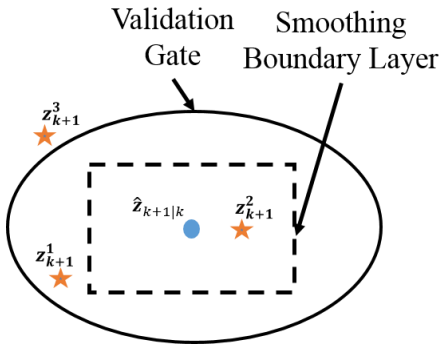

Figure 5.4 Validation gate and smoothing boundary layer rectangular

With respect to (5.37), the boundaries beyond which a measurement will cause a chattering signal is given below.

$$\left|z - \hat{z}_{k+1|k}\right| = \boldsymbol{\psi}_{z,k+1} \tag{5.57}$$

which represents the equation of a hyper-rectangular. For the measurements which are inside the gate ellipsoid, but outside the boundary hyper-rectangular there exists a chattering signal. The magnitude of this chattering signal abides by the distribution (5.42). To compare the gate ellipsoid with the boundary hyper-rectangular, a conservative way is to compare the gate ellipsoid with the bounding ellipsoid of the boundary hyper-rectangular. There are an infinite number of bounding ellipsoids for one hyper-rectangular, among which the bounding ellipsoid with the same proportions as the hyper-rectangular is assumed. The equation representing such ellipsoid is as follows.

$$\left[z - \hat{z}_{k+1|k}\right]' \left(m\Psi_{z,k+1}^2\right)^{-1} \left[z - \hat{z}_{k+1|k}\right] = 1 \tag{5.58}$$

where m is the dimension of the measurement vector. The axes of ellipsoid (5.58) are the eigenvalues of $m\Psi_{z,k+1}^2$. Therefore, assuming that the off-diagonal elements of $\Psi_{z,k+1}$are negligible, the vector consisting of axes for such ellipsoid is $\sqrt{m}\boldsymbol{\psi}_{z,k+1}$.

With respect to (5.3) and (5.16), the smoothing boundary layer matrix is calculated as follows.

$$\Psi_{z,k+1} = S_{k+1} {P_{k+1|k}^{11}}^{-1} diag(E_{z,k+1}) \tag{5.59}$$

The following theorem from [83] is used to find upper and lower bounds for the smoothing boundary layer.

Theorem [83]: Let A and B be m dimensional positive definite matrices. Let $\lambda_1(B)$ and $\lambda_m(B)$ denote the smallest and the largest eigenvalues of B, and the eigenvalues of A and AB are ascendingly ordered. Then,

$$\forall k\ , 1 \le k \le m: \lambda_k(A)\lambda_1(B) \le \lambda_k(AB) \le \lambda_k(A)\lambda_m(B) \tag{5.60}$$

To apply (5.60) to (5.59), assume that $A = S_{k+1}$ and $B = {P_{k+1|k}^{11}}^{-1} diag(E_{z,k+1})$. S_{k+1} is a positive definite matrix. Also, the product of a positive definite matrix (${P_{k+1|k}^{11}}^{-1}$) and a diagonal matrix with positive diagonal elements ($diag(E_{z,k+1})$) is a positive definite matrix. Therefore, the conditions of the theorem hold and the below inequalities are valid.

$$\begin{cases} \lambda_{S_1}\lambda_1(B) \le \sqrt{m}\psi_1 \le \lambda_{S_1}\lambda_m(B) \\ \vdots \\ \lambda_{S_m}\lambda_1(B) \le \sqrt{m}\psi_m \le \lambda_{S_m}\lambda_m(B) \end{cases} \tag{5.61}$$

If the upper bound of inequality (5.61) is smaller than the eigenvalues of $\gamma^{-1}S_{k+1}^{-1}$ as in (5.56), then the gate ellipsoid will encompass the boundary layer hyper-rectangular. Therefore, the following inequality should hold.

$$\begin{cases} \lambda_{S_1}\lambda_m(B) \le \sqrt{\gamma}\sqrt{\lambda_{S_1}} \\ \vdots \\ \lambda_{S_m}\lambda_m(B) \le \sqrt{\gamma}\sqrt{\lambda_{S_m}} \end{cases} \tag{5.62}$$

Inequality (5.62) is rearranged as follows.

$$\left[\sqrt{\lambda_{S_1}}\right]\lambda_m(B) \leq \sqrt{\gamma} \tag{5.63}$$

The term $\lambda_m(B)$ in (5.63) is a function of predicted state covariance matrix $P^{11}_{k+1|k}$ and the error vector $E_{z,k+1}$. Inequality (5.63) defines the criteria that if it holds for any measurements, that measurement is inside the validation gate, but outside the smoothing boundary layer. For such measurement chattering signal is observed. The magnitude of the chattering signal is used to discriminate this measurement against other measurements with less or no chattering magnitude. Therefore, if a validated measurements is inside the smoothing boundary layer, it will be weighted with a higher association probability relative to a validated measurement which is outside the smoothing boundary layer. For the case that the condition (5.63) does not hold, the boundary layer is larger than the validation gate. Therefore, none of the validated measurements cause a chattering signal. Since no extra information exists, for this case, the APDA coincides the conventional PDA.

5.6 Results

5.6.1 Simulation Examples

The following scenario of a highly maneuvering target trajectory in clutter is considered. The true trajectory is as depicted in Figure 5.5 and detailed in Table 5.1.

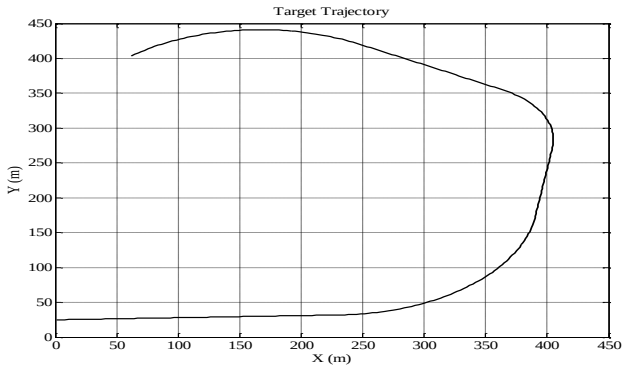

Figure 5.5 True trajectory of the maneuvering target in X-Y plane

Table 5.1 Detail of the true trajectory of simulation scenario (Sampling Time = 0.1 Sec)

Initial State	Maneuver	Duration
$x_0 = 1\ m$ $y_0 = 25\ m$ $v_{x_0} = 33\ m/s$ $v_{y_0} = 1\ m/s$	a non-maneuvering near constant velocity	0.0-7.0s
	a maneuvering coordinated turn motion with angular velocity of $\omega = 0.2\ rad/s$	7.1-14.0s
	a non-maneuvering near constant velocity	14.1-17.0s
	a maneuvering coordinated turn motion with angular velocity of $\omega = 0.4\ rad/s$	17.1-20.0s
	a non-maneuvering near constant velocity	20.1-24.0s
	a maneuvering coordinated turn motion with angular velocity of $\omega = 0.2\ rad/s$	24.1-30.0s

For the motion model a two-dimensional discrete constant velocity model is implemented as follows [6]. The state vector is defined as $\boldsymbol{x} = [x\ y\ v_x\ v_y]$, where x and y are the position in Cartesian coordinates, and v_x and v_y are the respective velocities. In this model, the accelerations of the target between two sequential samples are assumed to be constant with discrete-time zero mean white Gaussian noise. The motion model is defined as follows.

$$x(k+1) = Fx(k) + Gv(k) \tag{5.64}$$

where the state transition matrix and process noise gain matrix are defined as follows.

$$F = \begin{bmatrix} 1 & 0 & T_s & 0 \\ 0 & 1 & 0 & T_s \\ 0 & 0 & 1 & 0 \\ 0 & 0 & 0 & 1 \end{bmatrix}, \qquad G = \begin{bmatrix} T_s^2/2 & 0 \\ 0 & T_s^2/2 \\ T_s & 0 \\ 0 & T_s \end{bmatrix} \tag{5.65}$$

The white acceleration noise covariance matrix is defined as follows.

$$Q = cov\{v(k)\} = \begin{bmatrix} \sigma_v^2 & 0 \\ 0 & \sigma_v^2 \end{bmatrix} \tag{5.66}$$

The measurement model, matrix, and noise covariance are defined respectively as follows.

$$z(k) = Hx(k) + w(k) \tag{5.67}$$

$$H = \begin{bmatrix} 1 & 0 & 0 & 0 \\ 0 & 1 & 0 & 0 \end{bmatrix} \tag{5.68}$$

$$R = cov\{w(k)\} = \begin{bmatrix} \sigma_w^2 & 0 \\ 0 & \sigma_w^2 \end{bmatrix} \tag{5.69}$$

For the purpose of simulations, the following parameters are assumed: $\sigma_v^2 = 6^2$, $\sigma_w^2 = 1$, and $T_s = 0.1\ s$. Also, the clutter is generated from a uniform distribution with the number of false measurements, or clutter points obtained from a Poisson's distribution. The simulation is performed for several values of spatial densities for the clutter and compares the performance of APDA-SVSF, the PDA-SVSF and the PDA-KF for different values of clutter densities.

For the first simulation the spatial density equals $\lambda = 1/m^2$, in the surveillance window. All three methods were able to track the target. Table 5.2 shows the root mean squared estimation error (RMSE) for three methods, PDA-KF, PDA-SVSF, and APDA-SVSF, for 500 Monte Carlo runs. Based on the RMSE results the SVSF-based methods outperform

the KF based method. This is the consequence of the robustness of the SVSF against modeling uncertainties.

Table 5.2. RMSE of State Estimations for Target Tracking Case

States	PDA-KF	PDA-SVSF	APDA-SVSF
$\boldsymbol{x}$	0.56	0.29	0.08
$\boldsymbol{y}$	0.51	0.35	0.07
$\boldsymbol{v_x}$	2.09	1.99	1.61
$\boldsymbol{v_y}$	2.07	2.01	1.36

The second simulation is performed with the spatial density of clutter equal to $\lambda = 10/m^2$. Figure 5.6 shows a sample run of the tracking scenario for APDA-SVSF, PDA-SVSF and PDA-KF. Both APDA-SVSF and PDA-SVSF are able to handle the tracking scenario. However, the PDA-KF fails to track the target in its maneuvering motion, since the maneuver imposes a modeling uncertainty to the filtering system. Table 5.3 shows the root mean squared estimation error (RMSE) for APDA-SVSF and PDA-SVSF, for 500 Monte Carlo runs. Because of the proposed augmented probabilistic association technique, the RMSE of APDA-SVSF is dramatically decreased compared to original PDA-SVSF. The APDA-SVSF provides a more efficient set of association probabilities that in turn translates to lower estimation errors. More specifically, if the spatial density of the clutter further increases, the PDA-SVSF also fails to track the clutter in this very highly cluttered condition. However, the APDA-SVSF still performs well, with almost similar estimation error range, thanks to extracting extra information in the augmented association probability calculation procedure.

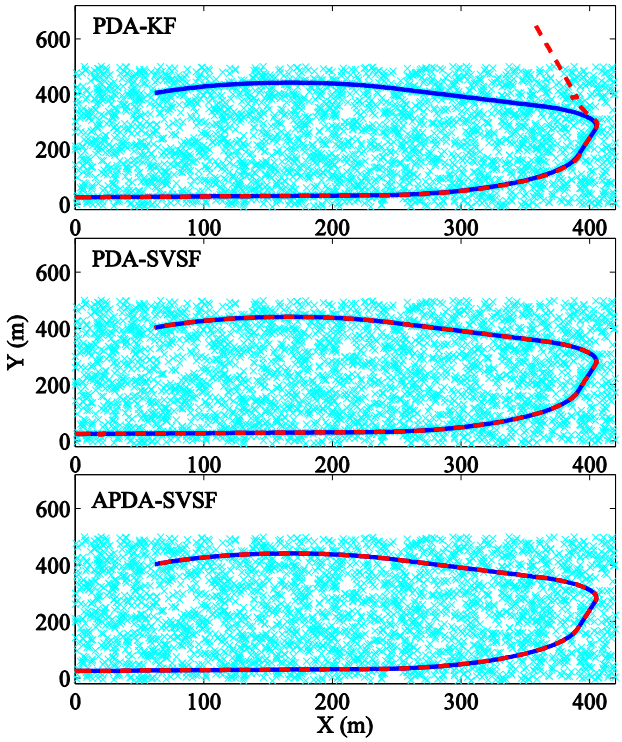

Figure 5.6 Illustration of the operation of PDA-KF, PDA-SVSF, and APDA-SVSF in the presence clutter (shown by cyan cross marks) with spatial density $\lambda = 10/m^2$

Table 5.3. RMSE of State Estimations for Target Tracking Case

States	PDA-SVSF	APDA-SVSF
$\boldsymbol{x}$	0.28	0.09
$\boldsymbol{y}$	0.34	0.08
$\boldsymbol{v_x}$	2.13	1.98
$\boldsymbol{v_y}$	2.04	1.11

5.6.2 Experimental Results

The proposed APDA-SVSF algorithm has been tested on a number of processed LiDAR data sets acquired in actual driving in a highway linking two cities (Hamilton and Toronto

in Canada along a highway called the Queen Elizabeth Way (QEW)). The experimental setup for data acquisition consists of a Ford escape car equipped with a Velodyne HDL32 LiDAR sensor. The driving path and the experimental setup is shown in Figure 5.7.

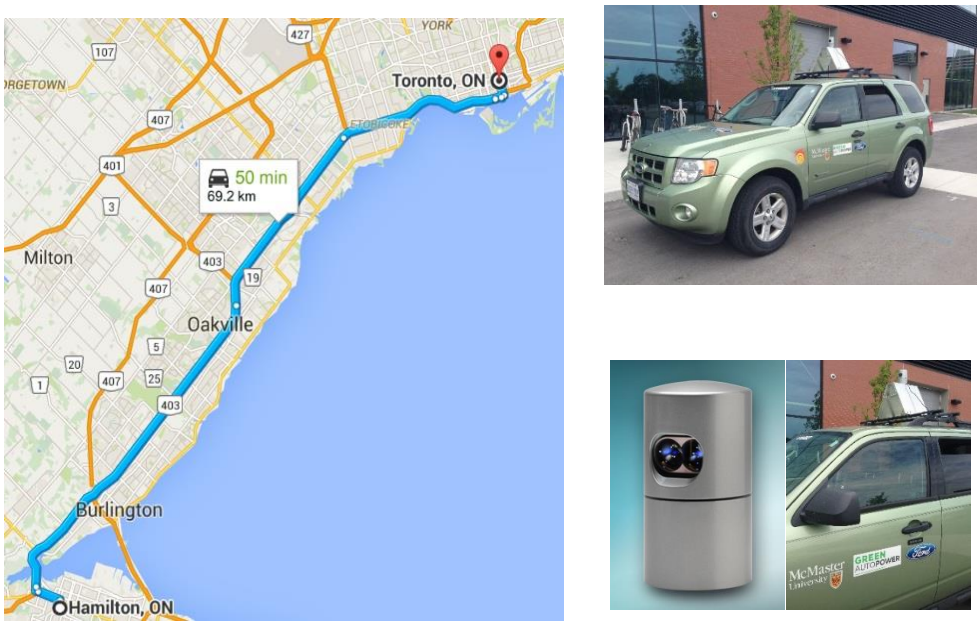

Figure 5.7 Driving path for experimental data gathering and the experimental set up

The LiDAR provides a dense 3D point cloud in each frame with a frame rate of 0.1 second, which requires to be processed before feeding into tracking algorithm. The data processing algorithm includes a segmentation phase followed by a clustering phase. The output of this algorithm are the positions of the centre point of vehicle like objects, which are fed into a data association and tracking system, as shown in Figure 5.8.

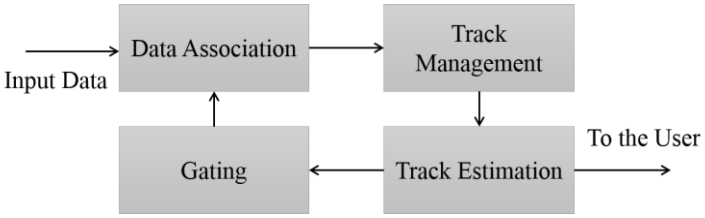

Figure 5.8 Conventional data association and tracking system components

Figure 5.8 provides a pictorial representation of the overall algorithm. It should be noted that the gating, the data association, and the track estimation blocks are those discussed in sections 5.35.4 and 5.4. These complement the new chattering based data association method proposed in section 5.5.

The track management block is required to carry out the track initiation, maintenance and termination. The initiation of a track means forming the initial track state and its associated covariance matrix. The tracks are managed through a rule based process using track score functions. Track score function is a likelihood ratio which is defined and iteratively updated for each track [1]. In each update, the track score is compared to a deletion threshold and a confirmation threshold. An illustration of the implemented track management block is shown in Figure 5.9.

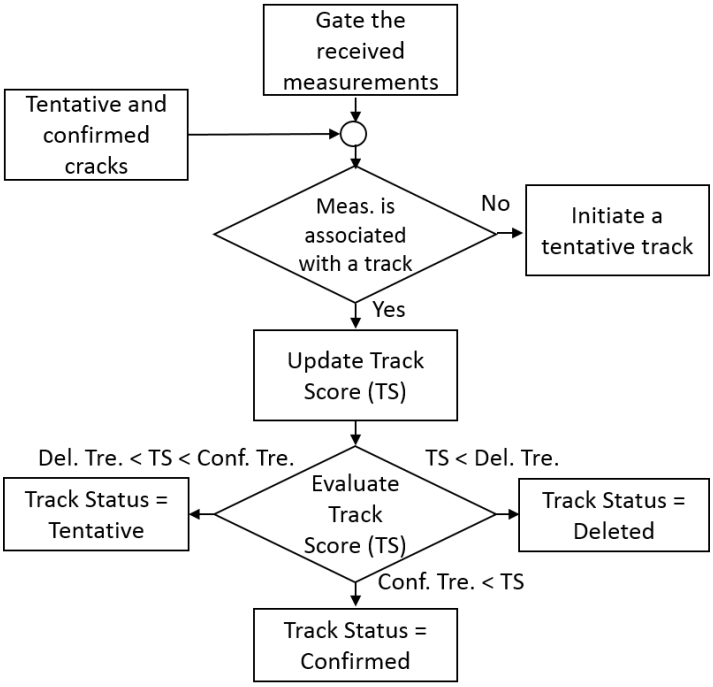

Figure 5.9 The flowchart of the track maintenance algorithm

The performance of the two algorithms, the PDA-KF and the APDA-SVSF, for experimental data is summarized and compared in Table 5.4. Note that the table provides the true positive (TP %), i.e. the percentage of correctly tracked objects, and false positive (FP %), i.e. the percentage of falsely tracked objects, attained by the algorithms. The track break-ups rate is an index that shows the number of relabeled tracks. The relabeling may occur if for any reason a previously confirmed target is missed over a number of frames, and then in the case of redetection, it is treated as a new track, with a new label. From Table 5.4, the proposed algorithm has improved the TP (%) by around 10% and the rate of track break-ups by 4%.

Table 5.4. The performance evaluation of multiple car tracking algorithms comparing JPDA-KF and JPDA-GVBL-SVSF

MTT Strategy	Total # of frames	TP (%)	FP (%)	Rate of Track Break-ups (%)
JPDA-KF	4275	84.21	14.79	7.3
JPDA-GVBL-SVSF		93.42	6.58	3.1

5.7 Conclusion

In this paper, a new data association method has been proposed that extracts extra information using the SVSF method. This novel method, named augmented probabilistic data association-SVSF (APDA-SVSF) uses the chattering information and introduces new set of augmented association probabilities. The APDA-SVSF is derived and then compared with PDA-KF and PDA-SVSF strategies under a designed simulation scenario. The comparison is in terms of estimation accuracy and robustness under different clutter densities. The proposed method significantly improves the performance of the tracking under highly cluttered scenarios. Also, the algorithm is tested on a processed data set from an experimental traffic monitoring system based on LiDAR. The overall performance of the multiple target tracking system is compared to PDA-KF in terms of TP (%), FP (%) and the rate of track break-ups. The proposed algorithm made a more reliable performance for the car tracking experimental data.

Chapter 6

General Conclusion

This thesis mainly deals with further development and formulation of the smooth variable structure filter (SVSF) for single and multiple target tracking in the presence of measurement origin uncertainty. The SVSF is demonstrated to be robust to modeling uncertainties and also giving extra measures of performance, such as the magnitude of the chattering signal. The objective of this research was to elaborate on these characteristics and modify and use them in target tracking and data association. The performance of the SVSF, in its current form for the case when there is fewer measurements than states can be improved by an optimal derivation and by deriving and using its error covariance. Expanding on the current form of the SVSF and preparing it for its combination with data association techniques yields many opportunities for its applications to target tracking problems as well as estimation.

The general overview of the research and the results is shown in Figure 6.1. Considering the interesting characteristics of the SVSF, the research considered the combination of the SVSF with advanced data association algorithms, namely PDA and JPDA. The outcome of this stage was three published conference papers that constituted the first chapter of this thesis.

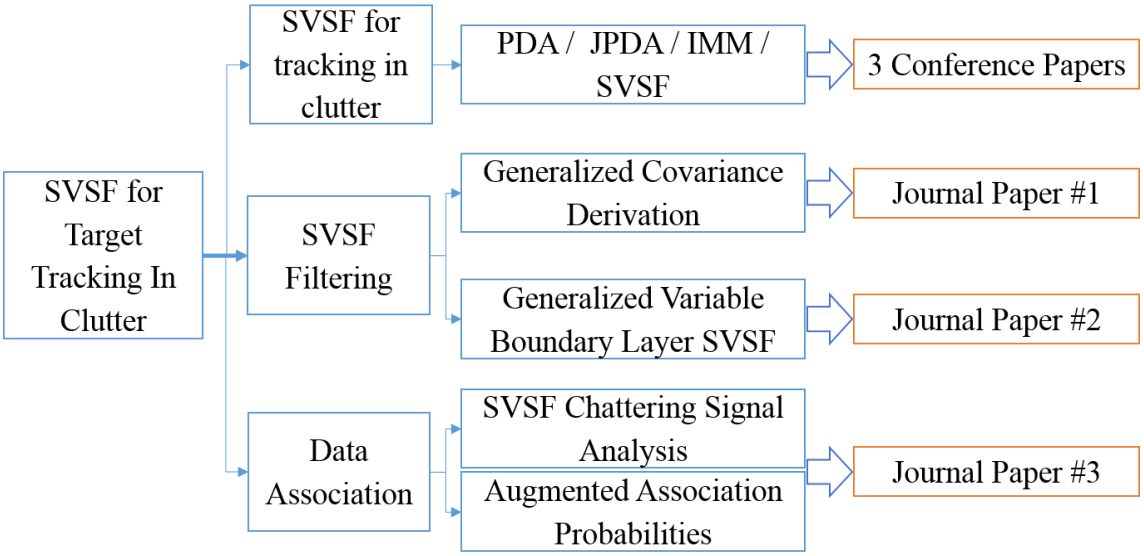

Figure 6.1 Research Flowchart and Outcome

As a second contribution from this research, the covariance of the SVSF was generalized for the cases where the number of the measurements is less than the number of states. This is an essential step in the optimal derivation of the SVSF and in the context of multiple target tracking systems; in a generic tracking system, a number of states describe the dynamics of the system and do not necessarily have a direct measurement associated with them. The proposed covariance formulation of the SVSF is based on the Luenberger observer derivation of the SVSF gain and gives a general formulation of the SVSF covariance. The so called covariance-modified SVSF, CM-SVSF, was then used in combination with probabilistic data association methods, including probabilistic data association (PDA) and joint probabilistic data association (JPDA), and applied to a number of single and multiple target tracking scenarios. The outcome of this research contribution is described in a manuscript submitted to the IEEE Transaction on Aerospace and Electronic systems, and is currently under the second revision.

To further develop the formulation of the SVSF, a generalized variable boundary layer SVSF (GVBL-SVSF) was derived. This new derivation gave an estimation method that is optimal in the MMSE sense when the system does not encounter severe modeling uncertainties; in the existence of modeling uncertainties in the system, the GVBL-SVSF switches back to the SVSF and preserves the robustness of the SVSF to modeling uncertainties. The generalized covariance of the SVSF was used to derive the GVBL-SVSF, hence the algorithm was well equipped to deal with systems with less measurements than states. The GVBL-SVSF was then combined with probabilistic data association methods and tested for a number of tracking scenarios in simulation as well as experimentally. The experimental setup for this study used a LiDAR (light detection and ranging) sensor attached to a car to monitor its surrounding traffic using a dense point cloud. The point cloud is processed and clustered into vehicle-like objects. The centre-point of these objects make the input to the tracking system. The outcome of this step was a journal paper published in IEEE Transaction on Intelligent Transportation Systems.

The SVSF provides extra performance measures including the magnitude of the chattering signal. This performance measure is potentially another source of information to discriminate the measurements and perform the data association more effectively. In the last chapter of this thesis, to examine the above hypothesis, the magnitude of the chattering signal is probabilistically analyzed. The probability distribution function (pdf) of the magnitude of the chattering signal is then calculated. The calculated pdf is used to improve the association probabilities. A Bayesian inference is used to formulate a new set of association probabilities which included the pdf of chattering information. The proposed augmented probabilistic data association (APDA) method in conjunction with GVBL-SVSF constitutes another contribution of this thesis. The APDA-GVBL-SVSF was tested for a number of simulation scenarios as well as LiDAR-based experimental data. The

outcome of this step was a journal paper submitted to IEEE Transaction on Aerospace and Electronic Systems.

This thesis expands the theory of the smooth variable structure filter and provides a general form of the SVSF. This general form opens the path to use the SVSF in several application and research areas in a more efficient manner. Furthermore, the interesting characteristics of the SVSF is examined and demonstrated to be beneficial and effective in the MTT systems. With the introduced concepts and algorithms of this thesis, a new set of tools are now available to solve different multiple target tracking problems.

Bibliography

[1] S. Blackman and R. Papoli, Design and Analysis of Modern Tracking Systems, Norwood, MA: Artech House, 1999.

[2] F. Bengtsson, Models for Tracking in Automotive Safety Systems, Goteborg: Chalmers University of Technology, 2008.

[3] L. Danielsson, Tracking and Radar Sensor Modelling for Automotive Safety Systems, Gothenburg, Sweden: Chalmers University of Technology, 2010.

[4] Y. Bar-Shalom and X. R. Li, Multitarget-Multisensor Tracking: Principles and Techniques, Storrs, CT: YBS Publishing, 1995.

[5] Y. Bar-Shalom, F. Daum and J. Huang, "The Probabilistic Data Association Filter, Estimation in the Presence of Measurement Origin Uncertainty," *IEEE Control Systems,* vol. 29, no. 6, pp. 82-100, Dec 2009.

[6] Y. Bar-Shalom, X. R. Li and T. Kirubarajan, Estimation with Applications to Tracking and Navigation, John Wiley and Sons, 2001.

[7] R. E. Kalman, "A New Approach to Linear Filtering and Prediction Problems," *ASME Journal of Basic Engineering,* vol. 82, pp. 35-45, 1960.

[8] R. Kalman and R. Bucy, "New Results in Linear Filtering and Prediction Theory," *ASME Journal of Basic Engineering,* vol. 83, pp. 95-108, March 1961.

[9] S. J. Julier, J. K. Ulhmann and H. F. Durrant-Whyte, "A New Method for the Nonlinear Transformation of Means and Covariances in Filters and Estimators," *IEEE Trans. on Automatic Control,* vol. 45, pp. 472-482, March 2000.

[10] G. Welch and G. Bishop, "An Introduction to the Kalman Filter," 2006.

[11] D. Simon, Optimal State Estimation: Kalman, H-Infinity, and Nonlinear Approaches, Wiley-Interscience, 2006.

[12] B. Ristic, S. Arulampalam and N. Gordon, Beyond the Kalman Filter: Particle Filters for Tracking Applications, Artech House, 2004.

[13] L. Xie, C. Soh and C. E. Souza, "Robust Kalman Filtering for Uncertain Discrete-Time Systems," *IEEE Trans. Autom. Control,* vol. 39, no. 6, pp. 1310-1314, 1994.

[14] X. Zhu, Y. C. Soh and L. Xie, "Design and Analysis of Discrete-Time Robust Kalman Filters," *Automatica,* vol. 38, no. 6, pp. 1069-1077, 2002.

[15] S. Habibi, "The Smooth Variable Structure Filter," *Proc. IEEE,* vol. 95, no. 5, pp. 1026-1059, 2007.

[16] S. R. Habibi and R. Burton, "The Variable Structure Filter," *ASME J. Dyn. Sys., Meas., Control,* vol. 125, pp. 287-293, 2003.

[17] S. A. Gadsden, Smooth Variable Structure Filtering: Theory and Applications, PhD Thesis, Hamilton, Ontario: McMaster University, 2011.

[18] E. Mazor, A. Averbuch, Y. Bar-Shalom and J. Dayan, "Interacting Multiple Model Methods in Target Tracking: A Survey," *IEEE Trans. on Aerospace & Electronic Systems,* vol. 34, no. 1, pp. 103-123, 1998.

[19] X. R. Li and V. P. Jilkov, "Survey of Maneuvering Target Tracking. Part V: Multiple-Model Methods," *IEEE Trans. On Aerospace & Electronic Systems,* vol. 41, no. 4, pp. 1255-1321, 2005.

[20] H. A. P. Blom and Y. Bar-Shalom, "The Interacting Multiple Model Algorithm for Systems with Markovian Switching Coefficients," *IEEE Trans. Autom. Control,* vol. 33, pp. 780-783, 1988.

[21] H. A. P. Bolm, "An Efficient Filter for Abruptly Changing Systems," in *Proceedings of the 23rd IEEE Conference on Decision and Control*, Las Vegas, NV, Dec. 1984.

[22] G. A. Ackerson and K. S. Fu, "On State Estimation in Switching Environments," *IEEE Trans. on Automatic Control,* Vols. AC-15, no. 1, pp. 10-17, Jan 1970.

[23] D. Musicki and S. Suvorova, "Tracking in Clutter Using IMM-IPDA-Based Algorithms," *IEEE Trans. on Aero. Elec. Sys.,* vol. 44, no. 1, pp. 111-126, 2008.

[24] N. Kaempchen, K. Weiss, M. Schaefer and K. C. J. Dietmayer, "IMM Object Tracking for High Dynamic Driving Maneuvers," in *IEEE Intelligent Vehicles Symposium*, Parma, Italy, June 14-17, 2004.

[25] X. R. Li and Y. Bar-Shalom, "Performance Prediction of the Interacting Multiple Model Algorithm," *IEEE Trans. on Aerospace and Electronic Systems,* vol. 29, no. 3, pp. 755-771, 1993.

[26] D. P. Bertsekas, "The Auction Algorithm: A Distributed Relaxation Method for the Assignment Problem," *Annals of Operations Research,* vol. 14, pp. 105-123, 1988.

[27] K. Jo, J. Kim and M. Sunwoo, "Real-Time Road-Slope Estimation Based on Integration of Onboard Sensors With GPS Using an IMMPDA Filter," *IEEE. Trans. Intell. Trasp. Syst.,* vol. 19, no. 2, pp. 910-918, Dec. 2013.

[28] D. Musicki, R. Evans and S. Stankovic, "Integrated Probabilistic Data Association," *IEEE Trans. Autom. Control,* vol. 39, no. 6, pp. 1237-1241, 1994.

[29] Y. Bar-Shalom and E. Tse, "Tracking in Cluttered Environment with Probabilistic Data Association," *Automatica,* vol. 11, no. 5, pp. 451-460, September 1975.

[30] Y. Bar-Shalom and W. Dale Blair, Multitarget-Multisensor Tracking: Applications and Advances Vol. III, Norwood, MA.: Artech House, 2000.

[31] T. E. Fortmann, Y. Bar-Shalom and M. Scheffe, "Sonar Tracking of Multiple Targets Using Joint Probabilistic Data Association," *IEEE J. Ocean. Eng.,* vol. 8, no. 3, pp. 173-184, 1983.

[32] D. B. Reid, "an Algorithm for Tracking Multiple Targets," *IEEE Transaction on Automatic Control,* vol. 24, no. 6, pp. 843-854, 1979.

[33] R. L. Streit and T. E. Luginbuhl, "Probabilistic Multi-Hypothesis Tracking," NUWC-NPT Technical Report 10,428, Newport, Rhode Island, 15 February 1995.

[34] D. F. Crouse, M. Guerriero and P. Willet, "A Critical Look at the PMHT," *J. Adv. Inf. Fusion,* vol. 4, no. 2, pp. 93-116, Dec 2009.

[35] B. Vo, S. Singh and A. Doucet, "Sequential Monte Carlo Methods for Multi-Target Filtering with Random Finite Sets," *IEEE Trans. Aero. Elec. Sys.,* vol. 41, no. 4, p. 1224–1245, 2005.

[36] R. Mahler, "PHD Filters of Higher Order in Target Number," *IEEE Trans. Aero. Elec. Sys.,* vol. 43, no. 4, pp. 1523 - 1543, Oct 2007.

[37] B. Vo and W. Ma, "A Closed-Form Solution for the Probability Hypothesis Density Filter," in *8th Int. Con. Inf. Fusion, Vol. 2*, Philadelphia, PA, July 2005.

[38] R. W. Sittler, "An Optimal Data Association Problem in Surveillance Theory," *IEEE Trans. on Military Electronics,* Vols. MIL-8, no. 2, pp. 125-139, 1964.

[39] I. Velodyne LiDAR, "velodynelidar," September 2015. [Online]. Available: http://velodynelidar.com/docs/manuals/63-9113%20HDL-32E%20manual_Rev%20H_Sept.pdf. [Accessed 2 December 2015].

[40] Y. S. Kim and K. S. Hong, "An IMM Algorithm for Tracking Maneuvering Vehicles in an Adaptive Cruise Control Environment," *International Journal of Control, Automation, and Systems,* vol. 3, no. 2, pp. 310-318, 2004.

[41] D. M. Lane, M. J. Chantler and D. Dai, "Robust Tracking of Multiple Objects in Sector-Scan Sonar Image Sequences Using Optical Flow Motion Estimation," *IEEE Journal of Oceanic Engineering,* vol. 23, no. 1, pp. 31-46, 1998.

[42] A. Yilmaz, O. Javed and M. Shah, "Object Tracking: A Survey," *Journal of ACM Computing Surveys (CSUR),* vol. 38, no. 4, p. Article 13, 2006.

[43] P. Abolmaesumi and M. R. Sirouspour, "An Interacting Multiple Model Probabilistic Data Association Filter for Cavity Boundary Extraction From Ultrasound Images," *IEEE Trans. Medical Imaging,* vol. 23, no. 6, pp. 772-784, 2004.

[44] B. Hammarberg, C. Forster and E. Torebjork, "Parameter Estimation of Human Nerve c-Fibers Using Matched Filtering and Multiple Hypothesis Tracking," *IEEE Transactions on Biomedical Engineering,* vol. 49, no. 4, pp. 329-336, 2002.

[45] B. G. EP, G. M. Jenkins and G. C. Reinsel, Time Series Analysis: Forecasting, Wiley, 2013.

[46] J. C. McCall and M. M. Trivedi, "Video-Based Lane Estimation and Tracking for Driver Assistance: Survey, System, and Evaluation," *IEEE Trans. Intell. Transport. Sys.,* vol. 7, no. 1, pp. 20-37, 2006.

[47] I. K. Moon, K. Yi, D. Caveney and J. K. Hedrick, "A Multi-target Tracking Algorithm for Application to Adaptive Cruise Control," *Journal of Mechanical Science and Technology,* vol. 19, no. 9, pp. 1742-1752, 2005.

[48] A. Petrovskaya and S. Thrun, "Model Based Vehicle Detection and Tracking for Autonomous Urban Driving," *Autonomous Robots,* vol. 26, no. 2, pp. 123-139, April 2009.

[49] J. Levinson, J. Askeland, J. Becker, J. Dolson, D. Held, S. Kammel, J. Kolter, D. Langer, O. Pink, V. Pratt, M. Sokolsky, G. Stanek, D. Stavens, A. Teichman, M. Werling and S. Thrun, "Towards Fully Autonomous Driving: Systems and Algorithms," in *IEEE Intelligent Vehicles Symposium (IV)*, Baden, Baden, 5-9 June, 2011.

[50] B. D. O. Anderson and J. B. Moore, Optimal Filtering, Englewood Cliffs: NJ: Prentice-Hall, 1979.

[51] S. A. Gadsden, M. Al-Shabi and S. R. Habibi, "Estimation Strategies for the Condition Monitoring of a Battery System in a Hybrid Electric Vehicle," *ISRN Signal Processing,* 2011.

[52] S. A. Gadsden and S. R. Habibi, "A New Form of the Smooth Variable Structure Filter with a Covariance Derivation," in *IEEE Conference on Decision and Control*, Atlanta, Georgia, 2010.

[53] D. Musicki and R. Evans, "Joint Integrated Probabilistic Data Association: JIPDA," *IEEE Transaction on Aerospace and Electronic Systems,* vol. 40, no. 3, pp. 1093-1099, 2004.

[54] M. Attari, S. A. Gadsden and S. R. Habibi, "Target Tracking Formulation of the SVSF as a Probabilistic Data Association Algorithm," in *Proceedings of the American Control Conference*, Washington D.C., June 2013.

[55] S. Blackman, Multiple Target Tracking with Radar Applications, Norwood, MA: Artech House, 1986.

[56] Y. Bar-Shalom, K. C. Chang and H. A. P. Blom, "Automatic Track Formation in Clutter with a Recursive Algorithm," in *Proceedings of the 28th Conference on Decision and Control*, Tampa, Florida, December 1989.

[57] M. Attari, A. Gadsden and S. Habibi, "A Multi-Target Tracking Formulation of the SVSF with the Joint Probabilistic Data Association Technique," in *ASME Dynamic Systems and Control*, San Antonio, Texas, October 2014.

[58] H. Blom and E. Bloem, "Combining IMM and JPDA for Tracking Multiple Maneuvering Targets in Clutter," in *Proceedings of the Fifth International Conference on Information Fusion*, Annapolis, MD, USA, July 2002.

[59] S. A. Gadsden, Y. Song and S. Habibi, "Novel Model-Based Estimators for the Purposes of Fault Detection and Diagnosis," *IEEE/ASME Trans. on Mechatronics,* vol. 18, no. 4, pp. 1237-1249, AUGUST 2013.

[60] M. S. Lee and Y. H. Kim, "An Efficient Multitarget Tracking Algorithm for Car Applications," *IEEE Trans. on Industrial Electronics,* vol. 50, no. 2, pp. 397-399, April 2003.

[61] C. Premebida and U. Nunes, "a Multi-Target Tracking and GMM-Classifier for Intelligent Vehicles," in *2006 IEEE Intelligent Transportation Systems Conference*, Toronto, Canada, September 2006.

[62] H. Gauvrit, J. P. Le Cadre and C. Jauffret, "A Formulation of Multi-Target Tracking as an Incomplete Data Problem," *IEEE Trans. Aero. Elec. Sys.,* vol. 33, no. 4, pp. 1242-1257, 1997.

[63] Y. Ruan, P. Willett and R. Streit, "The PMHT for Maneuvering Targets," in *American Control Conf.*, Philadelphia, Penn., June 1998.

[64] R. Mahler, "Multitarget Bayes Filtering via First-Order Multitarget Moments," *IEEE Trans. Aero. Elec. Sys.,* vol. 39, no. 4, pp. 1152-1178, Oct. 2003.

[65] A. Houles and Y. Bar-Shalom, "Multisensor Tracking of a Maneuvering Target in Clutter," *IEEE Transactions on Aerospace and Electronic Systems,* vol. 25, no. 2, pp. 176-188, 1989.

[66] T. Kim, "Model-Based Condition Monitoring and Power, PhD Thesis," University of Nebraska-Lincoln, Lincoln, NE, 2015.

[67] S. Chen and F. Yan, "Trapped Unburned Fuel Estimation and Robustness Analysis for a Turbocharged Diesel Engine With Negative Valve Overlap Strategy," *J. Dyn. Sys., Meas., Control,* vol. 137, no. 6, pp. 061004,1-13, 2015.

[68] X. Huang and J. Wang, "Robust Sideslip Angle Estimation for Lightweight Vehicles Using Smooth Variable Structure Filter," in *ASME Dyn. Sys. Cont. Conf. (DSCC)*, Palo Alto, CA, USA, Oct 21–23, 2013.

[69] C. Davis, "The Norm of the Schur Product Operation," *Numerische Mathematik,* vol. 4, no. 1, pp. 343-344, 1962.

[70] S. Sivaraman and M. Manubha, "Looking at Vehicles on the Road: A Survey of Vision-Based Vehicle Detection, Tracking, and Behavior Analysis," *IEEE Trans. Intell. Trasp. Syst.,* vol. 14, no. 4, pp. 1773-1795, Dec. 2013.

[71] S. A. Askeland and T. Ek, "Tracking With a High-Resolution 2D Spectral Estimation Based Automotive Radar," *IEEE Trans. Intell. Transp. Syst.,* no. 99, 2015, DOI: 10.1109/TITS.2015.2407571.

[72] M. Attari and S. R. Habibi, "Automotive Tracking Technique Using a New IMM Based PDA-SVSF," in *ASME Int. Mech. Eng. Cong. Exp.*, Montreal, QC, Nov, 2014.

[73] M. Attari, S. A. Gadsden and S. R. Habibi, "Target Tracking Formulation of the SVSF with Data Association Techniques," *IEEE Transaction on Aerospace and Electronic Systems,* Under Review, Dec. 2014.

[74] K. B. Petersen and M. S. Pedersen, The Matrix Cookbook, Copenhagen, Denmark: Technical University of Denmark, 2008.

[75] X. Wang, B. L. Scala and R. Ellem, "Feature Aided Probabilistic Data Association for Multi-Target Tracking," in *11th Int. Conf. Information Fusion*, Cologne, Germany, Jul 2008.

[76] C. S. Agate and K. J. Sullivan, "Signature-Aided Tracking Using Association Hypotheses," in *Signal Processing, Sensor Fusion, and Target Recognition*, Orlando, FL, April 2002.

[77] S. J. Julier and J. K. Uhlmann, "New Extension of the Kalman Filter to Nonlinear Systems," in *Signal Processing, Sensor Fusion, and Target Recognition*, Orlando, FL, April, 1997.

[78] S. A. Gadsden and S. R. Habibi, "A New Robust Filtering Strategy for Linear Systems," *ASME J. Dyn. Sys., Meas., Cont.,* vol. 135, no. 1, p. 014503, 2013.

[79] M. Attari, Z. Luo and S. Habibi, "An SVSF-Based Generalized Robust Strategy for Target Tracking in Clutter," *IEEE Trans. Intell. Transport. Sys.,* DOI: 10.1109/TITS.2015.2504331, 23 Dec. 2015.

[80] T. Kirubarajan and Y. Bar-Shalom, "Probabilistic Data Association Techniques for Target Tracking in Clutter," *Proc. IEEE,* vol. 92, no. 3, pp. 536-557, Mar 2004.

[81] A. K. Chakraborty and M. Chatterjee, "On Multivariate Folded Normal Distribution," *Sankhya: The Indian Journal of Statistics,* Vols. 75-B, no. Part 1, pp. 1-15, 2013.

[82] V. A. Zorich, Translated by Cooke, R.; Mathematical Analysis I, Chapter 8, Springer-Verlag Berlin Heidelberg, 2004.

[83] R. Bhatia, Matrix Analysis, New York: Springer-Verlag, 1997.